UNIVERSITY OF MINNESOTA

This is to certify that I have examined this bound copy of a doctoral thesis by

Carolyn Lee Erickson

And have found that it is complete and satisfactory in all respects and that any and all revisions required by the final examining committee have been made.

_____

Professor Kenneth Heller
(Faculty Advisor)

_____

GRADUATE SCHOOL

Nuclear Emulsion Analysis Methods of Locating Neutrino Interactions

A THESIS
SUBMITTED TO THE FACULTY OF THE GRADUATE SCHOOL
OF THE UNIVERSITY OF MINNESOTA
BY

Carolyn Lee Erickson

IN PARTIAL FULFILLMENT OF THE REQUIREMENTS
FOR THE DEGREE OF
DOCTOR OF PHILOSOPHY

December, 2006

Acknowledgements

Now, finally, I get to thank some of the people who helped make this expedition through graduate school possible.

First, my advisor, Ken Heller - thank you so much for your confidence, encouragement, guidance, and patience. Thank you, too, for the opportunity to work on this exciting experiment. I would also like to thank the entire DONUT collaboration for the opportunity to work on this experiment. It was excellent to be part of an important experiment that was small enough for me to experience all phases and aspects of a particle physics experiment.

A number of post doctoral and graduate students made my work easier, as well as more enjoyable, including Jason Sielaff, Reinhard Schwienhorst, Emily Maher, John Trammell, Judd Wilcox, and Ben Speakman. Thank you.

To my teachers Padmini Joshi and David Ober, thank you for the spark. To my friend and mentor Andy Ouderkirk, thank you for seeing me before I could see myself.

Jim Wineski, thank you for saving my life. I guess it goes without saying that without your help this would not have been possible. Cheryl, thank you for guiding me to the entrance. Karen, thank you for your trustworthy guidance throughout.

So many other friends have helped me through this process. I probably can not name them all, but I can try. Mary, thank you for your love, encouragement, and for showing me how to have some fun even when I didn't want to. I wish I had let go a little more. Thank you Kim, Barb, Paula, Laura, Cyndee, Sue, Brenda, Judith, Denne, Michael, Lori, Rob, Susan, Catherine, Carolyn, Rita, and the rest of the Monday night group, Harriett and the Monday afternoon group, Maureen, Alison, Shanna, Emily, and Markus.

To my partner Mame - thank you so much for your kindness, love, support, and for your hours and hours of technical assistance. I would not be finished yet without your help.

To my mother and father, Yvonne and Arnold, thank you for your unfailing love and support – always. Thank you Paul, Luann, Dean, Lynn, and all other family members who have given me support and encouragement throughout. And thank you,

my dear sister Elizabeth, for everything. Especially for believing in me always. Everyone should be so lucky to have a sister like you.

Dedication

This dissertation is dedicated to the memory of my grandmother, Edyth Miller.

Nuclear Emulsion Analysis Methods of Locating Neutrino Interactions

By Carolyn Lee Erickson

Under the supervision of Professor Kenneth Heller

ABSTRACT

The Fermilab experiment 872 (DONUT) was the first to directly observe tau neutrinos in the charged current interaction $\nu_\tau + N \rightarrow \tau + X$. The observation was made using a hybrid emulsion-spectrometer detector to identify the signature kink or trident decay of the tau particle. Although nuclear emulsion has the benefit of sub-micron resolution, its use incorporates difficulties such as significant distortions and a high density of data resulting from its continuously active state. Finding events and achieving sub-micron resolution in emulsion requires a multi-pronged strategy of tracking and vertex location to deal with these inherent difficulties. By applying the methods developed in this thesis, it is shown that event location efficiency can be improved from a value of 58% to 87%.

Table of Contents

List of Tables

List of Figures

1 History and Motivation

In December of 1930 Wolfgang Pauli wrote to a group of physicists attending a conference about radioactive beta decay in which he proposed the existence of a new particle[1]. The motivation for his postulate was to account for the missing energy in β decay. It had been observed that the energy of electrons emitted in β decay was a spectrum rather than being a single value expected from a two body decay of a particle at rest. Pauli called his particle the neutron, but after Chadwick used that name for a different particle Pauli's particle came to be called the neutrino. In his letter Pauli wrote "I have done a terrible thing. I have postulated a particle that can not be detected". And so the history of this seemingly phantom particle began - with a bold postulate and acknowledgement of its inherent illusiveness. Indeed, it was not until 26 years later that the first neutrino was detected by Cowan and Reines at the Savannah River nuclear reactor in South Carolina[2]. Utilizing the anti-electron neutrinos produced from β decay, which result from nuclear fission, they observed inverse β decay in the interaction $\overline{\nu_e} + p^+ \rightarrow e^+ + n$. In 1963 a second neutrino type was discovered by Schwartz, Steinberger, Lederman, and colleagues at Brookhaven National Laboratory[3]. Using a proton beam on a massive target they created a ν_μ beam and observed the interaction $\overline{\nu_\mu} + p^+ \rightarrow \mu^+ + n$. They did not, however, observe an occurrence of the interaction $\overline{\nu_\mu} + p^+ \rightarrow e^+ + n$. They confirmed that the electron and muon each had a neutral partner and that the muon-ness or electron-ness was apparently a conserved quantity within an interaction. This idea had previously been suggested by B. Pontecorvo in 1960[4]. Therefore in 1975 when Martin Perl and colleagues discovered the tau lepton it was assumed that it too should have a neutral partner, the tau neutrino[5], to fit into the Standard Model.

Although recent neutrino oscillation experiments have indicated that the Standard Model needs to be revised, it is still the best existing theory of matter and its interactions[6,7]. In the Standard Model all matter is composed of quarks and leptons

which exist in three generations of doublets. There are also gauge bosons which mediate the interactions between the fundamental particles. Of the 12 fundamental particles, or 24 since each has an antiparticle, only the tau neutrino had not been directly observed prior to Fermilab experiment 872. It was the primary purpose of E872, otherwise known as DONUT (Direct Observation of Nu Tau), to make the first observation of the charged current interaction $\nu_\tau + N \rightarrow \tau + X$. Prior to DONUT, there was indirect experimental evidence of the tau neutrino's existence. In observing the tau lepton decay it is apparent that there is missing energy and momentum consistent with an undetected neutrino[8]. Furthermore the width of the Z boson is consistent with three light Standard Model neutrinos[9]. After almost 30 years of neutrino studies, however, interactions of the tau neutrino had still not been observed in the same direct manner as the muon and electron neutrinos.

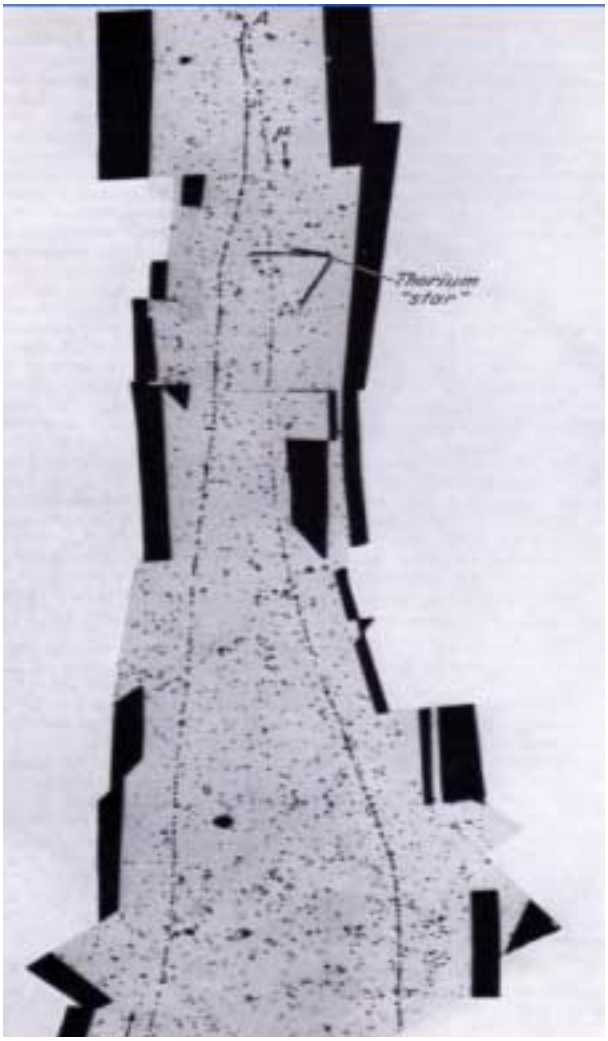

Figure 1-1 Emulsion image of the first observation of the pion. The pion is on the left. It decays at point A at the top of the image. The daughter muon travels down the right side. The thicker part of the pion track at the top indicates the particle is slowing down. The spacing of grains near the top of the muon track indicate a minimum ionizing particle. Image from reference 9.

A secondary purpose of E872 was to develop and test a new type of nuclear emulsion detection technology that could successfully detect both the initial neutrino interaction and the subsequent decay of the short lived tau lepton. One of the keys to the success of DONUT was the use of a hybrid detector comprised of an electronic spectrometer and sheets of

approximately 51 liters of nuclear emulsion sandwiched between thing steel plates. The combination of these two types of detectors allowed for a triggered experiment in which the spectrometer limited the search for a neutrino interaction to a small volume and verified that the tracks in the emulsion were from that interaction. The spectrometer also measured the properties of the particles resulting from the interaction.

Nuclear emulsion, essentially thick photographic film, was the heart of the detector because it has a spatial resolution of better than 1micron. It is an old technology which was used in such historic particle physics experiments as the first detection of the

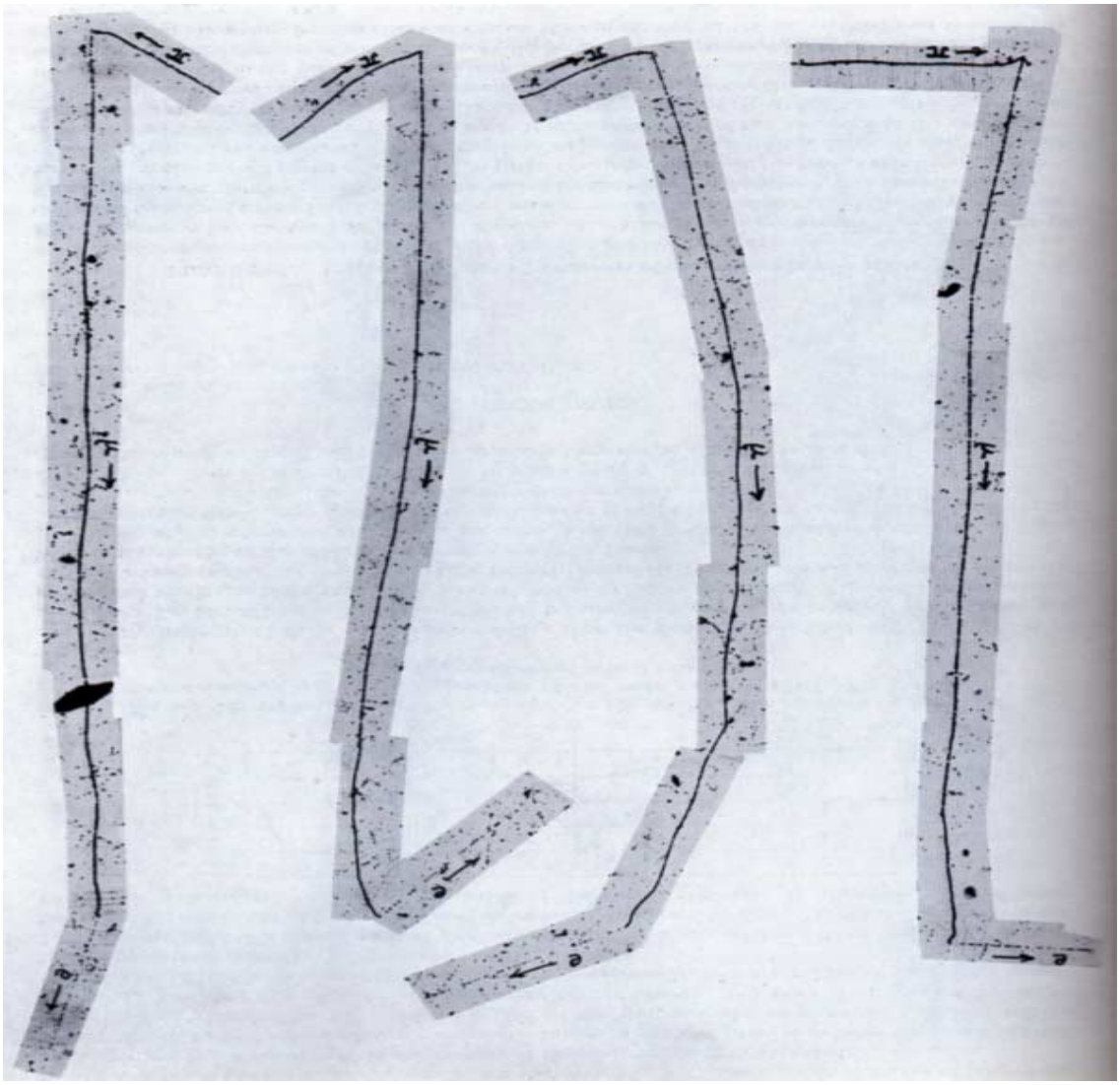

Figure 1-2 These emulsion images show pions decaying to $\mu + \nu_\mu$ with the μ subsequently decaying to $e + \nu_e + \nu_\mu$. . The images are from Powell, Fowler, and Perkins (reference 9).

pion and muon[10] (figure 1-1). Although emulsion had been an important particle detector early in the history of particle physics, its use faded with the improvement of electronic detectors. However, in recent years the use of nuclear emulsion has increased and it is again playing a significant role in experimental particle physics, particularly in the detection of short-lived particles. Since short-lived particles do not travel very far even at nearly the speed of light, the sub-micron resolution of emulsion makes it an important detector for this purpose. The reemergence of emulsion detectors has been made possible by automatic scanning techniques, primarily developed at Nagoya University, together with increased computer processing power that allows electronic pattern recognition. Currently a state of the art automatic scanning station is capable of collecting the same amount of data in 1 hour that previously required 20,000 hours of manual scanning by an individual peering through a microscope[11].

Although emulsion has excellent resolution it does have its drawbacks. First, it is expensive. Emulsion costs about 5,000 dollars per liter. For this reason, one of the techniques used in E872 was the application of emulsion in a sampling detector where the emulsion was used for tracking but steel sheets provided the mass for particle interactions. In this detector, emulsion sheets were interspersed with 1mm plates of steel. The use of steel allowed the 50 liters of emulsion to sample a larger mass than just that of the emulsion.

One weakness of emulsion is that it is always active. This produces two problems: 1) It provides no time stamp for an event, and 2) The level of background ionization is cumulative trough the course of its exposure. As with many particle physics experiments one of the primary challenges of DONUT was sorting through large amounts of data to find a small number of signal events. The fact that emulsion is always active coupled with the fact that a high intensity beam is required in order to see an occurrence of the infrequent neutrino interactions creates a situation in which the task is comparable to finding a needle in a haystack. Because all of the charged particles going through the emulsion, of which there are many, are recorded in the emulsion (fig 1-3), effective data reduction and event location techniques played a central role in determining the success of the experiment.

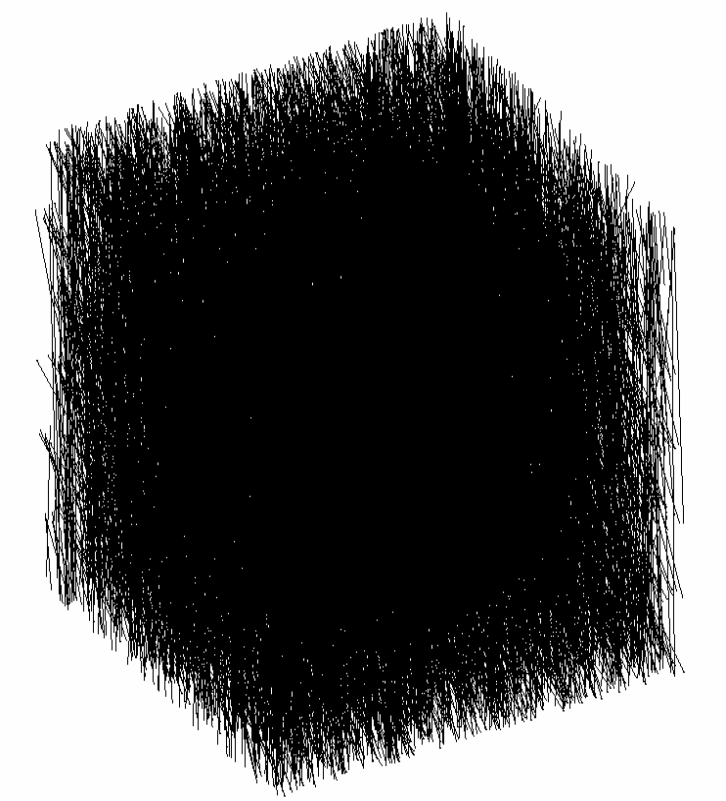

Figure 1-3 This image contains about 10% of the emulsion data in a typical volume of scanned data. Only tracks with more than 5 segments are displayed in this 0.06cm^3 volume, which is ~¼ of the volume usually scanned for location purposes.

This thesis describes the methodology used for emulsion tracking and event location. After a general description of the experimental setup, the focus of this thesis will be narrowed to the nuclear emulsion detector. Tracking and event location techniques will be described and a small event sample will be considered in detail for the purpose of determining event location efficiency. Finally, two neutrino events, located using these techniques, will be presented with a brief analysis determining the probability that one of the events is a tau neutrino event. The thesis will conclude by stating the results of E872.

2 Experimental Setup

The basic requirements for achieving the expressed goal of observing tau neutrino interactions are: 1) producing tau neutrinos, 2) allowing them to interact, and 3) identifying the signature of their interactions. In this chapter the experimental setup which allowed these requirements to be successfully met is described. First, a description of the production and purification of the neutrino beam is given. After describing the neutrino beam, a description of the emulsion target/detector will be given. Finally a description of the magnetic spectrometer will be given in section 2.3.

2.1 Neutrino Beam

2.1.1 Production

A neutrino beam with a substantial tau neutrino component was created by first bombarding a 10cm x 10cm x 100cm tungsten target with 800GeV protons extracted from the Fermilab Tevatron. Among the products of the proton – nucleon collisions in the tungsten were D_s mesons, which have a decay channel to ν_τ ,τ with a branching ratio of 6.4%[12]. The lifetime of the D_s is a short 10^{-13} seconds so that it typically decayed before it could interact in the tungsten, which had an interaction length of 9.6cm. The D_s decay, which produces both a tau neutrino and an anti tau neutrino, was the primary source of tau neutrinos in the beam (fig 2-1). A simulation of the spectrum of the interacted neutrinos is shown in fig 2-2. As opposed to the D_s the

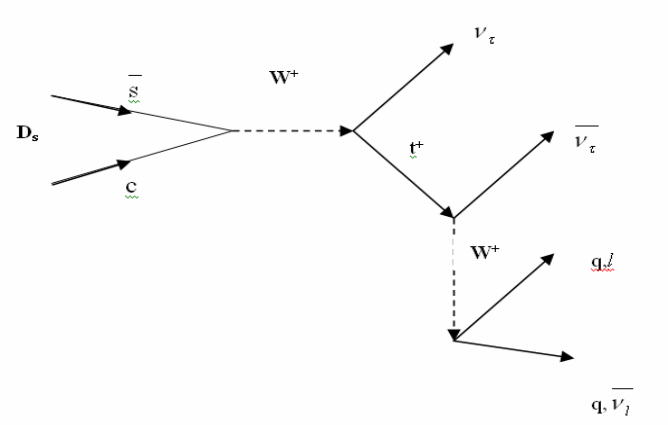

Figure 2-1 The Ds meson decays to produce a tau neutrino and anti tau neutrino.

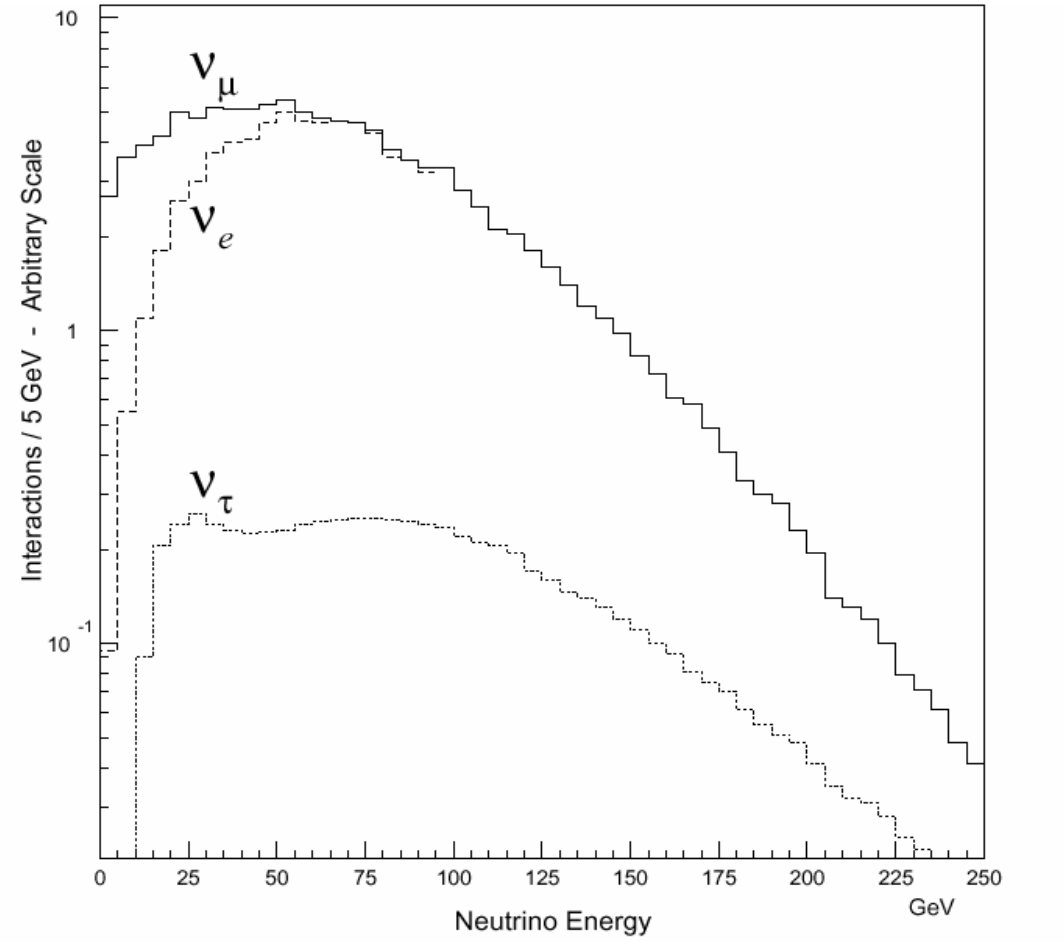

Figure 2-2 Simulation of the spectrum of the interacted neutrinos. [ref. 18]

lighter mesons have longer lifetimes, 2.6×10^{-8} and 1.24×10^{-8} respectively for pions and kaons, so those particles usually interacted before they decayed. Those which did decay provided the primary source of non-prompt muon neutrinos in the beam. The decay of other short-lived particles, mainly $D^{\pm}$, B, and Λ_c, provided an additional prompt muon neutrino component to the beam. The decay of these charm particles also contributed an additional 10 % to the tau neutrino component so that the final beam composition was estimated to be 5% tau neutrinos, 47% muon neutrinos, and 48% electron neutrinos[13].

2.1.2 Beam Purification

With approximately $5x10^{12}$ protons on target during each 20 second spill the ionization from charged particles emerging from the beam dump would have blackened the emulsion in one spill. Based on previous experiments an upper limit of $5x10^{5}$ tracks/cm^2 was set for emulsion track density[14,15]. Simulations showed that the density of muons through the target area would have been on the order of 10^{11} tracks/cm^2 with no filtering. In order to reduce the muon flux by the requisite 10^{6} a system of active and passive shielding was utilized.

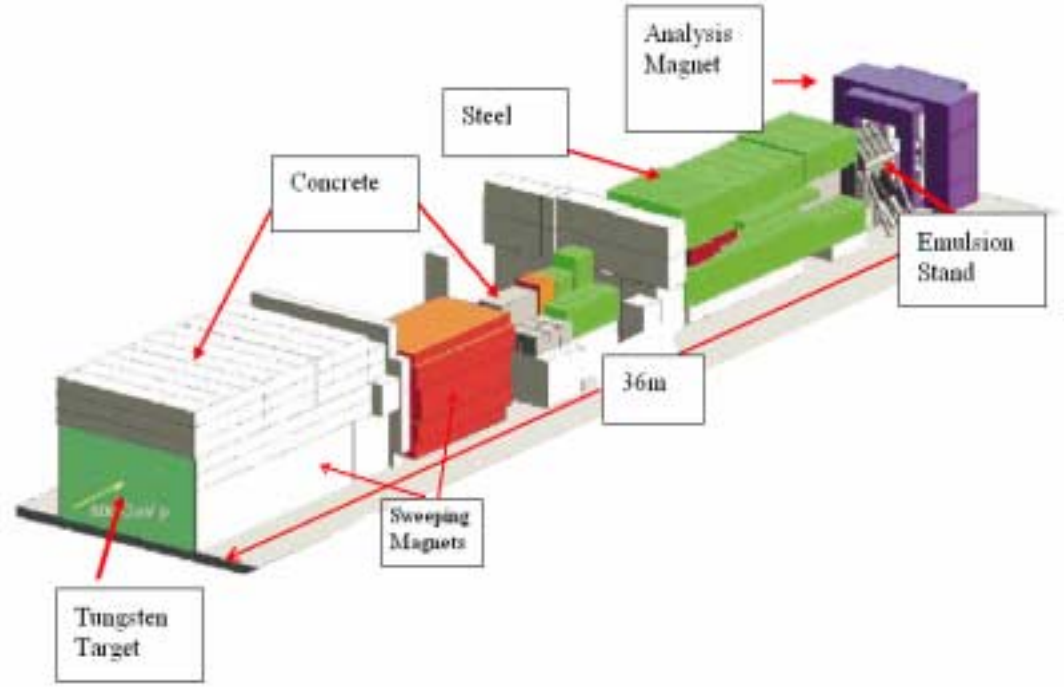

Figure 2-3 Neutrino beam active and passive shielding. The distance between the tungsten target and the emulsion was 36 meters.

The proton beam interacted with a tungsten target located in an enclosure with walls constructed of one meter of steel and two meters of concrete. Inside the enclosure, upstream of the target, bags of sand with 20% polyethylene beads and borated poly sheets were placed to reduce the backscattered low energy neutron flux. The active shielding consisted of two large sweeping magnets which were designed to remove most of the muons from the beam. The first of these, which surrounded the target, was 7 meters long and had a central field of 3.0 Tesla. This magnet was also surrounded by concrete. The field of this magnet provided a transverse momentum kick of 6.3 GeV/c which was large enough to sweep charged particles with momentum < 100 GeV to the sides of the emulsion target. However, some muons that were heading away from the emulsion were bent back into it by this first magnet. The purpose of the second magnet was to deflect those muons away from the emulsion target. The second magnet was 5 meters long with a field of 2.1 Tesla in steel in the path of the muons heading toward the emulsion. It had a region of non-magnetic air gap so as not to deflect particles that would miss the emulsion target.

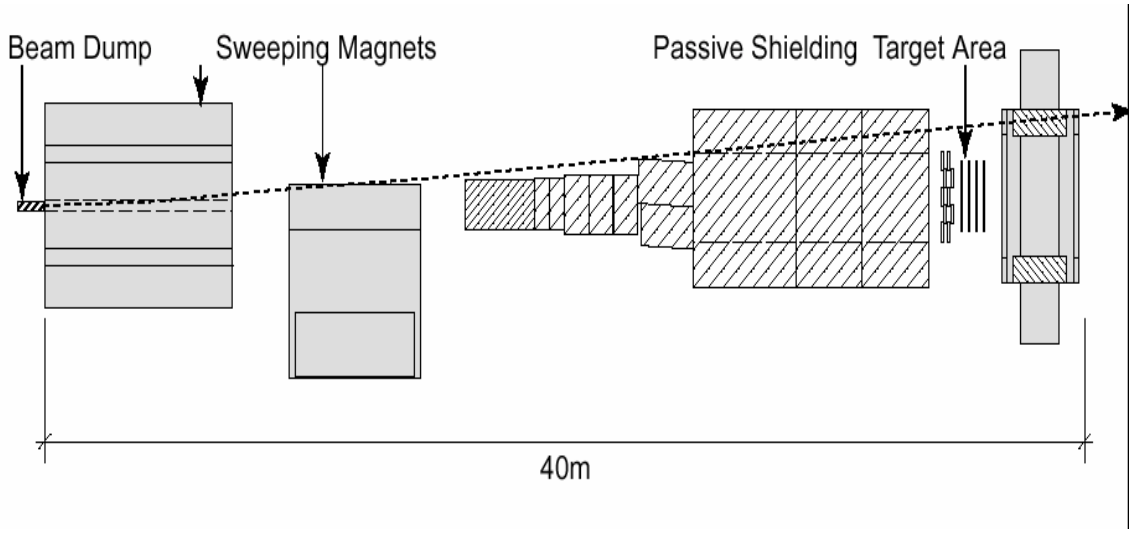

Figure 2-4 Plan view of active and passive shielding. The proton beam enters from the left. The dotted line represents a 400 GeV muon.

Downstream of the second sweeping magnet was a concrete wall to absorb remaining neutrons and 18 meters of steel to range out muons with energies less than 40GeV. The pattern of muons emerging from the magnets formed two plumes focused

on either side of the emulsion target. Because of the large flux in the plumes, cutouts were placed on each side of the 18 meters of steel to reduce the number of charged particles created by secondary interactions of muons in steel. Finally, the emulsion target itself was surrounded by 2cm of lead sheets on the sides and 12cm in the front to reduce the surviving photon flux from particle interactions in the shielding and air. The combination of active and passive shielding reduced the muon flux at the emulsion to about $1x10^5$ tracks/cm^2, sufficiently below the $5x10^5$ tracks/cm^2 limit.

2.2 Emulsion Target/Detector

2.2.1 Emulsion Composition

Nuclear emulsion is basically thick photographic film which provides high resolution for tracking ionizing particles which pass through it. Emulsion, a gelatin, is a fairly dense material so that in addition to providing excellent resolution as a detector it is also an interaction target. The emulsion used in E872, Fuji ET7C, has a density of 3.73gm/cm^3. It has a radiation length of 3.0 cm and the nuclear interaction lengths for pions and protons are 50cm and 35 cm, respectively[16]. Table 2.1 lists the composition of ET7C. The component which is key to track formation is silver bromide. A latent image is created at the location where silver atoms are formed from the combination of Ag+ ions and electrons liberated from Br- by ionizing particles passing through. When four or more silver atoms combine *grains* are formed which remain after the AgBr is washed away. The resolution of the final image, which appears as a series of grains, is largely determined by the initial crystal size of the AgBr. Figure 2.5 shows a plot of the crystal size for Fuji ET7C[17]. A more detailed description of the mechanisms responsible for image formation can be found in reference 18[18].

Table 2-2-1 Composition of Fuji ET7C

Element	Percent by Weight	Atomic Weight	% by number of Atoms
I	.3	126.90	.1
S	.2	32.06	.2
N	3.1	14.01	5.9
Br	33.4	79.90	11.1
Ag	45.4	107.87	11.2
O	6.8	16.00	11.3
C	9.3	12.01	20.6
H	1.5	1.01	39.6

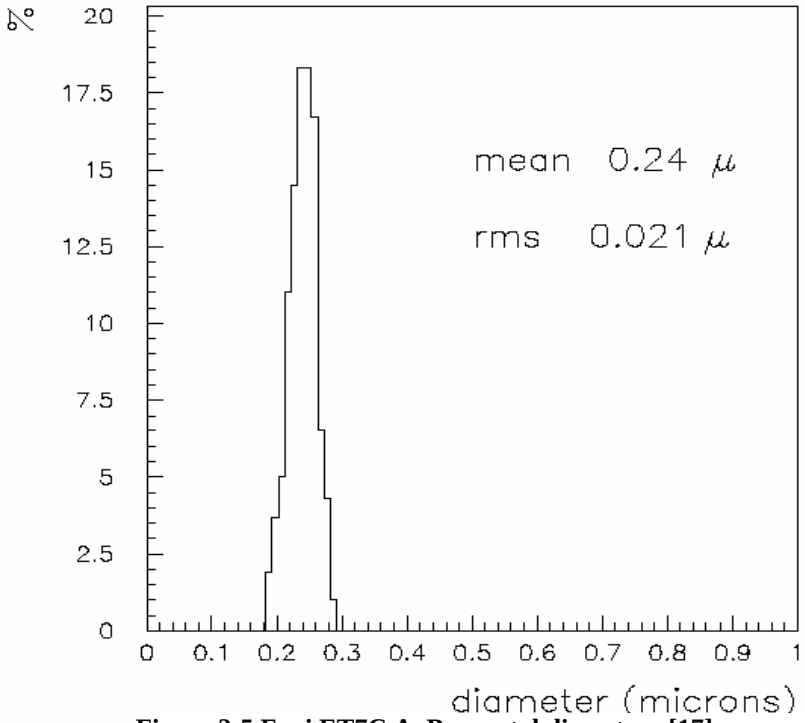

Figure 2-5 Fugi ET7C AgBr crystal diameter. [17]

2.2.2 Fabrication

The e872 emulsion target/detector was composed of seven 50 x 50 x 7 cm^3 *modules* which were oriented at 45^o from vertical and placed in an aluminum stand. As shown in figure 2-6 four modules fit in the stand at one time and modules were exchanged in the target station during the data run.

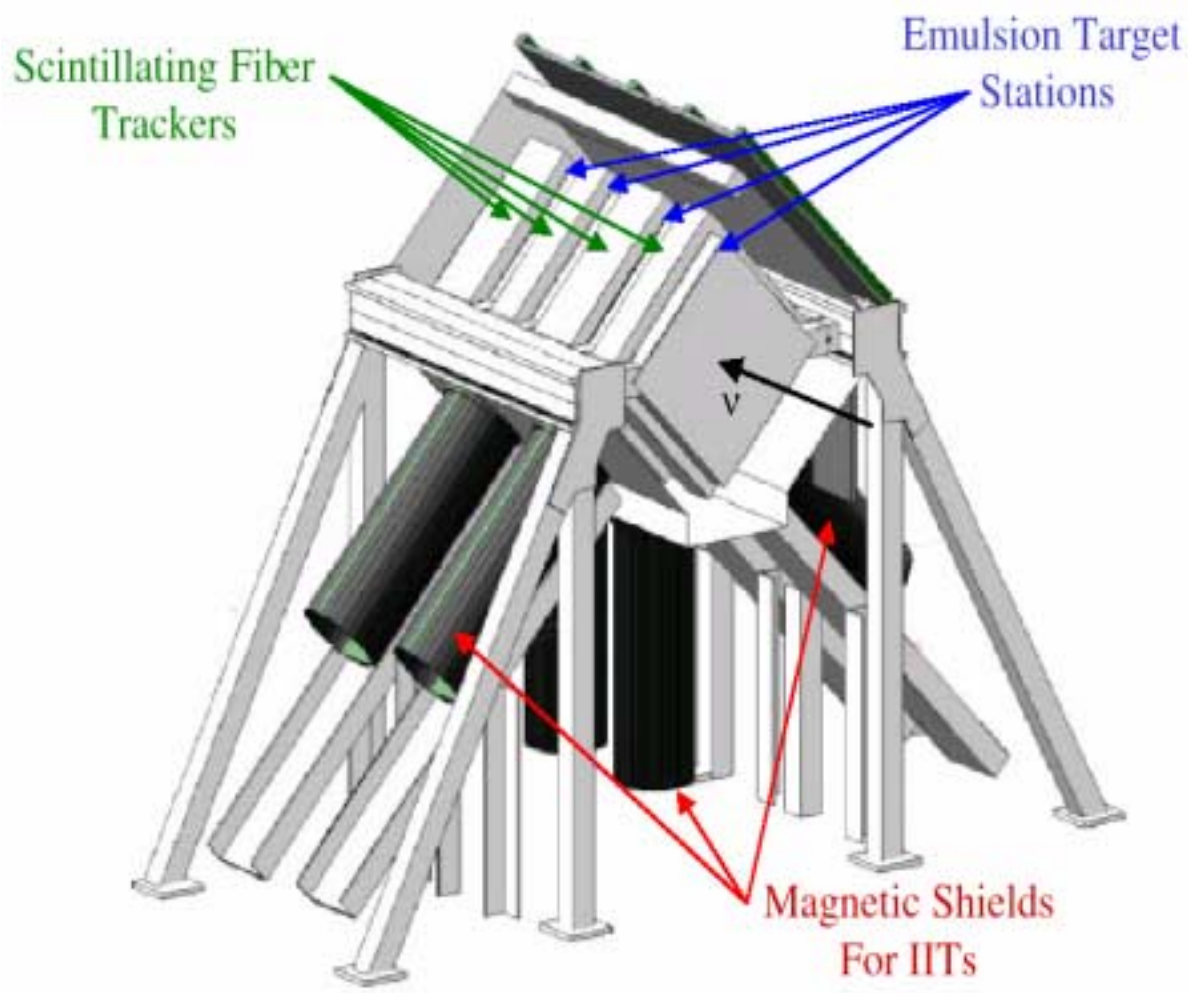

Figure 2-6 Aluminum target stand containing emulsion modules.

Fabrication of the modules involved pouring melted emulsion onto plastic sheets, allowing the sheets to dry, and stacking 47-87 of them together to form one module. Emulsion was melted at 40^{o}C and poured onto horizontally positioned plastic sheets, or plates. The purpose of the plastic was to provide rigid support for the emulsion. Inexpensive dummy gel, SiO_2 and gelatin, was poured around the edges of the ET7C emulsion and allowed to cool until it returned to its gelatinous state. After cooling, the plates were dried for an additional two days, flipped, and the process was repeated on the other side of the plates. During the drying phase the room temperature and humidity were maintained at 20^{o}C and 80%. Uniform drying was promoted by a system that provided uniform vertical air flow over the emulsion plates which were moved horizontally back and forth at a rate of 10cm/min. Uniform drying is critical to minimizing emulsion distortions. If drying is not uniform nonlinear stresses form which remain while the emulsion is being exposed. Later, when the emulsion is developed, the stresses are relieved which causes the final arrangement of grains in the emulsion to be distorted from the true (i.e. exposed) arrangement. A method for removing these distortions in software is the subject of section 3.2.3. After both sides, or faces, had been dried under these conditions the plates were allowed to dry for one more day at 20^{o}C and 60% humidity. Finally, seven centimeters of the edges, which is mostly dummy gel, were cut off to remove the worst part of the distortion which typically occurs at the edges.

Three different plate configurations were used in DONUT for the purpose of investigating the efficiency of the low cost sampling mode. The classical *bulk* configuration was composed of 350μm of emulsion coated on both sides of a 100μm acrylic base. (see Fig. 2-7). The two sampling type plates, ECC200 and ECC800, consisted of 100μm of emulsion coated on both sides of either 200 or 800 microns of lucite. Plate types ECC200 and ECC800 were interleaved between 1mm thick stainless steel plates. Once all plates had been prepared they were stacked into aluminum frames to form modules and placed under vacuum. The plate composition of each module is listed in table 2.2. During stacking the temperature and humidity were maintained at 20^{o}C and 60%. Maintaining low humidity is important during stacking because water vapor trapped

between plates will increase *fading*, which happens when the silver atoms containing the latent image return to Ag^{+}. Fading thus erases the latent image.

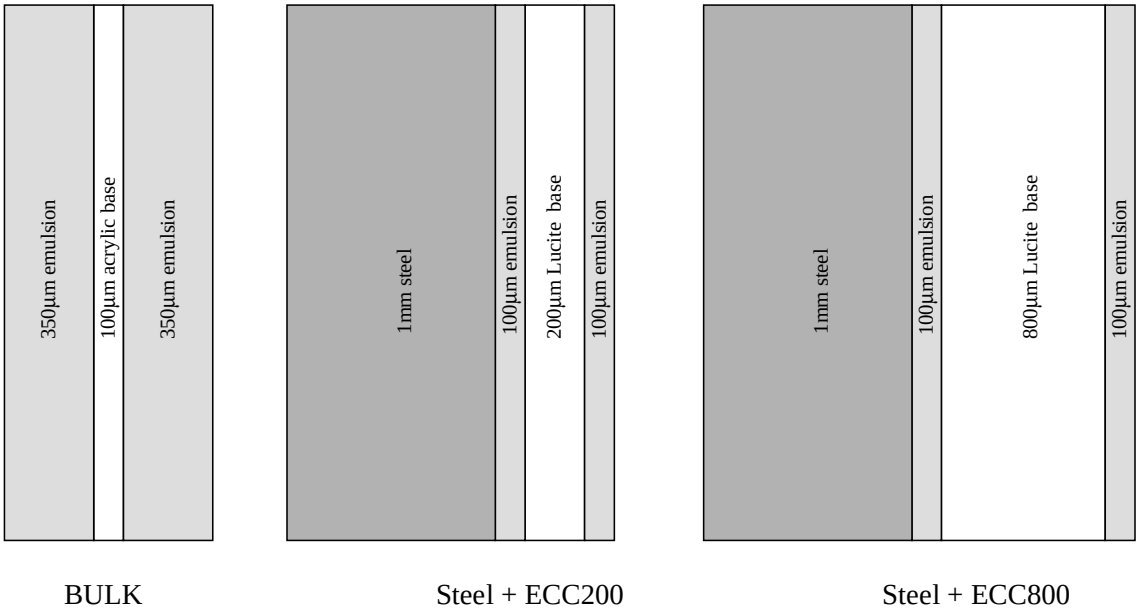

Figure 2-7 Cross sections of the three plate types.

Table 2-2 Plate configurations, mass, and number of protons on target for each of the seven modules.

Module		Plate Composition	Mass (Kg)	Protons on Target (x 10^{17})
number	type			
1	ECC1	(Fe+ECC200) X 47	105	2.57
2	ECC3	(Fe+ECC200) X 47	105	1.17
3	ECC/B1	(Fe+ECC800) X 21 + Bulk X 30	69.3	1.87
4	ECC/B2	(Fe+ECC800) X 19 + Bulk X 38*	67.9	3.35
5	ECC/B3	(Fe+ECC800) X 20 + Bulk X 32	66.5	3.35
6	ECC/B4	(Fe+ECC200) X 2 + (Fe+ECC800) X 7 + (Fe+ECC800) X 7 + Fe+(B+B+Fe) X 5+B X 43	64.44	1.99
7	B4	Bulk X 87	55.9	1.87

Fading and other climate induced problems such as emulsion expansion were also a concern during an exposure. For this reason a climate control room was built around the emulsion target and other nearby components of the detector. The temperature in the room was maintained at $22^{o}\pm1^{o}$C and humidity was maintained at 76%$\pm$2%.

2.2.3 Development

After each module was exposed for the length of time listed in table 2.2 it was disassembled for development. Before they were developed X-ray fiducial marks were made on each plate in the form of a grid with 1cm x 1cm spacing. The fiducial marks were necessary to preserve the exposed (i.e. true) spatial information since emulsion shrinks by about a factor of two during development.

The development of all plates was performed at Nagoya University. The developing process includes presoaking, development, stopping, fixing, rinsing, soaking again, and drying. Two aspects of development are particularly important for maintaining the quality of the emulsion. The first is adjusting the developing time and pH so as to both maximize the developed grain density AND produce uniform grain density throughout the emulsion. Uniform grain distribution is equally as important as high grain density because having developed grains exclusively near the surface diminishes the emulsion's usefulness as a three dimensional detector. In E872 the developing process was tuned to provide 28$\pm$2 grains/ 100μm for minimum ionizing particles in bulk and ECC800 plate types. Plates of type ECC200, which were the first processed, had a lower grain density which dropped as low as 20grains/100μm.

The other stage of development critical to maintaining emulsion quality is the drying phase. As stated above, uniform drying is important during the fabrication of the emulsion plates. Similarly, uniform drying at the end of the developing phase is also important for minimizing emulsion distortions. Alcohol is typically used to enhance uniform drying. When emulsion is soaked in alcohol some of the water is replaced by alcohol which then vaporizes more easily than the water. However, alcohol was not used

in the early part of the experiment because there was some concern that it might weaken the Lucite bases, which were being tested for the first time. In addition drafts in the drying room can also contribute to non-uniform drying. Despite these concerns, the efficiency of detecting track segments was maintained above 97% for all module types combined, so these drying issues were not a major problem.

2.2.4 Emulsion Data Acquisition

Emulsion data was acquired with an automated scanning system consisting of a microscope, a high precision moving stage, a 120 Hz CCD camera, an electronic track selector, and a computer. For each neutrino interaction identified in the spectrometer a typical volume of 5mm x 5mm x15mm was scanned in the emulsion. Depending on the plate configuration this requires scanning 8-19 plates. The time required for scanning this small volume was ten hours. With the available scanning equipment it would have required ~1000 years to fully scan all seven modules.

Segment data acquisition at the plate level involves digitizing the CCD image of each 120μm x 90μm microscope field of view within the requested scan area. For each such field an image is captured at 16 different depths of the emulsion to a final depth of 100μm. Electronics then sums the 16 digitized images and requires that a specified number, usually 8 or 9, of detected grains coincide. If this condition is met a segment is created at that horizontal position and is assigned a *pulse height* defined to be the number of focal depths with detected grains. Ionizing particles that do not pass perpendicularly through the emulsion would go undetected without an adjustment to the data. This is because the grains associated with such a track are not at the same horizontal position in successive layers and therefore would not add in coincidence to form a segment. (fig2-8). For this reason images from successive layers are systematically shifted horizontally and summed again electronically. The CCD pixel size is 0.3μm x 0.26μm so that a 1μm grain occupies about 9 pixels.

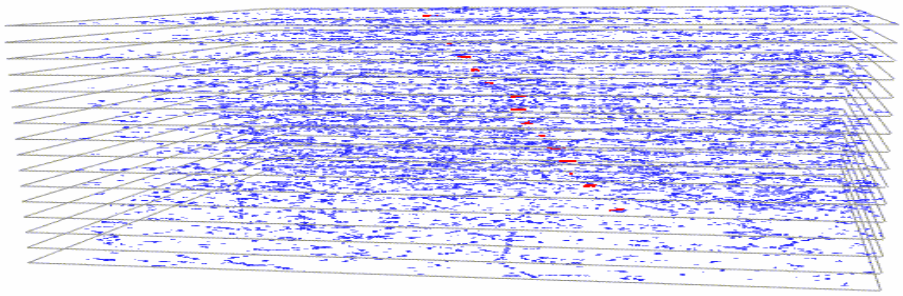

Figure 2-8 Images of digitized data from 16 focal depths of a portion of one emulsion sheet are shown. The spots represent hits associated with one particular track segment. Since this segment is not perpendicular to the emulsion sheet the detected grains will not add in coincidence to form a spike at a specific horizontal location.

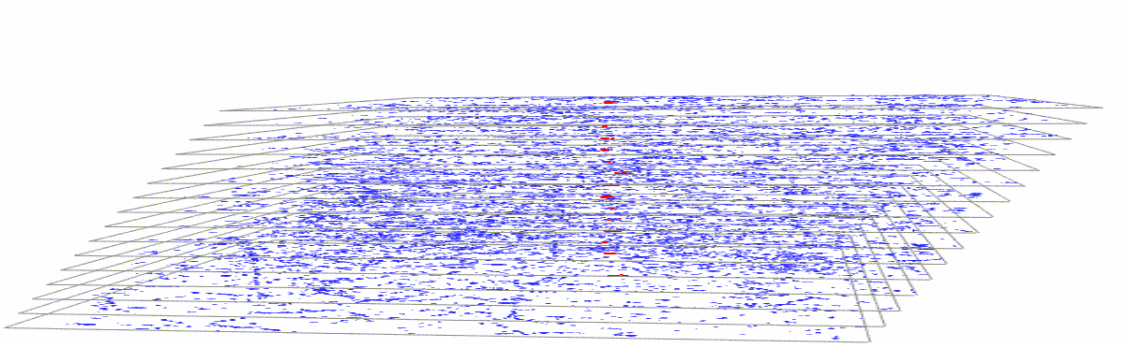

Figure 2-9 Data from successive layers are systematically shifted and summed again in order to detect segments such as the one in figure 2-8. After such a shift the signal will appear as in figure 2-10.

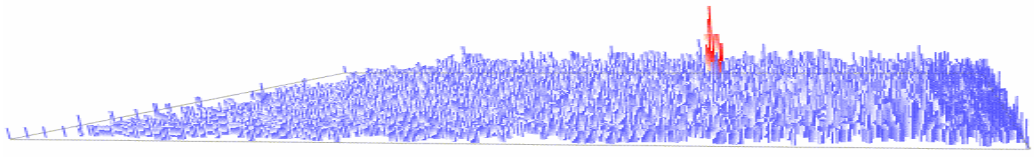

Figure 2-10 Sum of 16 shifted layers shown as a pulse height.

The electronic track segment recognition efficiency depends on the emulsion development process, distortion, and to some degree on fading. First of all, grain density is controlled largely by development, as discussed in the last section. If the density is too low the segment pulse height will be less than the value required to form a segment. Fading also reduces tracking efficiency by lowering grain density. Distortions do not lower grain density but reduce the number of hits which add coherently to form track segments (fig. 2-11c,d). The result smears the pulse height peak which then may be too

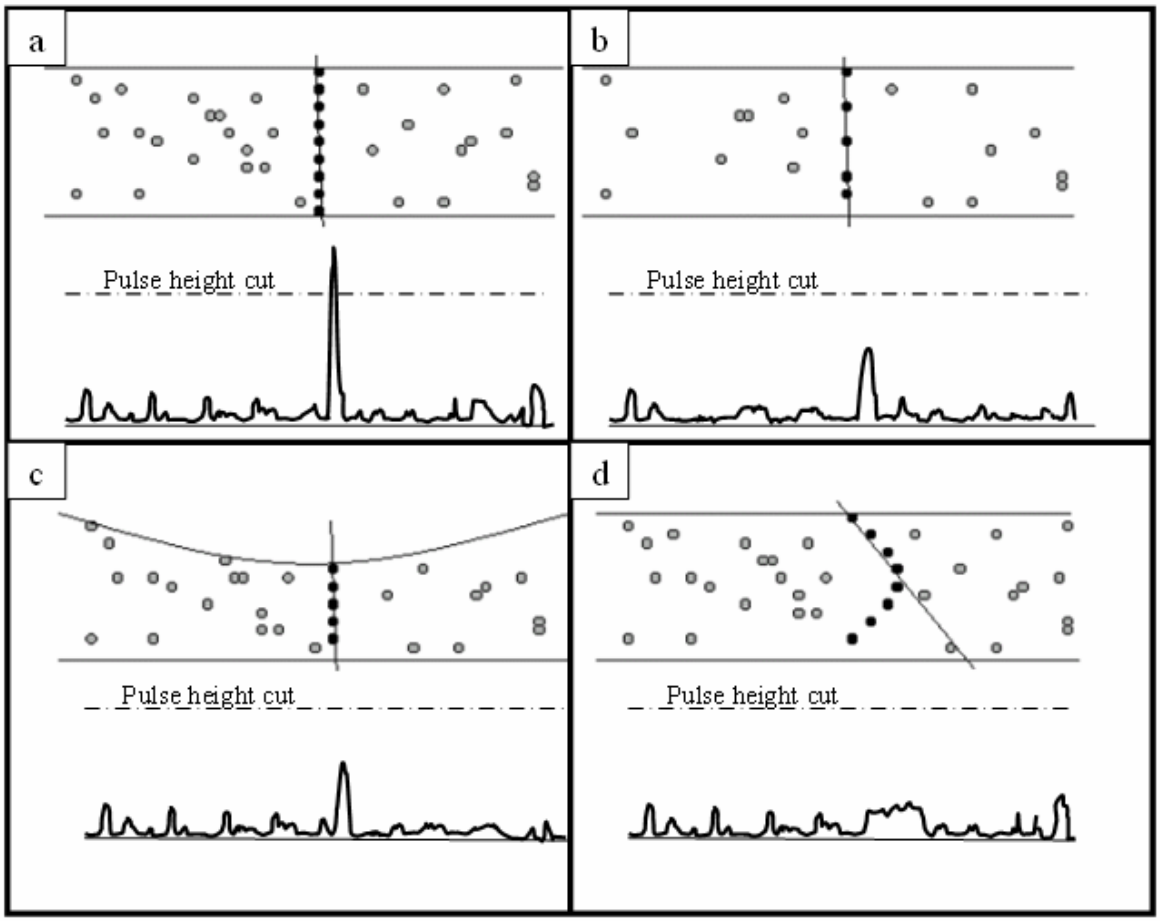

Figure 2-11 CAUSES OF SCANNING INEFFICIENCY. Each graphic depicts the cross-section of an emulsion sheet above its corresponding digitized data signal. The dashed line represents the signal level required for a segment to be identified. **a** depicts the ideal situation with high grain density and no distortion. The black dots represent the grains which add coherently to form a track segment in this plate. The grey dots represent background grains. Here the track segment signal is seen to peak above the pulse height cut. **b** shows the reduced grain density caused by bad development technique or fading. In this case the signal is too weak to pass the pulse height cut. **c** and **d** show two forms of distortion which also result in the signal not passing the pulse height cut.

low to pass the pulse height requirement. Scanning efficiency also has an angular dependence, as shown in figure 2-13, so that only track segments with $\theta < 450$ mrad were selected. Scanning efficiency can be found by calculating the percentage of segments missing from the straight tracks left by the large flux of penetrating muons. Efficiencies for the different plate types are shown in figure 2-13.

The spatial resolution of the electronic track selector is 0.3μm and the angular resolution is 3.0 mrad for a 100μm track segment. The resolution is determined mainly by the CCD pixel size, but also has contributions from stage vibrations and temperature and humidity variations during scanning. The final result of the plate scan for one 5mm x 5mm area is a data file containing pulse height, position, and angular information for each *track segment* traversing that area. Track segments are short three dimensional tracks formed from coincident grain images that traverse *one* emulsion face. They will be linked to form tracks that traverse more than one face by a software process described in section 3.2.

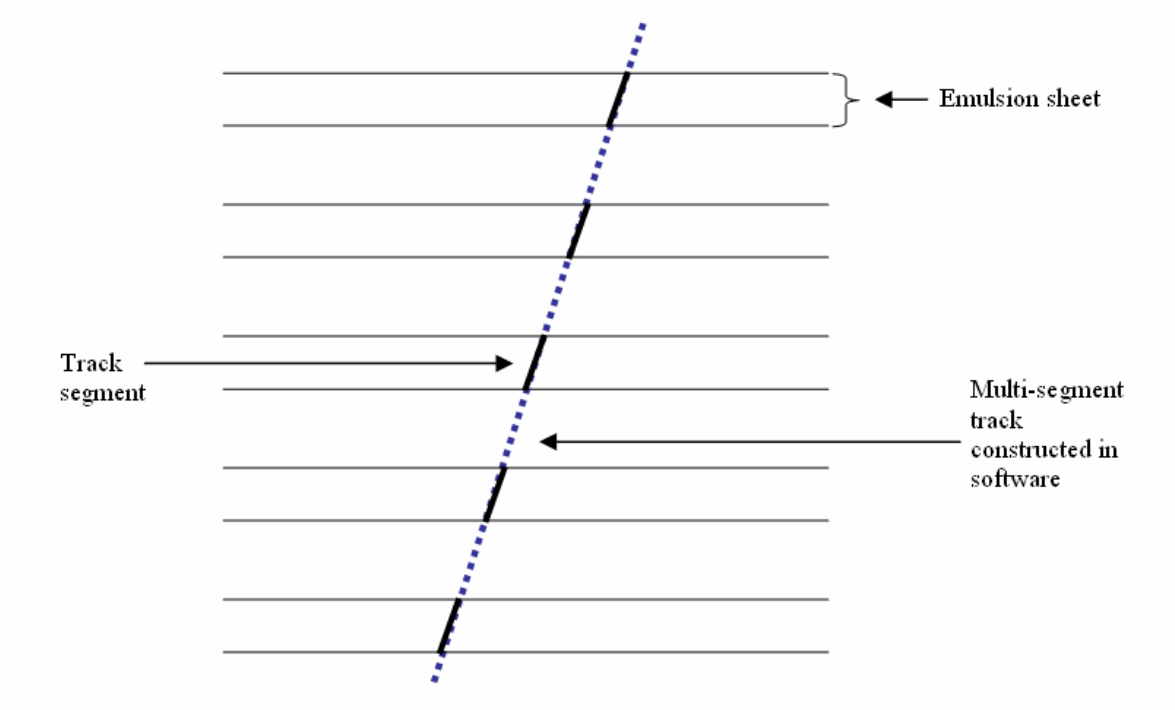

Figure 2-12 Segments are formed electronically from coincident grain images and traverse only one emulsion face, while tracks are formed in software from segment data and traverse multiple plates.

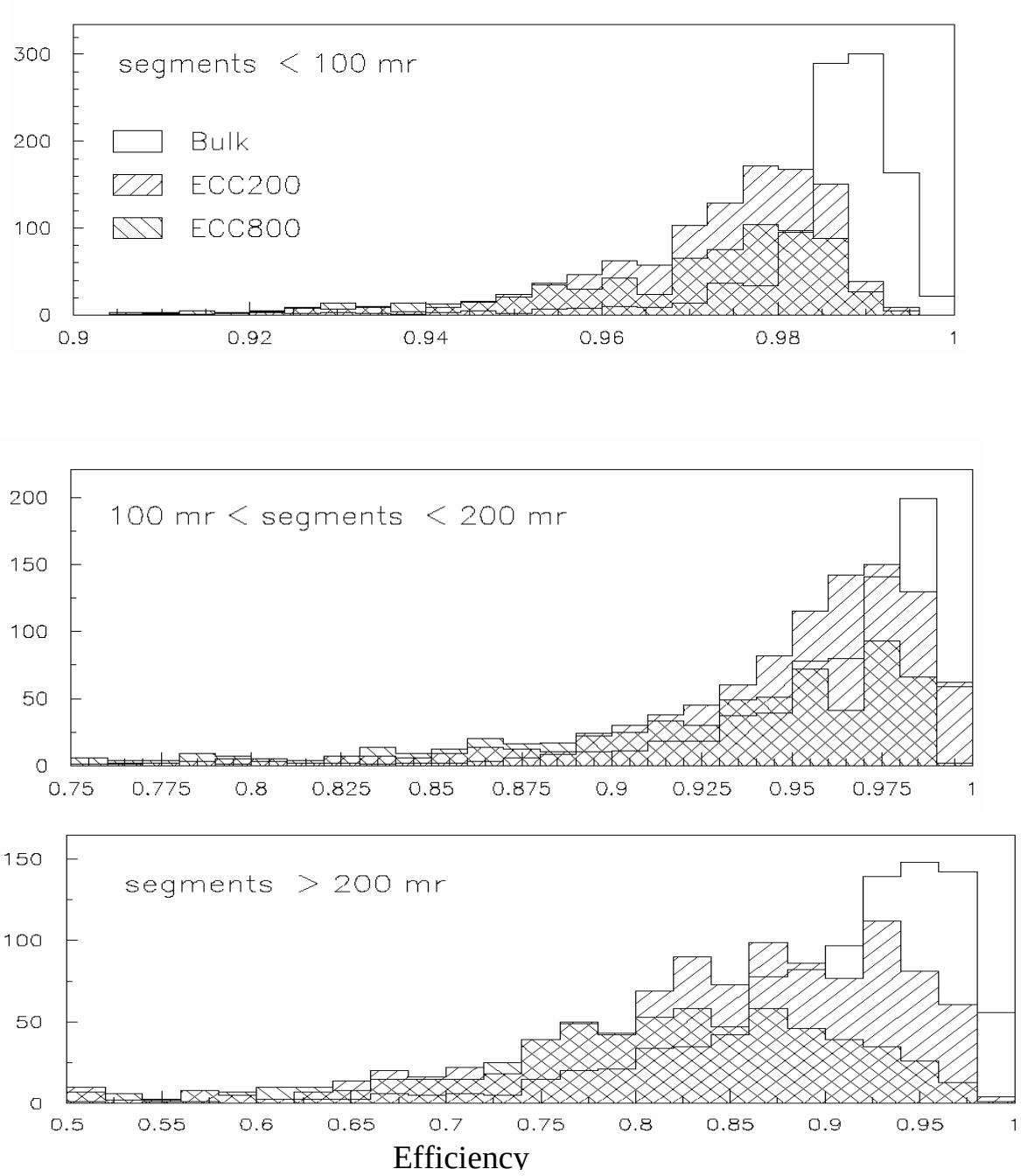

Figure 2-13 Scanning efficiencies for the three plate types in different angular regions. The top histogram gives the efficiency for tracks with angles < 100mrad relative to the beam direction. The middle shows the efficiency for tracks with angles >100mrad but <200mrad, and the bottom shows the efficiency for tracks with angles >200mrad. The three plate types are given different fill patterns in the histograms and are defined in the top histogram. [18]

2.3 Spectrometer

While the emulsion was the heart of the E872 detector, it alone was not enough to find the interaction ν_τ + N -> τ + X because, as mentioned above, the time required to fully scan all of the emulsion would have been ~1000 years. Therefore a primary purpose of the spectrometer was to identify the approximate location of the interaction vertex. Vertex predictions were typically precise enough so that a typical emulsion volume of only 5mm x 5mm x 15mm was scanned for each event (fig 2-15). In addition to providing vertex predictions the spectrometer was also needed for momentum measurements and particle identification.

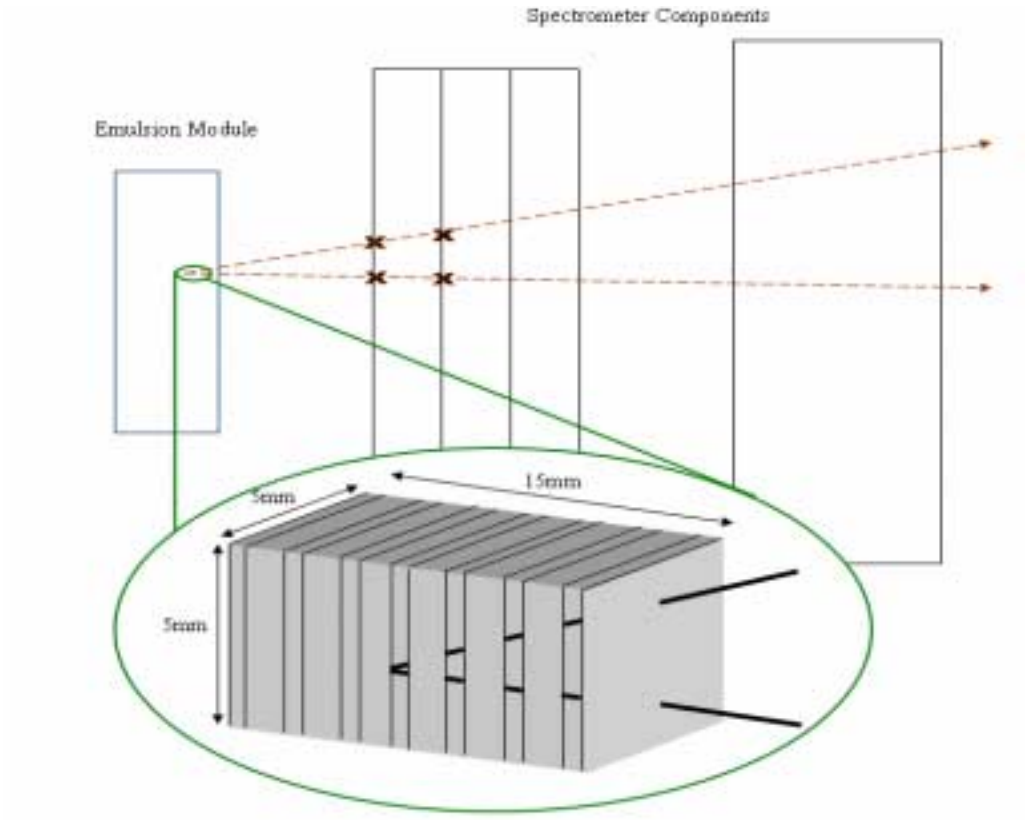

Figure 2-14 General event location idea. The spectrometer is used to identify the volume of emulsion to be scanned.

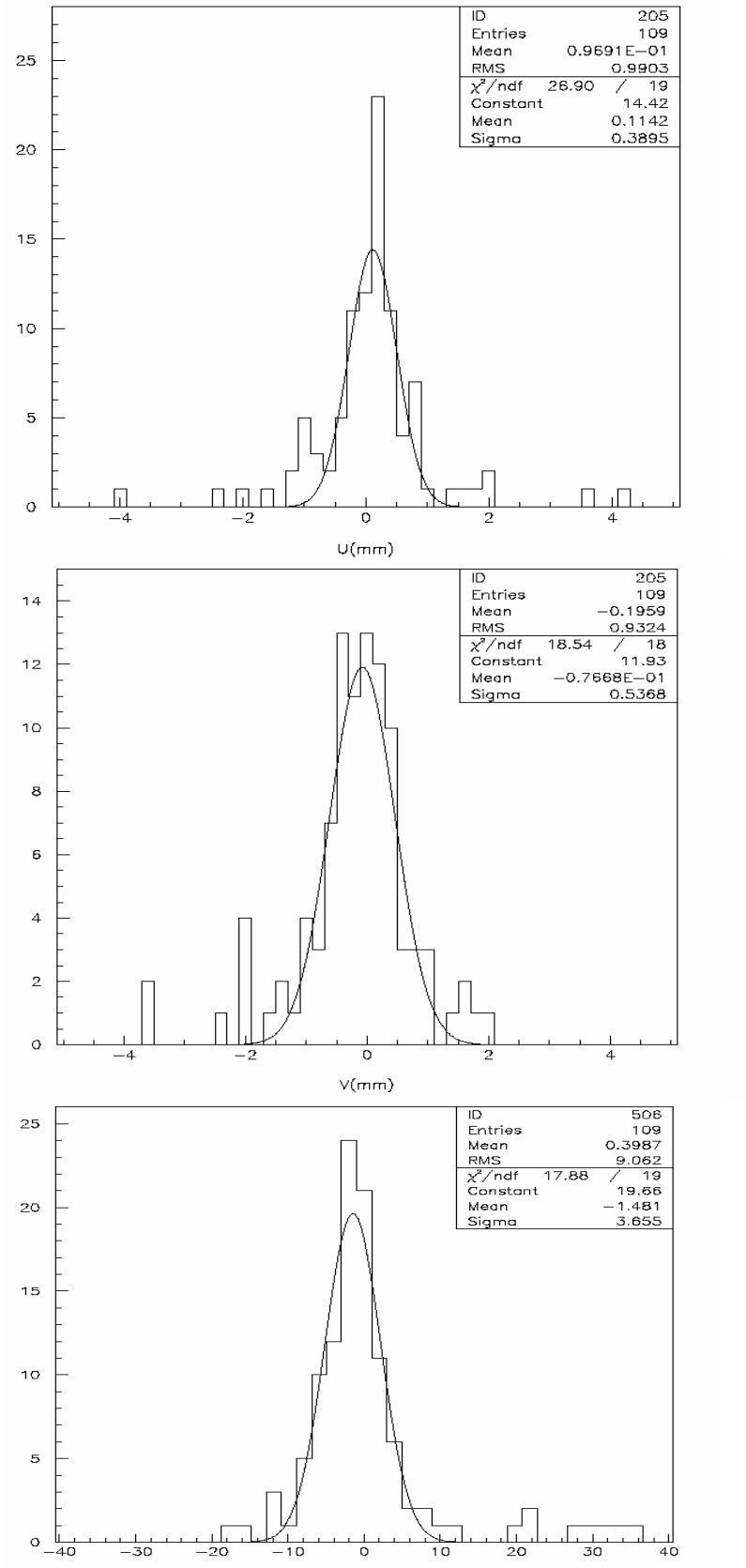

Figure 2-15 U, V, and Z difference between vertex predictions and actual positions for located events.

2.3.1 Trigger

The rate that the spectrometer could record data was limited by the CCD camera that read out the scintillating fiber tracker (sect. 2.3.2). The CCD cameras had a maximum data taking rate of ~30Hz. In order to keep the dead time below 15% a trigger rate of less than 5Hz was required. Essentially the trigger required that no charged particle enter the emulsion area and that more than one charged particle emerged, the signature of a neutrino interaction.

The E872 trigger consisted of a scintillating veto wall and three planes of scintillating counters interleaved between the emulsion modules. The veto wall was the most upstream component of the spectrometer (see Fig. 2.16). The wall was composed of two layers of five scintillation counters. Each of the 10 counters was 30.5cm x 10cm x 152cm and had an EMI 9791 photomultiplier tube on each end. The overall efficiency of the veto wall for a minimum ionizing particles was > 99% based on individual counter efficiencies of > 95%.

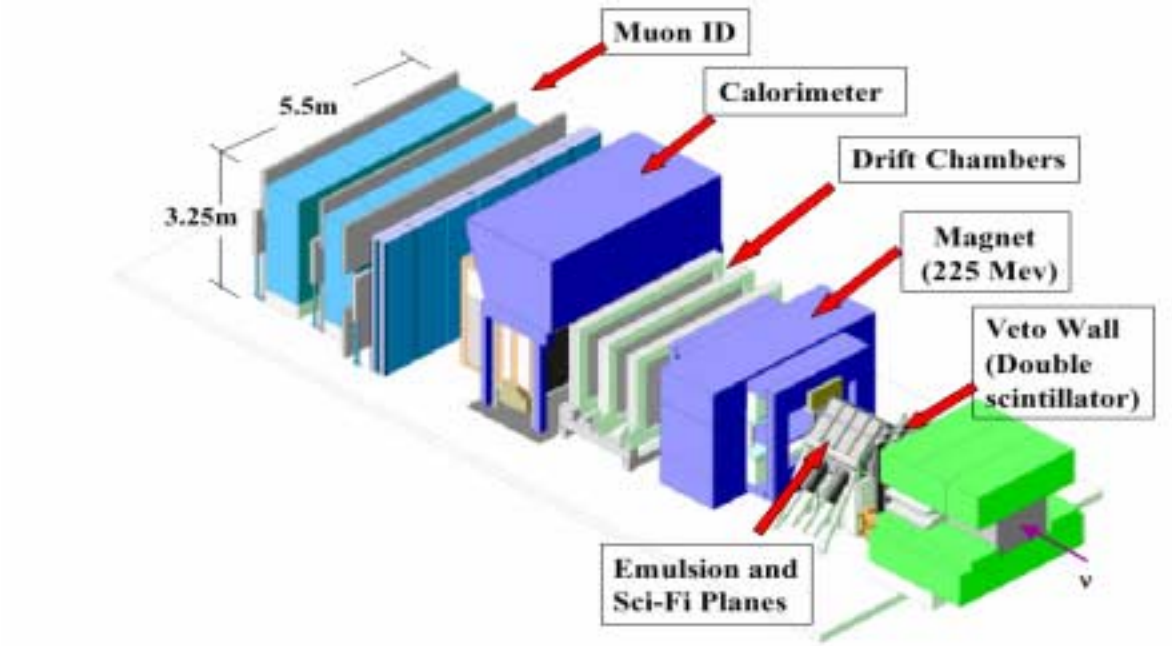

Figure 2-16 Components of the DONUT spectrometer. The most downstream end of the steel shielding in the beam line is also shown in green.

The next element of the trigger was a set of three planes of scintillation counters with transverse dimensions of 70cm x 70cm, large enough to shadow the emulsion modules. The three planes, called T1 T2 and T3, were placed after emulsion modules 2, 3, and 4 respectively. T1 consisted of 8 counters 10cm in width and T2 consisted of nine 10cm counters. The T1 and T2 counters were composed of a layer of scintillating fibers which were bundled together and read out on both ends by Hamamatsu R5600 photomultiplier tubes. T3 was composed of 10 scintillating plastic paddles read out on both ends by Phillips 12 stage tubes. The efficiency of all counters was greater than 97% for minimum ionizing particles.

The trigger logic was designed to select events with two or more charged tracks emerging from the emulsion with no charged tracks coming in. The two tracks were required to have an opening angle greater than 250 mrad. The reason for requiring two tracks was to reduce events caused by the muons that went through the emulsion. The condition of no charged tracks entering the spectrometer was accomplished by combining all 20 of the veto wall Photo Multiplier Tubes into a series of OR's. A hit in any of the

tubes vetoed that event. The two charged track requirement was met by a condition of *multiple adjacency* in (T1 and T2) or (T2 and T3) (Fig. 2.17).

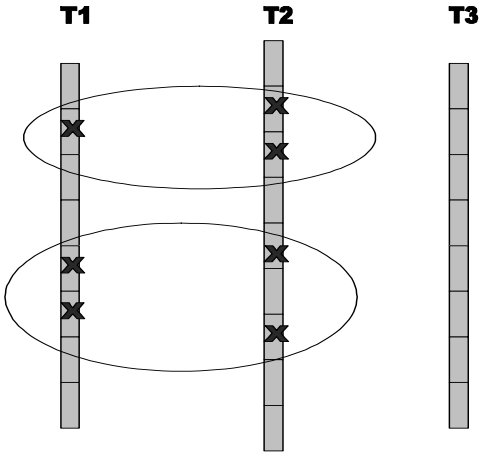

Figure 2-17 The two types of multiple adjacencies are shown. Either of these patterns in T1 and T2, as shown, would trigger the spectrometer. Similarly, either of these two patterns in T2 and T3 would also satisfy the trigger

2.3.2 Scintillating Fiber Tracker

A primary purpose of the spectrometer was to determine the location of the emulsion volume to be scanned. For this reason the tracking spectrometer elements nearest the emulsion needed to have both a high resolution and be able to function in a high rate environment. The most upstream element was a scintillation fiber tracker, or SFT. The fiber tracker consisted of 24 56cm x 56cm planes of fibers which were oriented either vertically or $\pm$ 45^{o} from vertical. As shown in figure 2-18 the planes were interspersed between emulsion modules. Each plane consisted of either two or four layers of 500μm

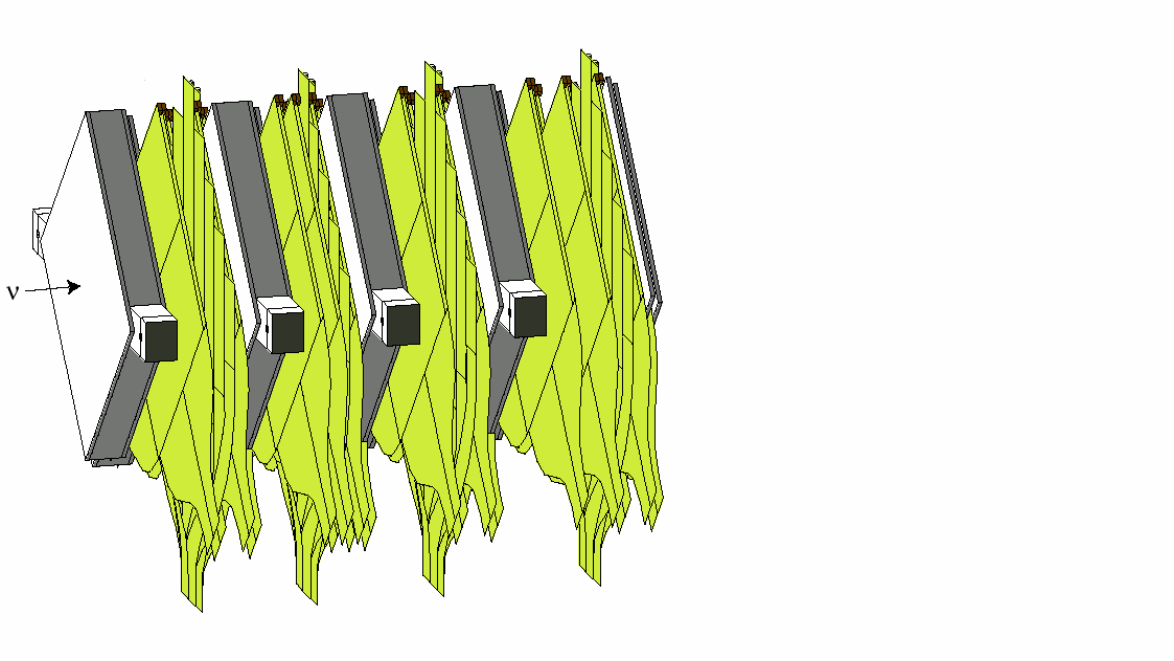

Figure 2-18
Emulsion modules are depicted as boxes with the scintillating fiber planes shown between.

diameter fibers glued to a polystyrene backing. The glue was a highly reflective TiO_2 based paint that was designed to reflect light escaping a fiber back into it and also reduce

crosstalk. The fibers were bundled into six groups which were each read out by an image intensifier with a CCD camera. This readout method was chosen to reduce the cost of reading out ~100K fibers. Large iron canisters around each image intensifier shielded them from the fringe field of a large gap analysis magnet, which was the next downstream element of the detector. After alignment, the resolution of the SFT was 200μm. The efficiency of the planes was 96% for uv planes and 99% for x planes[19].

2.3.3 Analysis Magnet

Following the emulsion/SFT/trigger assembly was a wide gap dipole magnet with an aperture of height 200cm and width 94 cm. It was 2m in length and provided a transverse momentum kick of 228 Mev/c. This magnet, in conjunction with the downstream tracking detectors, provided momentum measurements with an uncertainty, $\Delta p/p$, of better than 0.1 for p=10GeV and $\Delta p/p \leq 0.2$ for p=100GeV.

2.3.4 Drift Chambers

The three most downstream drift chambers, DC1, DC2, and DC3, had active areas of 330cm x 160cm. Each of these had four planes of sense wires with wire spacing of 1.905cm. Two of the planes had vertical wires which were set off from each other by 0.95cm (one-half cell size). The other planes were oriented at $\pm$ 17^o from vertical. The drift chambers contained a gas mixture of 50% Argon and 50% Ethane which was used as a quenching agent. The gas mixture was bubbled through ethanol at 0^o C. The efficiencies of each of the three chambers was 90%. In addition a 100cm x 70 cm vector drift chamber was positioned just upstream of the analysis magnet. This chamber usually contained too many hits to be useful in the initial selection of tracks to predict the location of an interaction in the emulsion but was used in the procedure to verify that an event had been located (see section 4.1.4)

2.3.5 Calorimeter

Following the drift chambers was a 375cm x 195cm calorimeter made of scintillating glass blocks in the center and lead glass blocks in the outer portion. The calorimeter provided identification and measurement of electromagnetic energy in the events. It also helped to determine the total energy of any interaction. The 400 blocks, arranged as shown in figure 2-19, were read out by photomultiplier tubes. The characteristics of the different block types are listed in (table 2.3).

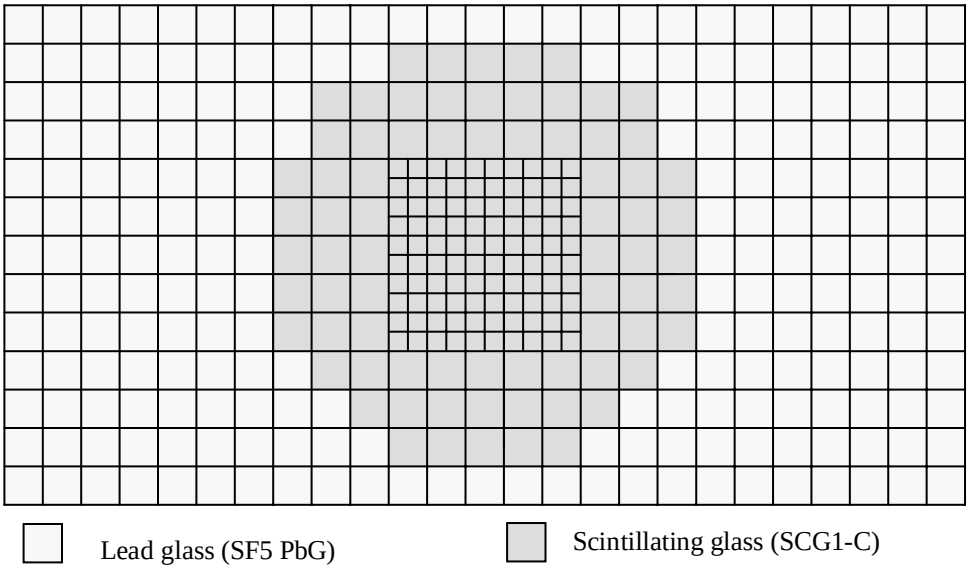

Figure 2-19 Arrangement of blocks in the electromagnetic calorimeter. The characteristics of the block types are listed in table 2.3.

Calibration of the calorimeter was performed by measuring the e/μ response for several blocks using test beams of known energy at Brookhaven National Laboratory. Utilizing this information, the responses of all other blocks were normalized at Fermilab using the PW5 muon beam which gave the response of each block to a minimum ionizing particle. During the data run, the performance of each block was monitored by measuring the signals produced by LEDs attached to each block as well as the signal from muons

passing through each block. LED measurements, and also pedestal measurements, were recorded between each beam spill.

The stability of pedestals was found to be better than 1%, and the stability of LED signals was ~2%. The overall energy resolution of the electromagnetic calorimeter was determined to be better than 20% at 1 GeV by tracking electrons through the spectrometer and comparing their momentum determined by bending in the magnet to the response of the calorimeter.[20]

Table 2-3 Characteristics of electromagnetic calorimeter blocks

Glass Type	Number of Blocks	Dimensions (cm)	Radiation Lengths	Nuclear interaction Lengths
SCG1-C	100	7.5 x 7.5 x 89	20.9	2.0
SCG1-C	74	15 x 15 x 89	20.9	2.0
SF5	224	15 x 15 x 89	16.8	1.0

2.3.6 Muon Identification System

The final element of the spectrometer was a muon identification system. It was composed of three planes of proportional tubes, each of which was located behind a steel wall. The purpose of the steel was to range out hadrons and thus allow for the identification of muons. Each plane consisted of two layers of proportional tubes, with one layer oriented in the x direction and the other layer in y. The tubes had a cross sectional area of 16cm x 4cm and contained four individual 4cm x 4cm cells. The dimensions of the most upstream wall was 3.7m x 6.25m with a thickness of 0.42m of steel. The other two walls measured 3.25m x 5.48m and were .91m thick. . The proportional tubes had an efficiency of 97% and provided position resolution of 4cm. The proportional tube coverage had a notch in its sides to avoid the high flux of muons in that region.

2.3.7 Data Acquisition

All signals from the spectrometer elements, except signals from the fiber tracker, were digitized by either LaCroy CAMAC ADCs or LaCroy CAMAC TDCs. The CCD signals from the fiber tracker were digitized by custom built flash ADCs. During the spill, a VME multi-processing bus was used to collect all event data. In the 40 seconds between beam spills, data was sent from the VME processor to a computer via Ethernet using TCP/IP protocol. The computer wrote the data to tape and processed it for diagnostic purposes. During the data run approximately 10^7 events were recorded to tape.

3 DATA REDUCTION

Before neutrino interactions can be identified in the emulsion, preliminary data processing and analysis are required. Track reconstruction and vertex identification in the spectrometer are done first followed by data filtering designed to reduce the number of non-neutrino interactions in the data set. Emulsion tracking also needs to be done before physics analysis can be accomplished. These procedures are the subject of this chapter.

3.1 Spectrometer Data

3.1.1 Tracking

Spectrometer track reconstruction is performed using the electronic signals from each component of the detector. The ionization produced by a charged particle passing through one of the detector planes is recorded as a hit with two spatial coordinates: Z, the plane position along the beam line, and an orthogonal coordinate which depends on the orientation of that particular detector plane. (fig. 3.1). Connecting hits from two such planes produces a line which is a candidate for a two dimensional projection of a particle's trajectory. To identify the three dimensional track representing that particle's trajectory, one must correctly combine two dimensional lines from two or more separate views. Hits in a third view or another component of the detector are used to resolve any ambiguity in determining this match.

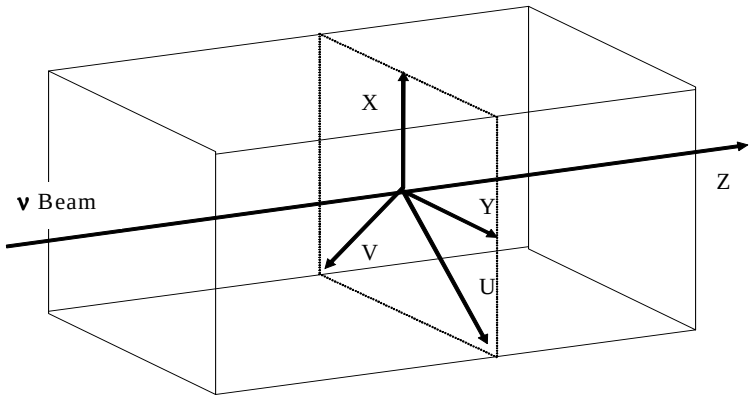

Figure 3-1 Experimental coordinate axes. The neutrino beam enters from the left .

3.1.2 Vertex Predictions

After spectrometer tracking, the vertex location for all candidate events was predicted. Several vertex finding algorithms were applied to the spectrometer data in order to predict the vertex location in the emulsion to within a typical volume of 5mm x 5mm x 15mm.

The first vertexing algorithm utilizes the two dimensional SFT lines from the U and V views separately. In this algorithm a list of all two track vertices in the U-Z plane is made. A single view vertex is simply defined as two or more lines which begin in the same module and have a distance of closest approach of < 1mm. After the list of two track vertices is created, each vertex is used as a constraint and all possible lines are connected to it. The vertex with the most lines is selected as the U view vertex. A vertex is then selected in the V view in the same manner. Finally, a three dimensional vertex is formed from the selected U and V vertices if they are within 10mm of each other in Z.

The next vertexing algorithm uses the combination of all two dimensional lines. All lines passing within a distance of 4mm from a.given point in one view are used to form a vertex. A vertex fit is performed using all of these lines and the track with the largest χ^2 is dropped and the vertex is refit. This fitting and track dropping procedure is repeated eight times or until $\chi^2<3$. A three dimensional vertex is formed from the selected U and V vertices if they are within 10mm of each other in Z.

The third algorithm is similar to the second except that 3-D tracks are used. That is, tracks which have been formed from the combination of two lines that have been determined, by another view or detector component, to belong together. This algorithm also differs from the second in that the tracks are weighted for their contribution to χ^2 of the vertex fit. The tracks are weighted using their multiple scattering uncertainties determined by their estimated momentum and their length from the vertex to the end of the emulsion target. The momentum estimate is based on the bending of the track through the

analysis magnet. If no information downstream of the analysis magnet is available, the momentum is assumed to be 0.5GeV.

The final vertexing algorithm requires the input of a seed vertex position which can be provided by one of the other algorithms or by a person viewing the track pattern. This algorithm steps through a grid around the seed in U-Z space. At each step, lines which radiate from that point are formed and the total number of hits which lie on those lines is counted. The step which contains the most hits on lines which radiate from it is chosen as the position of the vertex in the U view. The same procedure is done to determine the position of the vertex in the V view. The Z position of the final vertex is determined by the average of the z position of the U view vertex and the z position of the V view vertex.

The vertexing algorithms are used initially to assist in the data filtering which is described in the next section. They are used later as a guide to predict the event location in emulsion in order to define the volume of emulsion to be scanned. The automatic vertexing methods are not as efficient for this purpose as visual vertex selection but they provide a starting point. Visual vertex selection will be described in section 4.1.1.1.

3.1.3 Data Stripping

Only ~0.1% of the experimental triggers were neutrino interactions. Most of the triggers were caused by muon interactions in either the upstream steel, the target frame, or the analysis magnet. In order to remove non-neutrino events from the data set two filters were applied to the ~10^7 records on tape. The first of these was a software filter which required at least one of the following conditions to be met:

- One or more drift chamber tracks projects back to the most downstream emulsion module in the vertical (non-bend) view.
- A vertex is reconstructed with scintillating fiber tracks in both the U and V views of the same emulsion module.

- At least 30GeV is deposited in the electromagnetic calorimeter.

Events which satisfied at least one of these criteria were stored as stripped files. This filter reduced the data set to ~ 10,000 events.

The second filter was applied interactively by humans viewing a graphical display of each event. All events from the stripped files were examined by two people independently and selected events were required to satisfy the following conditions:

- The event had a vertex in both the U and V views of the scintillating fiber tracker with at least two tracks or a shower.
- The vertex was inside the emulsion volume.
- The total energy in the event was $\geq$ 5GeV.

After viewing the events independently the two people responsible for a given file would view the events together to form a consensus. After all stripped files had been filtered interactively 1020 predicted neutrino interactions remained in the data set.

3.2 Emulsion Data

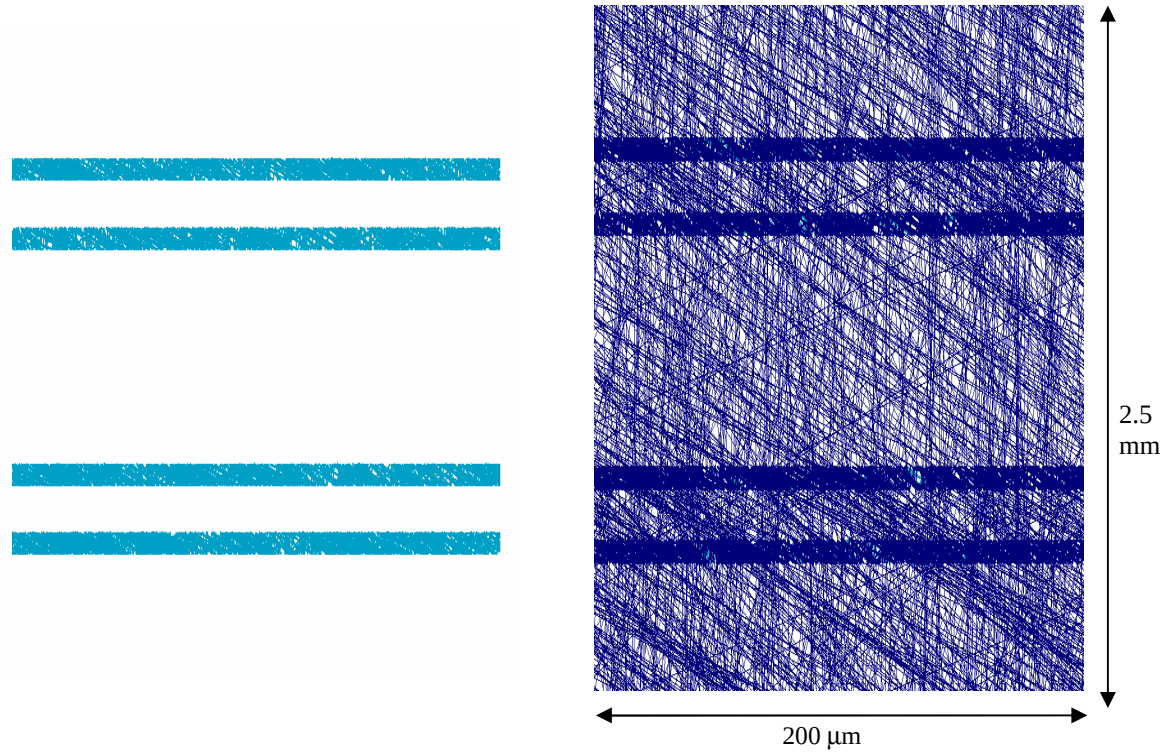

Figure 3-2 200micron x 200micron x 2.5mm emulsion volume. Single segments are shown on the left before any tracking has been done. The right image is the same volume after the tracking process.

Figure 3.2 is the two dimensional image of a 200micron x 200micron x 2.5mm volume of emulsion data. This volume is ~ 2.5×10^{-3} of the size of a typical scan volume. These images reflect the challenge of linking emulsion segments from plate to plate. The density of segments within a single emulsion plate is ~ $10^5/cm^2$. In this section, the procedure for linking single segments to form multi-segment tracks will be described. After that a procedure to perform fine local alignment will be detailed. Finally, a brief presentation of physics results which can be obtained from emulsion data will be given.

Before tracking is done, emulsion data exist as a set of *f_files* for each candidate event. f_files contain the raw data resulting from automatic scanning as described in section 2.2.3. The number of f_files for an event is given by the number of plates which span the scan volume surrounding the vertex prediction. Each separate f_file contains pulse height, position, and angular information for each segment traversing the scan area of one plate. The method for combining f_files and linking segment data between plates to form multi-segment tracks involves several steps. The first step is to determine the relative U,V positions of consecutive plates. After that segments are linked to form tracks using three algorithms. These processes are described next.

3.2.1 Plate to Plate Alignment

During the disassembly of emulsion modules the individual plates were marked with x-rays. These fiducial marks are used to make the first rough plate to plate alignment. With the plates roughly lined up a more precise plate to plate alignment is determined by maximizing the number of segment to segment links from one plate to the next. With the first plate fixed, the second plate is translated in the u-v plane and rotated in θ and ϕ until maximum segment to segment registration is found. With the first two plates thus aligned the same process is performed on the third plate, and the fourth plate, etc. until the relative positions and angles of all plates within the scan volume have been determined.

3.2.2 Track Formation

After the relative plate positions are determined segments from consecutive plates are linked to form tracks by cycling through three algorithms three times. The first algorithm uses the position and angle of a segment, called the *base segment*, to calculate the expected position and angle of a matching segment in the next emulsion plate. Before searching for matching segments, however, all segments in the scan volume are sorted into 500 micron regions depending on each segment's U and V positions and plate number. Since only segments from adjacent regions in the next plate need be considered,

this reduces the number of searches. (Fig 3-3) After sorting, the segment to segment linking algorithm is begun with a search for matching segments to each base segment within a given region. The search is made by examining all segments in the adjacent search regions that are within ~0.5mm of the projected position of the base segment. The

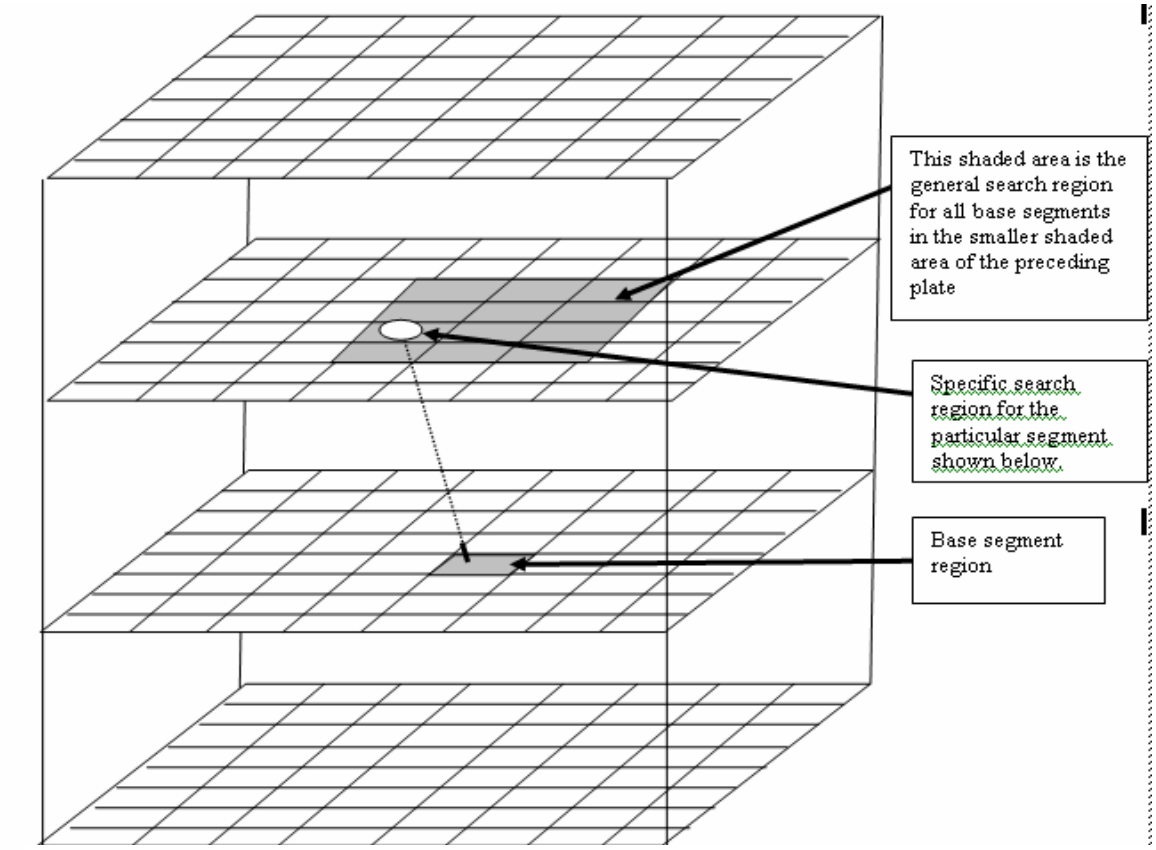

Figure 3-3 Segment data is sorted into regions according to U and V positions and plate number. This reduces the number of comparisons necessary to link segments.

size of the search area depends on the distance between scanned plates. If any matching segments are found which pass the position and angular criteria described below, they are stored until all candidate matches have been checked. The best matching segment, as defined below, is chosen and connected to the base segment to form a two segment track. In this algorithm all segments in the event are considered as base segments; That is, for every segment in the event a search is made in an adjacent plate for another segment which links to it. The connections are made beginning in the most downstream plate and linking upstream. As linking proceeds beyond the first plate, some of the base segments will already be connected to tracks because they have matched a base segment in the

previous plate. (fig 3.4a) In that case, if there is a matching segment in the following plate, the existing track will be extended to include the new match. (fig 3-4b)

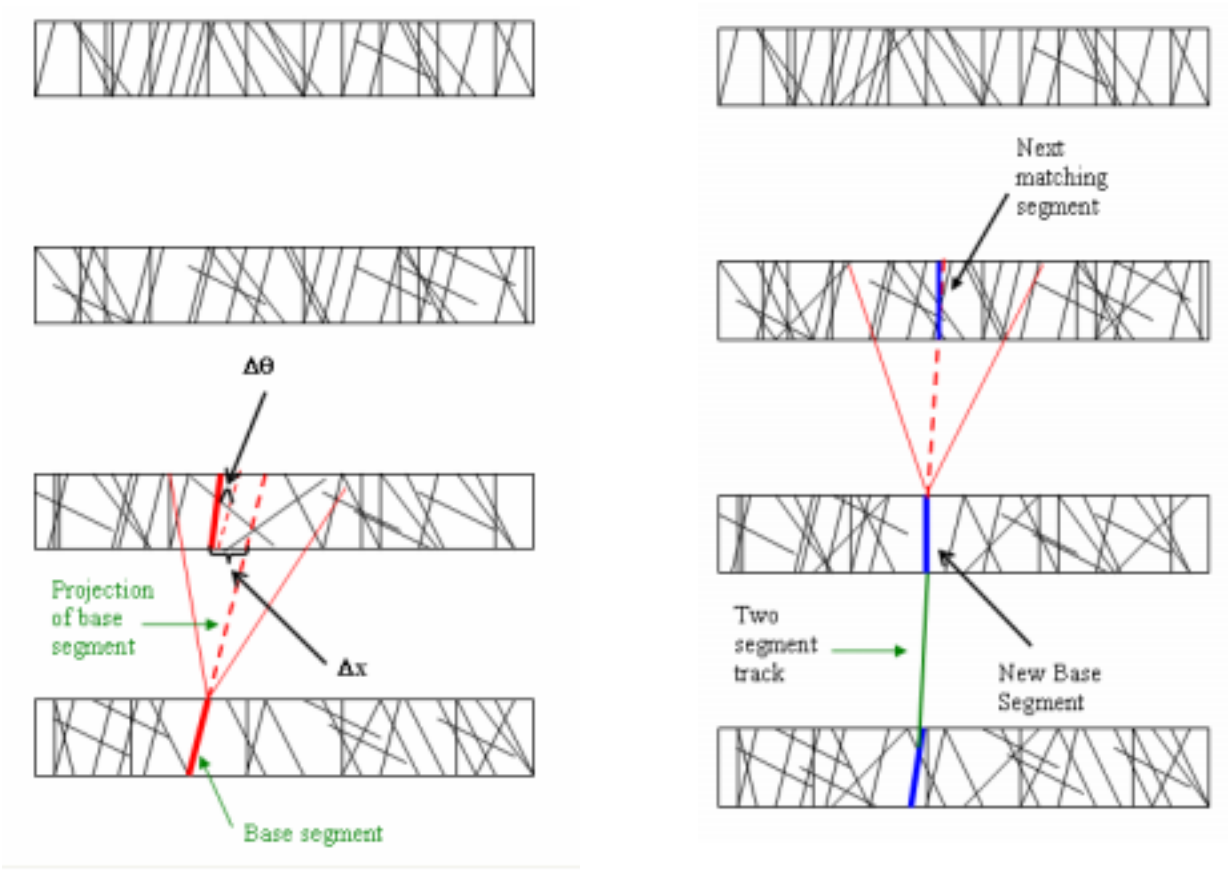

Figure 3-4 In the image on the left the base segment is the thick segment in the bottom emulsion plate. The position of that segment's projection to the next plate is used to find a matching segment that links with the first segment to form a track. The search area for a match to that base segment is defined by the cone shown between emulsion plates. The image on the right shows the process being continued to the following plate. What was the match segment is now a base segment in the next plate.

In the segment to segment linking function described above, as well as the track to segment functions described next, an attempt is made to form the higher momentum and straightest tracks first. This is accomplished by doing the tracking in 3 phases with successively looser matching requirements in each phase. The most well defined tracks are intentionally created first for two reasons: 1) The high quality tracks resulting from the first phase are used later as reference tracks for fine alignment, and 2) Connecting the best matching segments first minimizes mismatching segments. Since the tracking algorithms do not allow a particular segment to belong to multiple tracks, once a segment

has been connected to one track it can not be connected to a different track. Therefore the more poorly defined or low momentum tracks are not allowed to take segments away from the previously formed straight tracks.

Several criteria are used to select potential matching segments and to determine the best match. The criteria are described here and the numerical criteria are listed in table 3.1. A segment is said to *match* a base segment if the χ^2 of the match is less than the χ^2 criterion for that phase, where χ^2 is determined by the angular difference between the two segments and the position difference. The position difference, Δx, is the distance between the match segment's position and the base segment's projected position in the match segment's plate. (fig 3-4a). χ^2 is given by:

$$\chi^2 = \frac{(\Delta x)^2}{\sigma_x^2} + \frac{(\Delta \theta)^2}{\sigma_\theta^2}$$

where $\Delta\theta$ is the angular difference between the two segments, and σ_x and σ_θ are the uncertainties of the position and angular differences. σ_x depends on the parameters r and s, which represent the angular resolution of a segment and the degree of scattering respectively. σ_x is given by:

$$\sigma_x = s + r \times \Delta z$$

where Δz is the distance between the base segment plate and the matched segment plate. The uncertainties of the angular and position differences are increased in successive phases so that the straightest tracks are formed first.

Another criterion of the segment to segment tracking function relates to each segment's angle relative to the beam direction. Only segments less that the angle criterion listed in table 3.1 are considered in each phase. This last requirement arises from the fact

Table 3-1 Segment matching selection criteria.

Phase	Segment angle criterion (radians)	r (mrad)	s (μm)	σ_θ (mrad)	χ^2
1	0.06	3.5	0.5	6.0	1.0
2	0.20	3.5	1.0	7.0	1.3
3	0.50	3.5	3.5	9.0	1.6

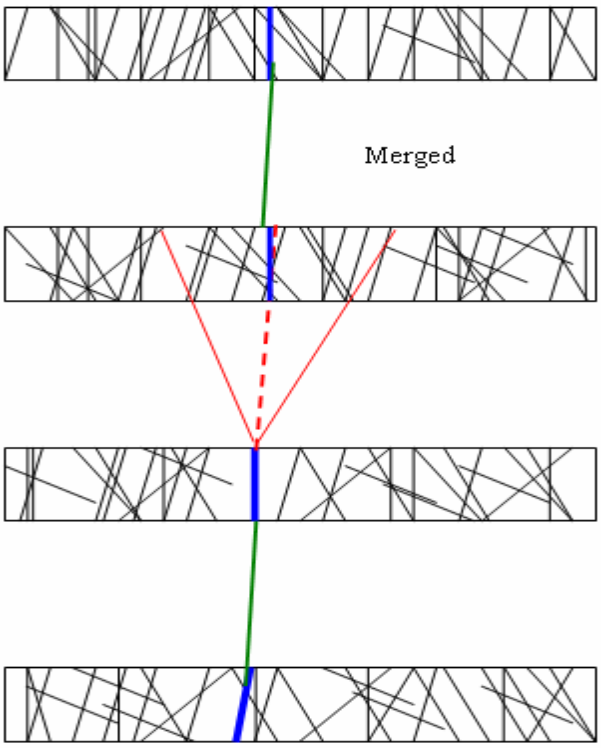

that most of the through going tracks are caused by muons, which have high momentum

and are traveling in the direction of the beam. By considering only segments with angles less than 0.06 radians relative to the beam direction in phase one we are assured that most of the tracks formed during that phase are high momentum straight through muon tracks.

Figure 3-5 In the above image, the projection of the track spanning the lower two plates matches an existing two segment track in the upper two plates. The two tracks will be merged to form one 4 segment track.

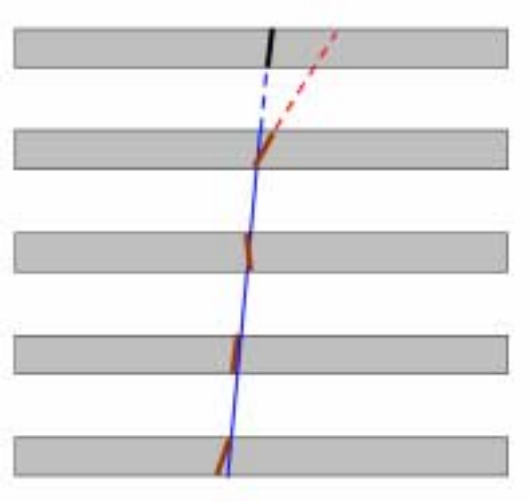

Figure 3-6 In the second tracking algorithm, the position of the extrapolated *track* is used to locate matching segments rather than the extrapolated base segment position.

After the segment to segment linking function is complete there exists a set of tracks ranging in length from 2 segments to the full depth of the scan volume (i.e. through all plates). The next tracking algorithm utilizes the projection of these tracks rather than single segment projections to locate matching segments. The tracks formed in step one are projected upstream in search of matching segments. If a matching single segment is found the base track is extended to include that segment. If the matching segment is the end segment of another track, the two tracks are merged. (fig 3-5) This procedure is continued for the resultant track until either two consecutive plates have not produced segment matches or the last plate is reached. Allowing tracks to have missing segments minimizes the effects of scanning inefficiencies due to distortion and other emulsion problems described in section 2.2.3. This track to segment linking function is performed on every multi-segment track that was formed in the first algorithm. The projection of tracks rather than single segments usually predicts the expected position of the next segment more precisely since it uses the data from all segments already belonging to the base track. (fig 3-6). Because of multiple scattering this is not the case, however, for low momentum tracks where the segment to segment linking function is better. (fig 3-7).

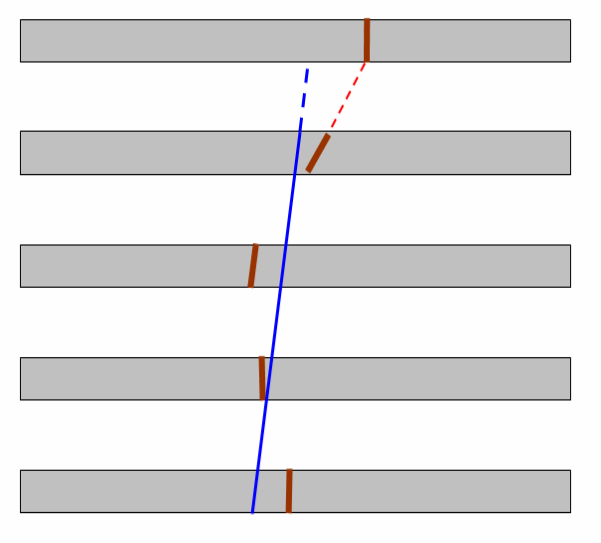

Figure 3-7 This graphic shows how the segment to segment linking function is better for low momentum tracks.

The third algorithm is almost identical to the second except that tracks are projected downstream rather than upstream. Occasionally emulsion distortion or multiple scattering is such that a track may link properly in one direction but not in the other. For this reason functions for linking both upstream and downstream are used. These three algorithms comprise the first phase of the emulsion tracking program. The emulsion data is cycled through these three algorithms two more times. Each subsequent cycle is performed with less restrictive selection criteria. This allows for the formation of lower momentum tracks while not compromising the integrity of the higher momentum tracks which were formed first. After each phase of tracking, a file, called an *m file*, containing all track and segment information is written out. Figures 3.8 and 3.9 show the progression of connecting segments and tracks through the 3 algorithms and 3 phases.

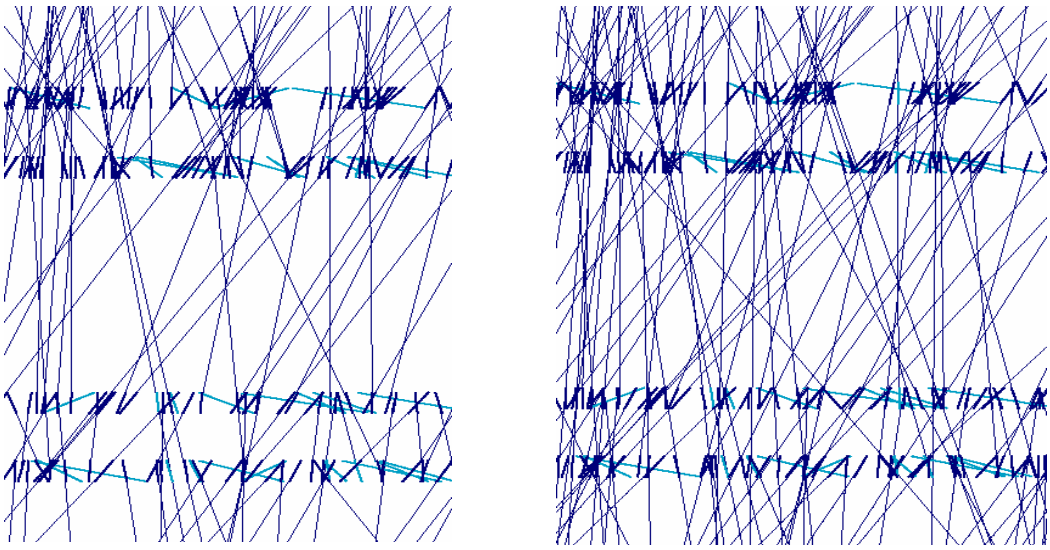

Figure 3.8 These images show the results of the tracking functions on the central 100μmx100μm x 2.5mm portion of emulsion displayed at the beginning of this section (fig 3-2). The images here and on the next page show tracks formed after each step of each of the three phases. The light blue lines are segments which have not yet been linked to tracks. The thick, short, dark blue lines are segments that have been linked to tracks. Multi-segment tracks are indicated by the thinner and longer dark blue lines. The left image above shows tracks formed in the segment to segment linking function of phase one. The right image above shows tracks formed after upstream track to segment linking in phase one. The left image below shows tracks after downstream track-segment linking of phase one. The right image below shows results of segment to segment linking of phase 2. Images of tracks formed during the remaining steps and phases are shown in figure 3-9. Note that the vertical distance shown is 25 times greater than the horizontal distance, so the segment and track angles are smaller than they appear.

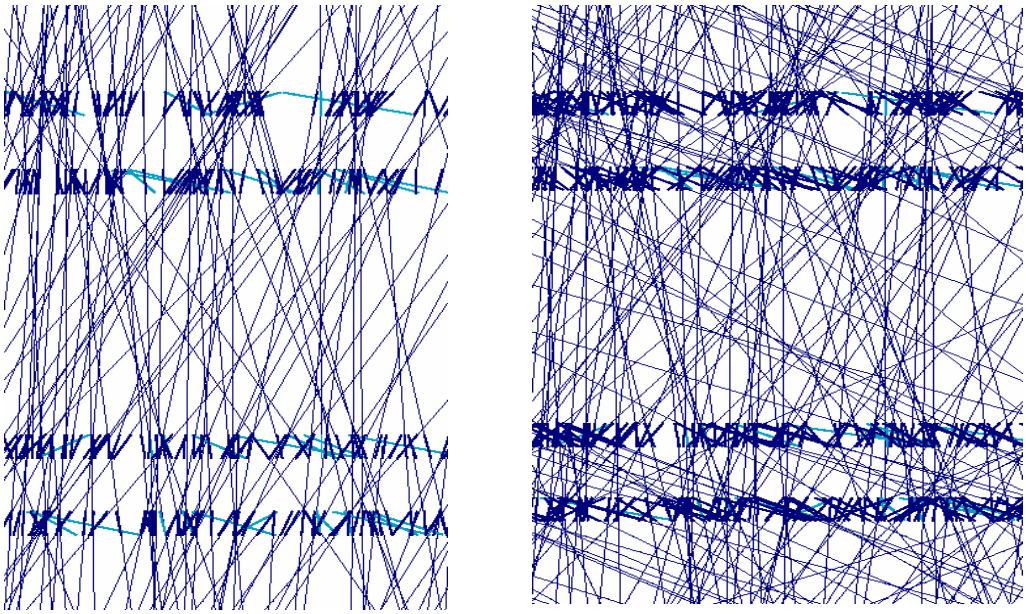

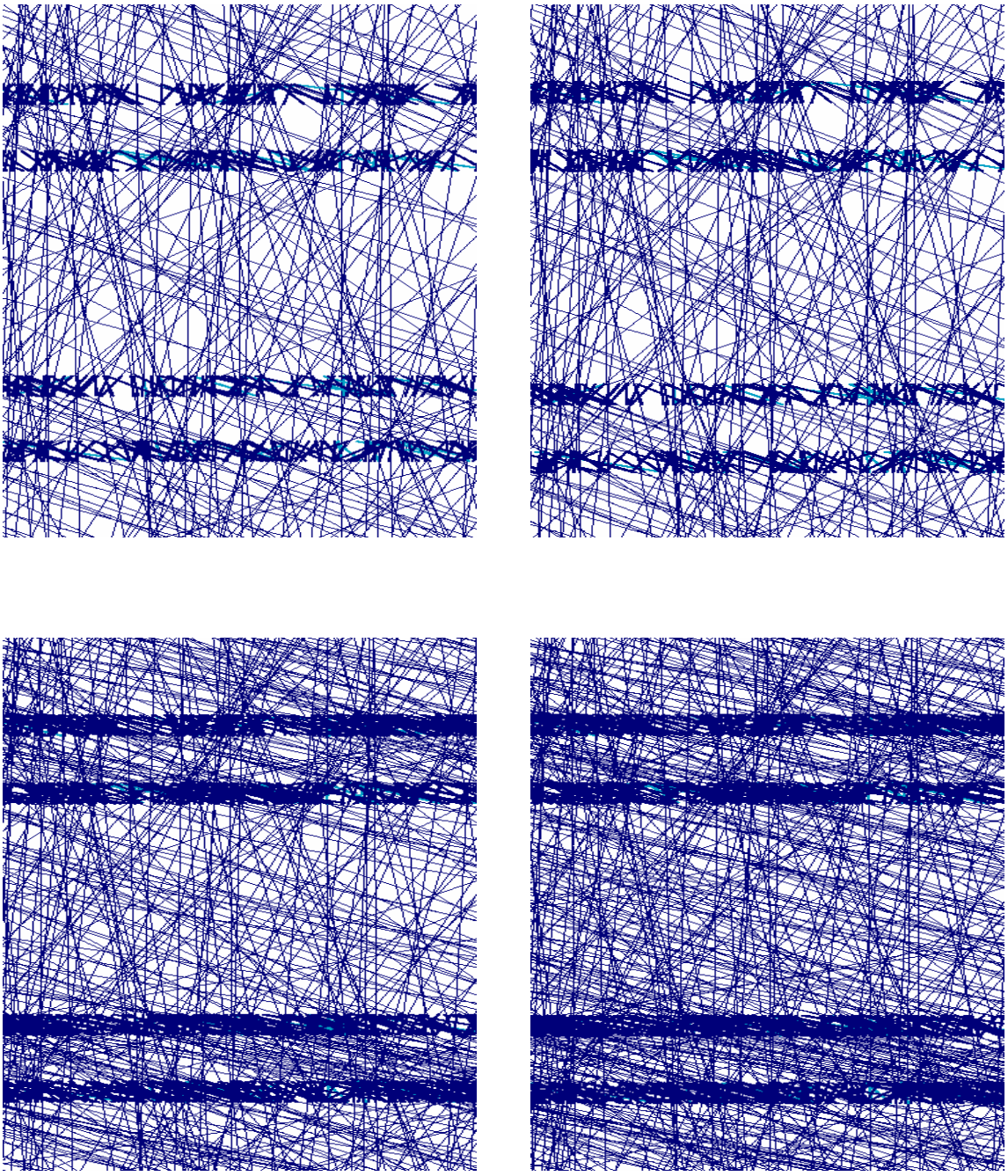

Figure 3.9 These images and those from figure 3-8 show the results of consecutive stages of the tracking process on a 100μmx100μmx2.5mm volume of emulsion. The above left image shows tracking results after phase 2 upstream track to segment linking. Above right shows tracks formed after phase 2 downstream track to segment linking. The bottom left image shows tracking results after phase 3 segment to segment linking, andthe bottom right shows tracks existing after phase 3 upstream track – segment linking has been done.

3.2.3 Fine Local Alignment

In order to determine the most accurate segment and track parameters it is necessary to perform a fine alignment procedure on the emulsion data. As discussed in section 2.3 both the plate preparation and development processes can lead to distortions in emulsion. Typically, when a sheet of emulsion becomes distorted, the segments in that sheet will point in a direction which is not the true direction of the penetrating particles. For example, say that a particle passes perpendicularly through an emulsion sheet. Later, when it is developed, some areas of the sheet may dry faster than others. The result is that the sheet shrinks in a non-uniform manner, shifting the grains from their true positions relative to each other. The direction of the segment formed by these grains will no longer be perpendicular to the surface but will be skewed. All other segments in the affected area will also be skewed in the same direction. For this reason, a fine alignment is applied locally to the emulsion data in order to remove this local distortion. (fig 3-10). It is found that regions of distortions on an emulsion plate are typically greater than 150μm x 150μm. It is therefore justified to apply the same correction to all segments within such a region. Local alignment is performed by determining the shift in position and in angle that segments of a given region are distorted and then applying a correction to all segments in that region. The alignment procedure is carried out on an entire scan volume by dividing each plate of the volume into 150μm x 150μm regions. The process is then applied to all regions of each plate.

The alignment procedure is done between phase one and phase two of the tracking procedures described in the last section. Since tracking criteria were held tight in the first stage tracks formed during that stage are by definition straight with minimal deviations of segments to tracks. These are likely high momentum tracks. Those tracks with four or more segments are chosen as the set of reference tracks for local alignment. By choosing high momentum tracks, the track to segment deviations due to multiple

scattering are minimized and the remaining deviations are due to the innate resolution of the emulsion and to distortion.

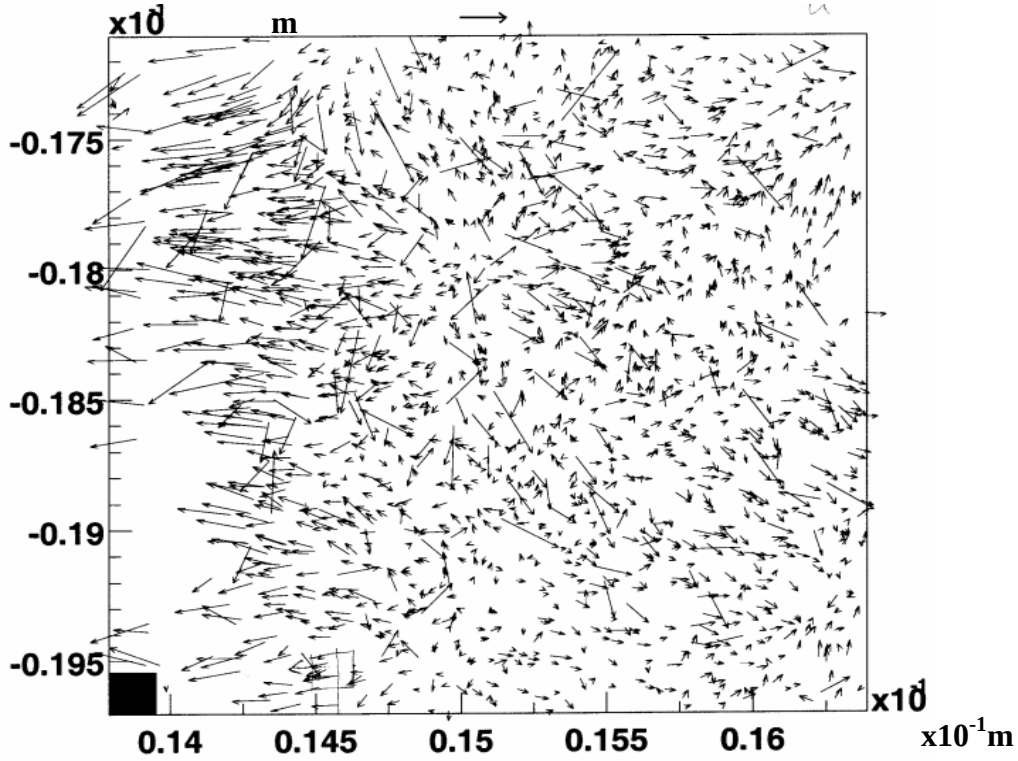
x10
m
-0.175
-0.18
-0.185
-0.19
-0.195
x10
0.14
0.145
0.15
0.155
0.16
x10-1m

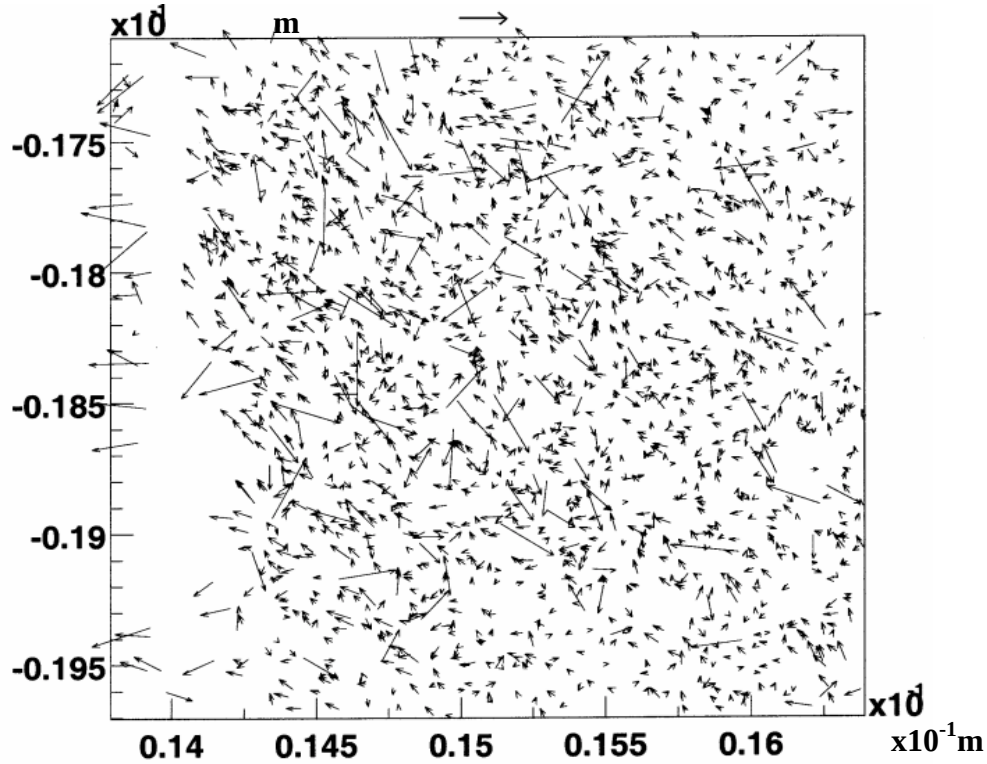
x10
m
-0.175
-0.18
-0.185
-0.19
-0.195
x10
0.14
0.145
0.15
0.155
0.16
x10-1m

Figure 3-10 Two images of the same 2.5mm x 2.5mm area in one emulsion plate. The upper image shows unaligned segments and the lower image shows aligned segments. The vectors represent angular deviations of segments from their parent tracks. The horizontal vector above each box gives the scale for a 20mrad deviation. Tracks are aligned in 150micron x 150micron regions which is the area represented by the small black box in the lower left of the top image.

Alignment corrections are calculated within a given region by finding the mean value of segment to track residuals for the reference set in that region. The position and angular residuals are taken to be the deviations due to distortion. These corrections are not applied immediately but rather stored until all areas of all plates in the scan volume have been considered. After that is done the appropriate corrections are applied to all segment in the scan volume. Figure 3-12 shows the effects of fine local alignment on a single track. As shown in figure 3-11 local alignment improves position resolution from 0.6μm to 0.4μm and angular resolution from 4.2mrad to 2.1 mrad.

It is an interesting fact that fine local alignment would not be possible without a high rate of background tracks. Before DONUT data was collected, a significant effort was made to lower the rate of background muons. This was in fact necessary because without any reduction the emulsion would have been immediately blackened and rendered useless. However, the sub-micron resolution of emulsion is retained with rates up to about $5x10^6$ tracks/cm^2. If the rate falls below about 10^4 tracks/cm^2 local alignment as described above can not be accomplished.

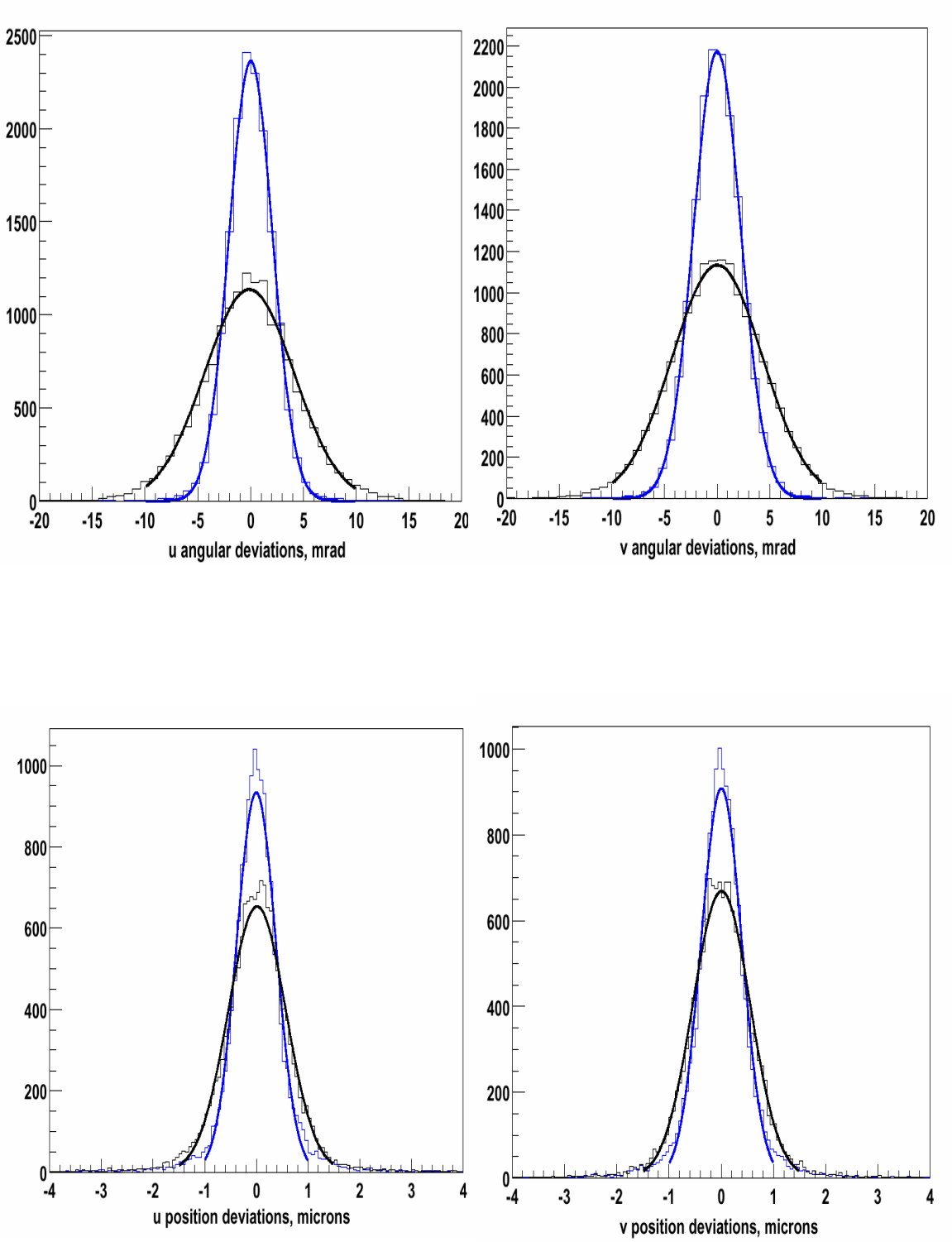

Figure 3-11 Deviations of individual segments from their parent tracks in position and angle. The outer histograms represent pre-alignment data and the inner histograms show data from the same event after fine alignment

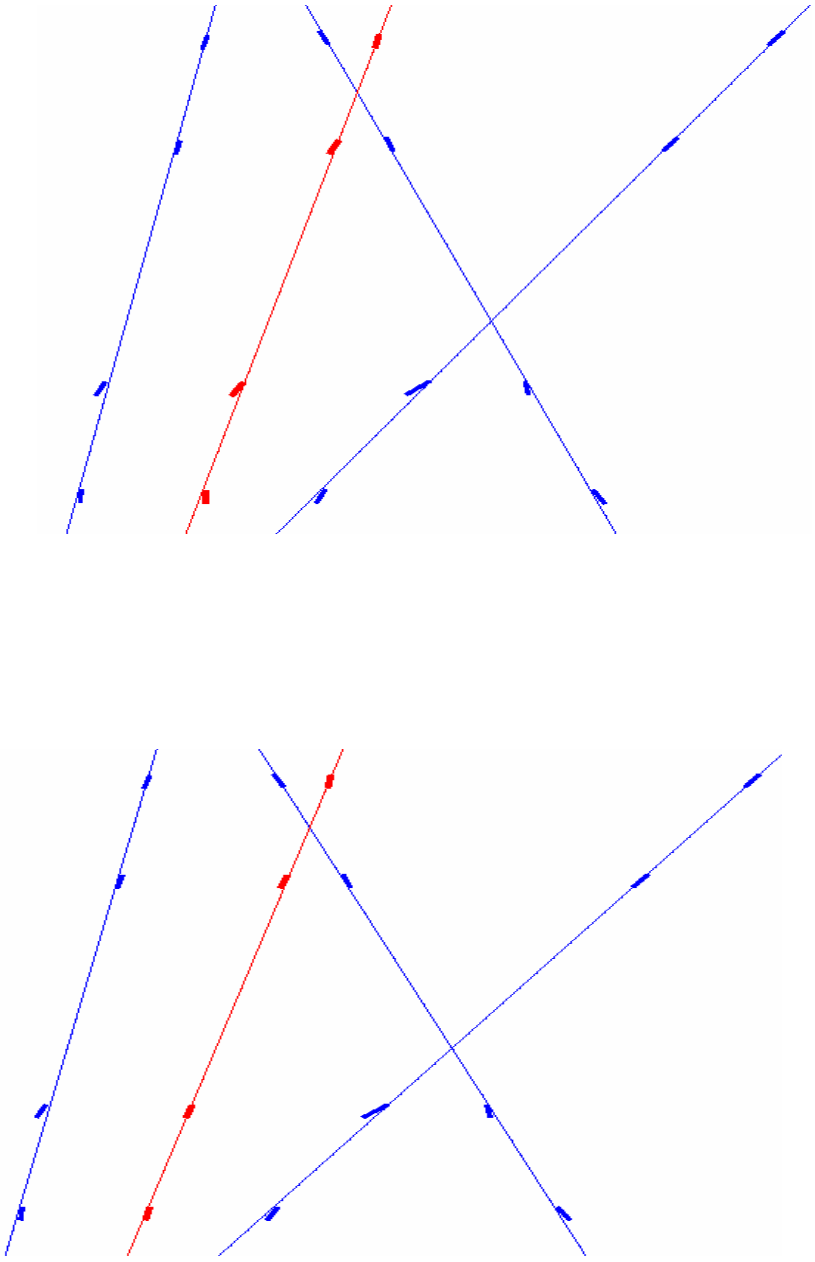

Figure 3-12 Shown here are emulsion data before (above) and after (below) fine local alignment. In these images only the track which is second from the left, is aligned. Notice how in the top image the segments of all four tracks are skewed in the same direction in the second plate from the bottom. The segments of the that track are seen to line up more closely with the parent track in the lower image. The fine alignment procedure is performed on all segments of all tracks during tracking.

3.2.4 Significance of Aligned Emulsion Tracks

When emulsion tracks are properly aligned there are useful physics results that can be obtained from the data. These include momentum measurements of tracks and electron identification. Momentum measurements are made in emulsion by considering a number of segment displacements due to multiple coulomb scattering. (fig 3-13). The amount of scattering is inversely proportional to momentum and is approximately given by

$$\theta_5 \cong \frac{K}{p\beta}|Z|\sqrt{\frac{t}{X_0}}$$

(5.1)

where K is the scattering constant, t is the thickness traversed, and X_0 is the radiation length of the material[21]. One can also measure the rms lateral displacement as[22]

$$< y^2 > \cong \frac{1}{6}\theta_s^2\ t^2$$

(5.2)

Substituting equation 5.1 into 5.2 gives

$$y_{rms} \propto \frac{t^{3/2}}{p\beta\sqrt{X_0}}$$

(5.3)

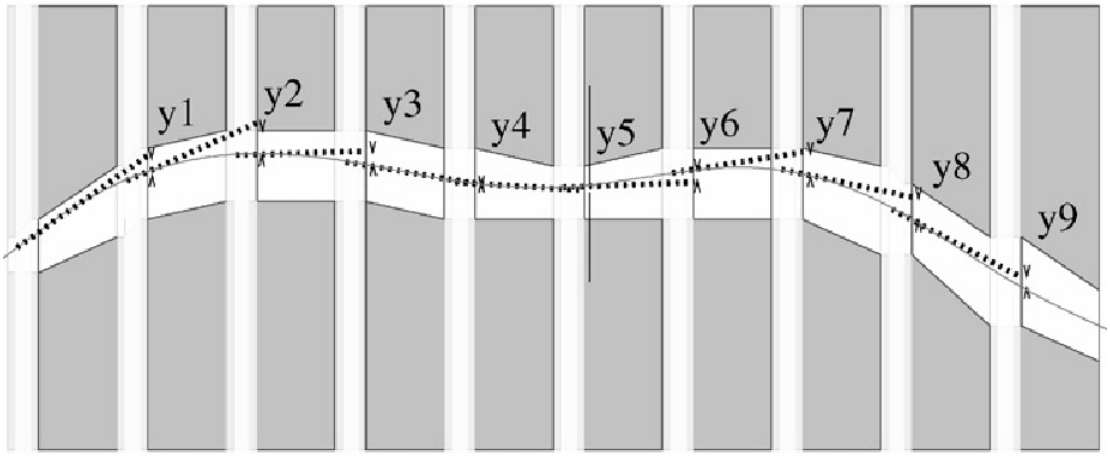

Figure 3-13 Measurements of lateral displacements from plate to plate, due to multiple scattering, are used to measure a particle's momentum.

The distribution is approximately Gaussian and y_{rms} can be measured with accuracy proportional to $\sqrt{2n}$ for n measurements. In the DONUT analysis each located event was rescanned and tracks were followed to the end of the module. The $t^{3/2}$ dependence of multiple scattering deviations allowed for ~30% accuracy in momentum measurements up to about 25GeV[23]. This momentum measurement method was checked using a 4GeV pion beam at KEK[24]. Particles with momentum < 20GeV were also compared to the momentum measurements provided for some particles by the spectrometer using the analysis magnet. Figure 3-14 shows that the results were consistent with the emulsion multiple scattering measurements.

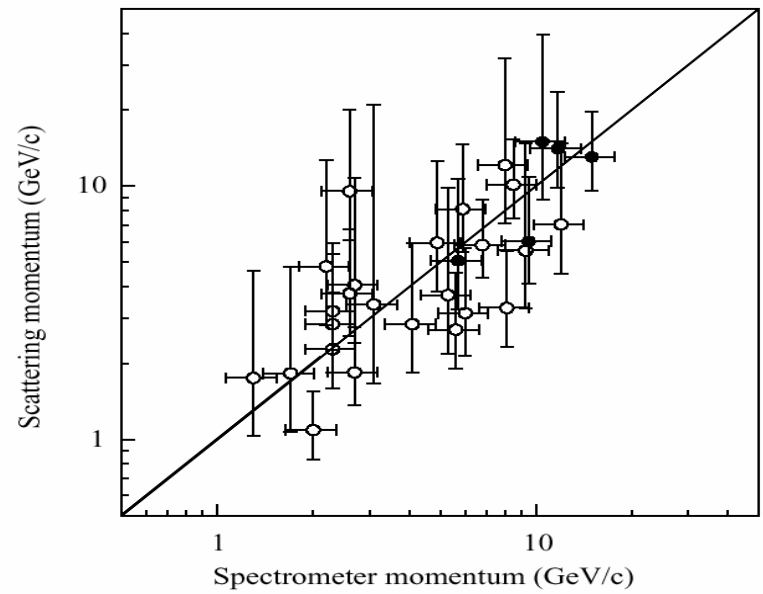

Figure 3-14 Comparison of momentum as measured by the spectrometer and measurements from multiple scattering in emulsion[23].

Emulsion data can also be used to identify electrons. Multiple scattering creates a different effect in electrons versus hadrons because of their typical values of momentum. This results in different values of χ^2 for electron and hadron tracks. By utilizing this difference in χ^2 a track can be characterized as electron-like or hadron-like. This information is used in conjunction with a check for electron positron pairs near the track to determine a particles identity. If pair production is indicated in the surrounding emulsion and χ^2 of a track indicates an electron, that particle is identified as an electron[25]. Pair production is identified simply by the density of isolated tracks which originate within a cone surrounding the track of interest. The efficiency of electron identification is a function of radiation lengths traversed and is estimated to be ~85% for a track which can be followed in the emulsion for[22] $\geq 2X_0$ (fig 3-15).

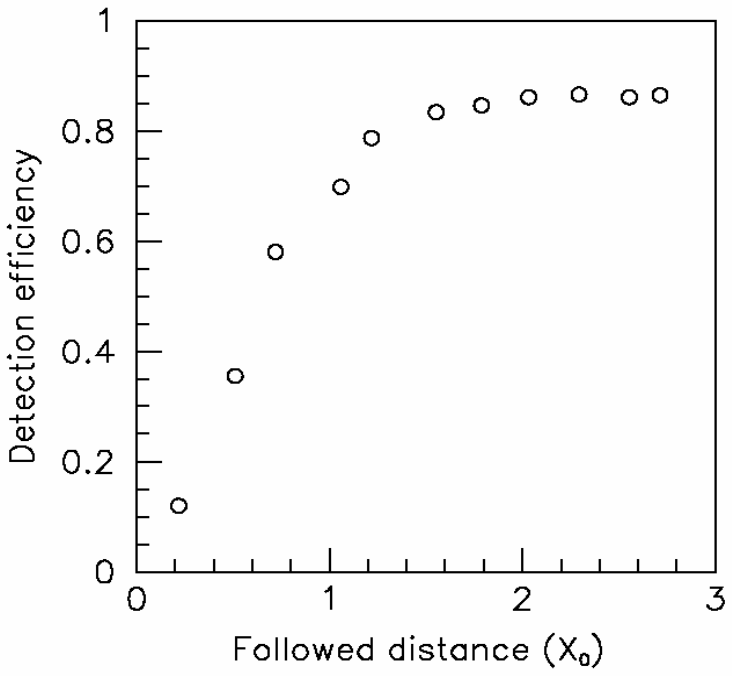

3.2.5

Figure 3-15 Estimated electron identification efficiency using emulsion data. [23].

Plate Slipping

One problem identified in DONUT emulsion data was that some emulsion plates shifted vertically within the modules during exposure (fig. 3-16). In these cases the vacuum applied to a module was insufficient to keep some plates from slipping. Plate slipping occurred randomly over time which resulted in multiple time dependent alignment configurations within a single module. Tracks that actually penetrated all plates within a module may or may not appear to have done so. Figure 3-17 depicts the slipping process over time. This situation can be remediated by using the high density of background muon tracks to determine the various plate configurations. Similar to the first tracking procedure described in chapter 4, plates are shifted relative to each other in

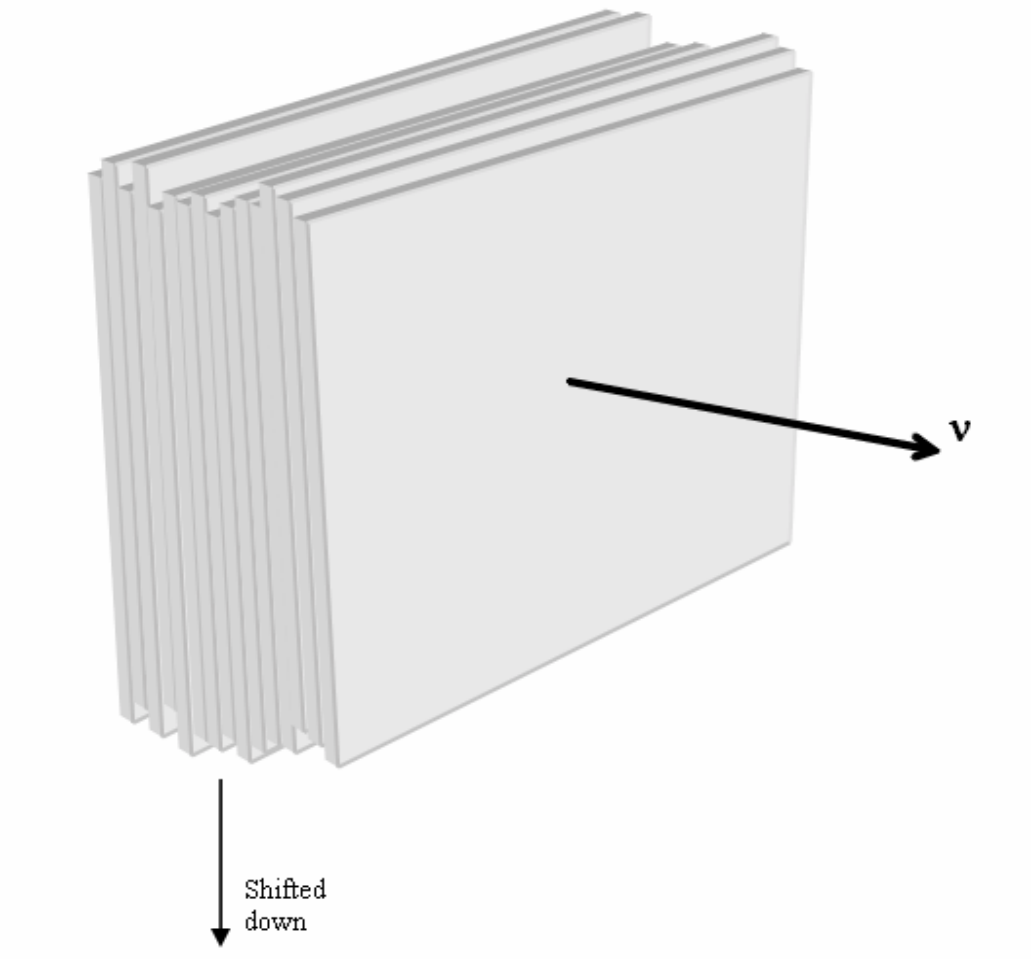

Figure 3-16 Some plates shifted vertically during exposure. Some were isolated plates and some moved together, typically less than 50 microns.

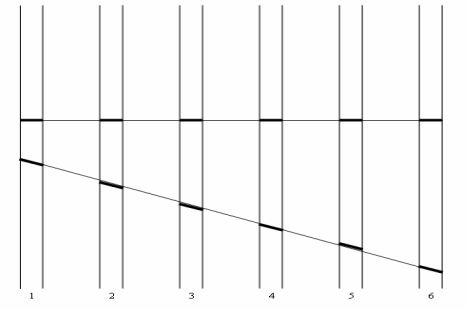

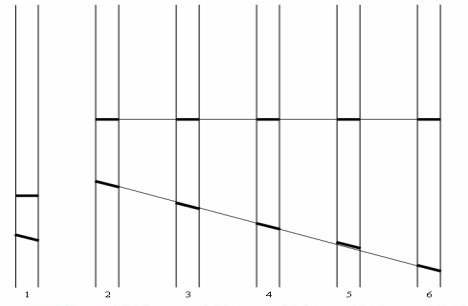

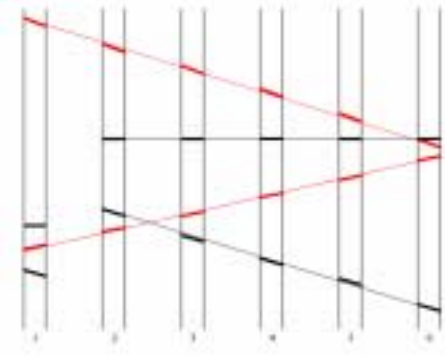

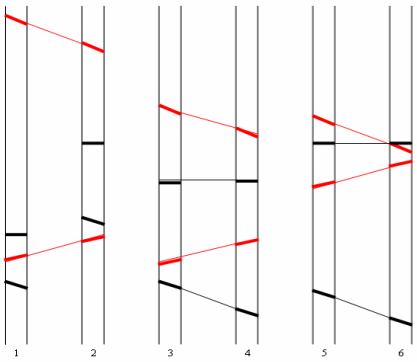

software until there is a significant increase in the number of penetrating tracks. The relative plate positions are recorded and then plates are shifted again until another such increase is found. This procedure is repeated until all plate configurations that produce a significant increase in the number of penetrating tracks have been found. Tracks identified as belonging to a particular configuration are excluded from all other configurations. The multiple resultant m_files of the same scan volume correspond to different time periods. Although this process is in principle not difficult, it was only performed manually on a few events using the 3D emulsion display as a guide. Automation of this process remains to be done which may help to recover some unlocated events.

Figure 3-17 These five schematics depict the results of plate slipping over time. Here three occurrences of slipped plates are represented. The various tracks were formed between successive slips. The order of events is 1) Two tracks are formed in the upper left image. 2) Plate one slips, and after that the more tracks are added. 3) Plates 3 and 4 slip together as shown in the lower left. 4) After that the final tracks are added as shown in the lower right.

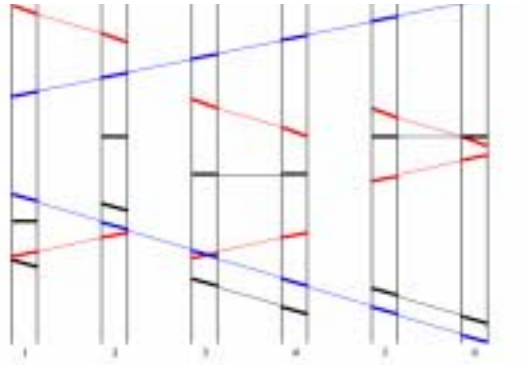

4 Event Location

In order to identify a particular interaction as a tau neutrino interaction, it is necessary to locate the neutrino interaction in the first place. In fact, locating an interaction in the emulsion can be more difficult than identifying the event as a tau neutrino interaction. Once the interaction vertex and tracks have been identified it is fairly simple to check the tracks for the signature tau kink.

In the initial stages of the development of event location strategies, simulated data were used. However, simulations do not include all of the defects of a real emulsion stack. Real data provided a better understanding of the emulsion and the procedures required for successful event location. A bootstrap technique was used. Initially some events were located by simple methods and it was possible to refine these methods with real data. A 3D emulsion display proved to be extremely helpful because it allowed humans to use their pattern recognition capabilities to determine when a software procedure was ineffective and to suggest new strategies.

The methodology for event location is the subject of this chapter. The methodology will be described first, followed by data from a sample study of 30 events. The results of the study will then be used to calculate the location efficiency.

4.1 Methods of event location

There are basically four different methods used for locating neutrino events in the emulsion. Each method is essentially a filter applied to the data. In all cases the purpose is to locate a small set of candidate events from which the true neutrino interaction vertex can be successfully chosen. Since the events present themselves in the emulsion as vertices the terms *vertex* and *event* will be used interchangeably in this chapter. The first two location methods described utilize the projection of spectrometer tracks to locate *specific* emulsion tracks from the interaction. Those spectrometer tracks originating from the interaction should necessarily have a corresponding emulsion track. Focusing on

those tracks is the philosophy of the first two methods. The third method does not utilize spectrometer tracks and is useful when there are large numbers of spectrometer tracks that are caused by showering or secondary interactions. This is a general method that utilizes all of the emulsion tracks. The last method uses single segment emulsion tracks and is particularly useful when the emulsion is distorted or there are other emulsion problems such as plate slipping.

The order in which the methods are applied to the data is: 1) the general method using all emulsion tracks. 2) The spectrometer track projection methods. 3) The single segment methods. This order is chosen because, although the general method requires more computer processing time, it requires less human interaction time. It is basically the easiest to use. The single segment method is used last because it is the most labor intensive both for humans and computers. In the next sections the spectrometer track matching method will be described first. While in practice it is not the first method used it is presented first because it contains the complete set of techniques used for the other methods. The description of the matching method provides a convenient reference for the procedures which also apply to the other methods.

4.1.1 Using 3D Spectrometer Tracks to Locate Interaction Vertex

The goal of this method is to use one or more three dimensional spectrometer tracks to assist in identifying at least one of the emulsion tracks formed in a particular neutrino interaction. By using the position and angular information of a spectrometer track projected backwards into the emulsion, a detailed search can be made to locate the matching emulsion track. Once one or more emulsion tracks from the interaction have been identified it is a fairly simple matter to search for other emulsion tracks which form a vertex with that track. The idea here is to reduce the number of possible background vertices in the emulsion by using the constraints provided by the spectrometer tracks.

4.1.1.1 Identifying three dimensional spectrometer tracks

Much of the spectrometer tracking has already been described in chapter 2, however the track requirements for event location are very specific. The spectrometer

tracking routines and event display are used here to interactively select one or more spectrometer tracks to assist in event location. The goal of this step is to identify the three dimensional tracks most likely to have come from the original neutrino interaction in order to maximize the probability of finding a matching emulsion track. Track selection is done using the criteria described below to determine the best tracks for this purpose.

Formation of a three dimensional track is accomplished by identifying associated pairs of two dimensional lines from orthogonal projections. The two associated lines are projections of the trajectory of a single particle. Forming such a 3D track is frequently a complex task because 1) one or both of the two dimensional lines may not be clearly defined due to other nearby fiber hits, and 2) Even if each 2D line is well defined the association of the pair may be ambiguous. If a 3D track has isolated projections in both the U and V views of the spectrometer *and* the 2D projections can be unambiguously paired the task is finished. More typically there are either no isolated tracks, or if there are isolated tracks downstream of the analysis magnet it is difficult to determine which scintillating fiber hits are associated with those tracks. Figures 4-1 and 4-2 show how the showering and secondary interactions can obscure the path of a muon through the scintillating fibers. Here the muon track would be more easily identified if an accurate vertex position were known. Therefore finding the desired 3D tracks involves an iterative process between estimating the vertex position and picking out which scintillating fiber hits form plausible tracks. The refined estimated vertex position will be used later to evaluate the event candidates.

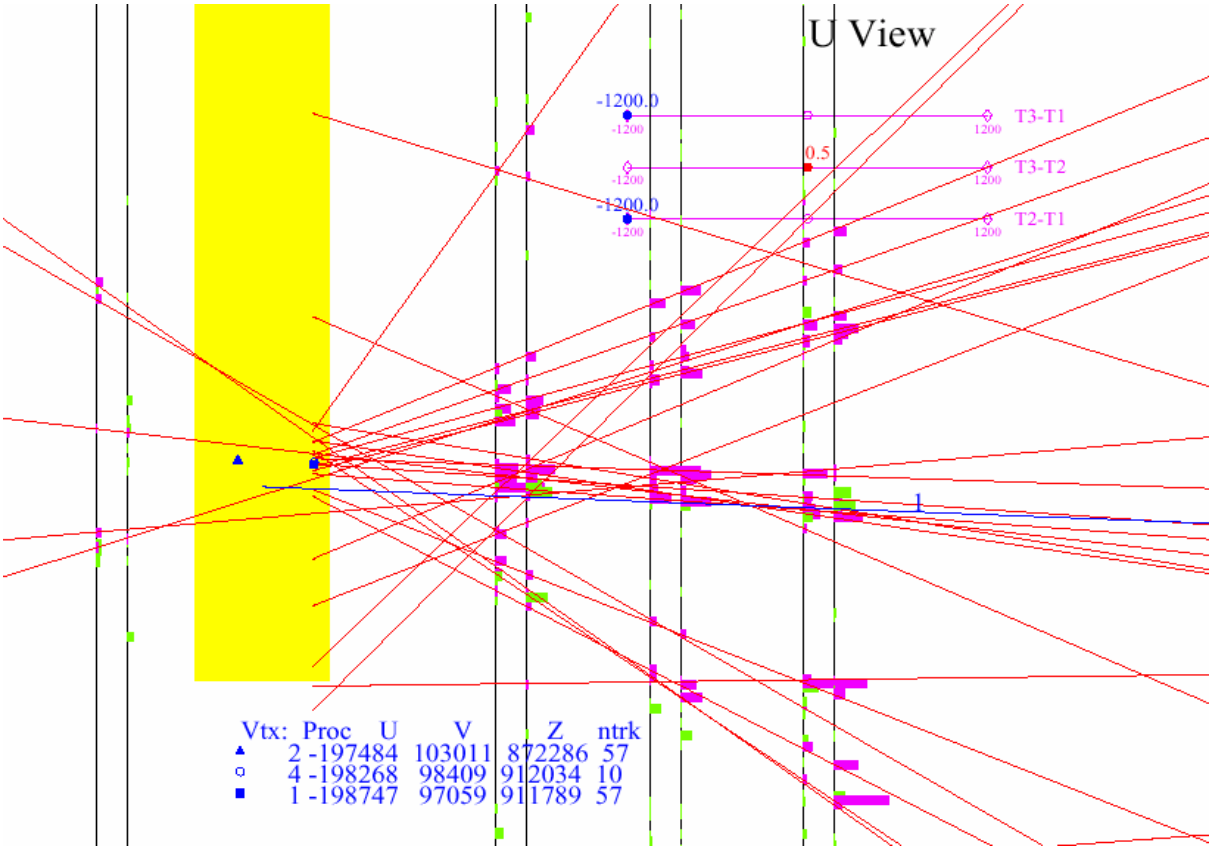

Figure 4-1 The vertical lines in this image depict the scintillating fiber planes with fibers oriented in the U direction. Neutrinos enter from the left along the Z (beam) direction. The rectangle on the left represents an emulsion module. Scintillating fiber hits are shown as small horizontal bars when no 3D tracks or 2D lines are associated. The longer horizontal bars are scintillating fiber hits associated with the pink 2D lines in the U-Z plane. The small spots inside the emulsion module are the positions where the automatic vertexing algorithms placed vertices (section 3.1.2). This image shows the result of automatic tracking and vertexing before manual adjustments. Track #1 (starting near dots) is identified as a muon in the muon ID. Here we see that when the muon is projected to the scintillating fiber tracker it is unclear which SFT hits are associated with the muon track. The V-Z plane is displayed in the next image.

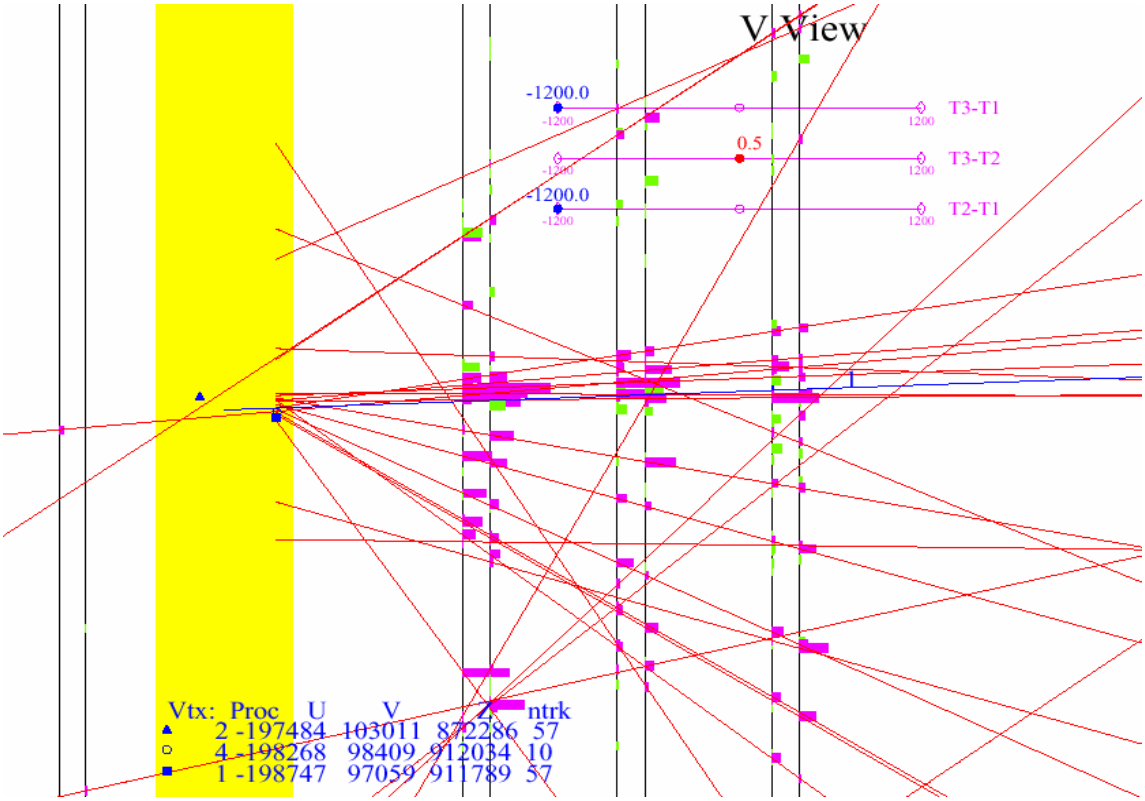

Figure 4-2 V-Z plane of the scintillating fiber tracker for the same event shown in figure 4-1. The projected muon track is indicated by the central line starting near the spots in the emulsion module.

The computer-aided human process of identifying 3D tracks is as follows. First, the plan view is displayed to get a general picture of the event. (fig 4.3). The drift chambers downstream of the analysis magnet are examined. These chambers typically have many fewer tracks than the scintillation fiber tracker because they are shielded from low momentum particles by the magnetic field of the analysis magnet. Any muon or other high momentum tracks in these drift chambers are identified. If such tracks are found, the scintillating fiber tracker is checked to see if there are any clear matches in both the U and V views. If these matches are found, a 3-D track is formed. If such a clear 3-D track cannot be found, the fiber tracker is searched for hits which together form plausible 2D lines that could be associated with the high momentum track. At this point the goal is not only to find 2D lines and 3D tracks, but also to make an improved estimate of the vertex position. A good estimate of the vertex position will aid in determining which hits in the spectrometer are most likely caused by the emulsion tracks from a vertex.

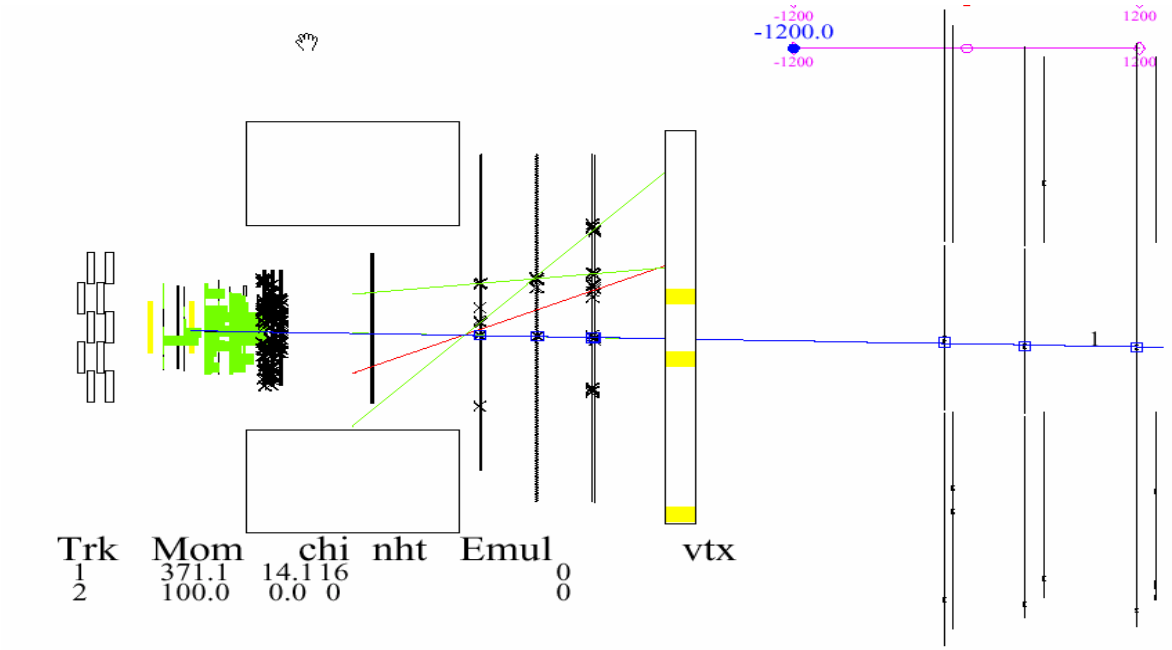

Figure 4-3 The spectrometer event display indicates a muon, track number 1, in this plan view of the detector.

Several factors should be considered in determining which SFT hits form the most reliable lines, and which 2D lines should be paired to form 3D tracks. These include:

1) Lines which traverse more than one emulsion module should be chosen because they are from higher momentum particles.

2) Lines which have a better χ^2 than others and lines which contain isolated hits are less ambiguous and are therefore good choices. If there are isolated hits along a candidate line interspersed between planes of scintillating fibers which have multiple surrounding hits, it is helpful to ignore the planes with multiple hits and only use planes with isolated hits

3) If a highly ionizing track, denoted by large pulse heights from the SFT, is evident in both views it is reasonable to assume that those two lines pair to form a 3D track. While such a track can be helpful one must be cautious since a highly ionizing track may have a low momentum and thus experience significant multiple scattering. It can be used as a guide but it may not point accurately to the vertex.

4) A line which exits the scintillating fiber tracker at a particular Z value may be matched to a line in the orthogonal view which simply stops at the same Z value. (fig 4.7).

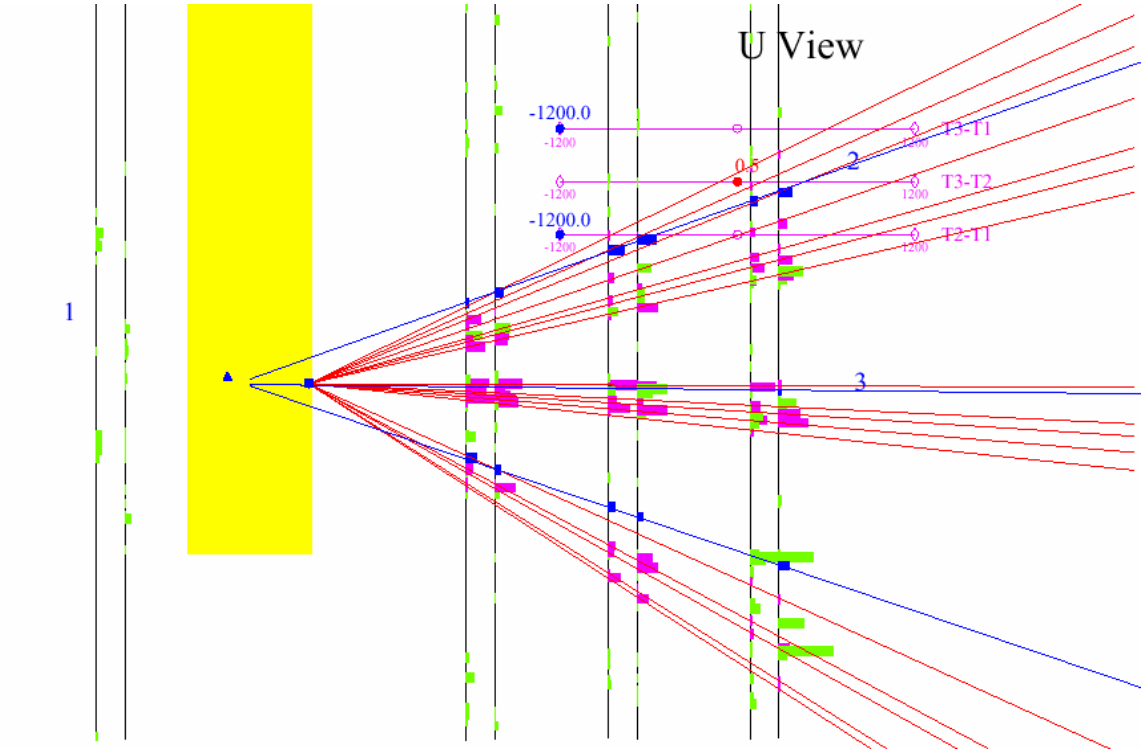

Figure 4-4 Here is the same event displayed in figures 4.1 and 4.2 after fitting. There is a secondary vertex at the downstream edge of the emulsion module. Now the muon track is more easily identified. It is the lower track which forms the primary vertex with the other blue tracks.

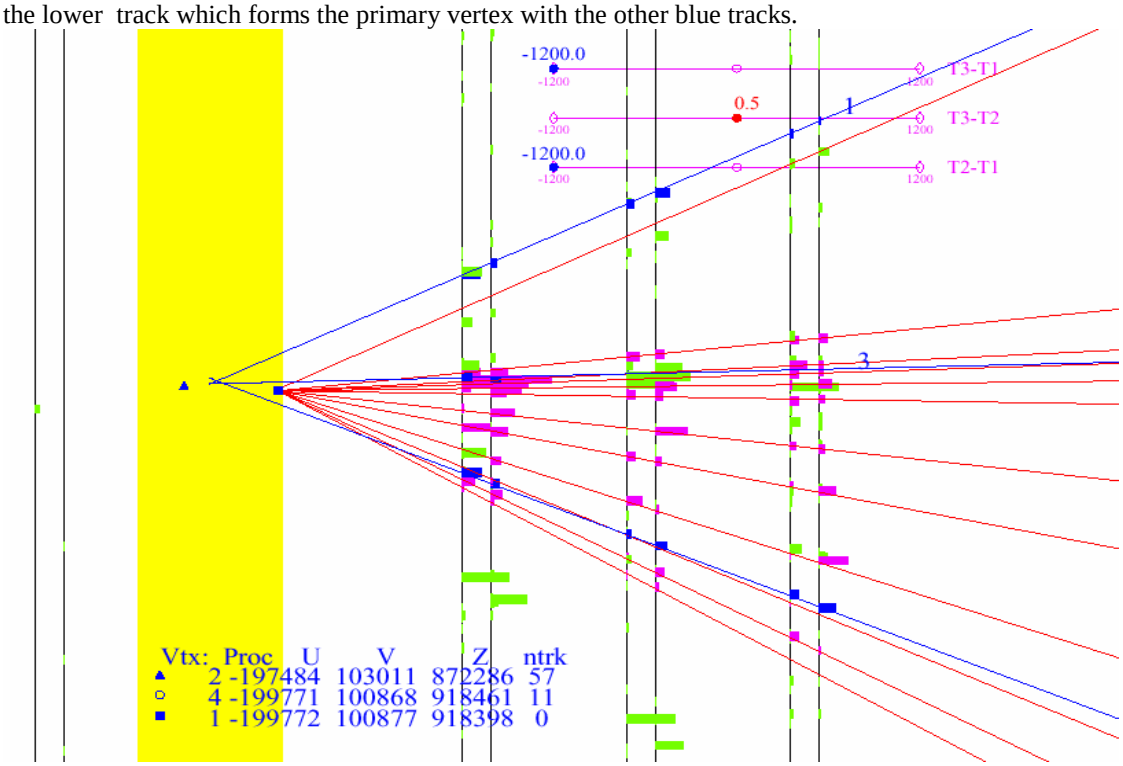

Figure 4-5 V view after fitting.

In choosing the vertex position, one determines which point has the greatest number of lines emanating from it. This point could be either a primary or a secondary vertex. It is probably a secondary vertex if there are any other lines that originate upstream of this point. (figs 4-4,4-5). The technique then is to identify two or more lines which originate upstream of that secondary interaction or shower. If one view is much clearer than the other, the clear view is done first. If the vertex position is apparent in one view the Z position is determined from that view. Then, in the orthogonal view, only one plausible line is necessary because the vertex should be on that line at the Z position determined in the previous view. (fig 4-6). If there is conflicting information or not enough information to place the vertex in one view, a vertex choice is made anyway and the orthogonal view is examined. Once the vertex position has been decided the process can be repeated. With a better vertex prediction other lines may become clear. Better defined tracks help clarify the vertex position.

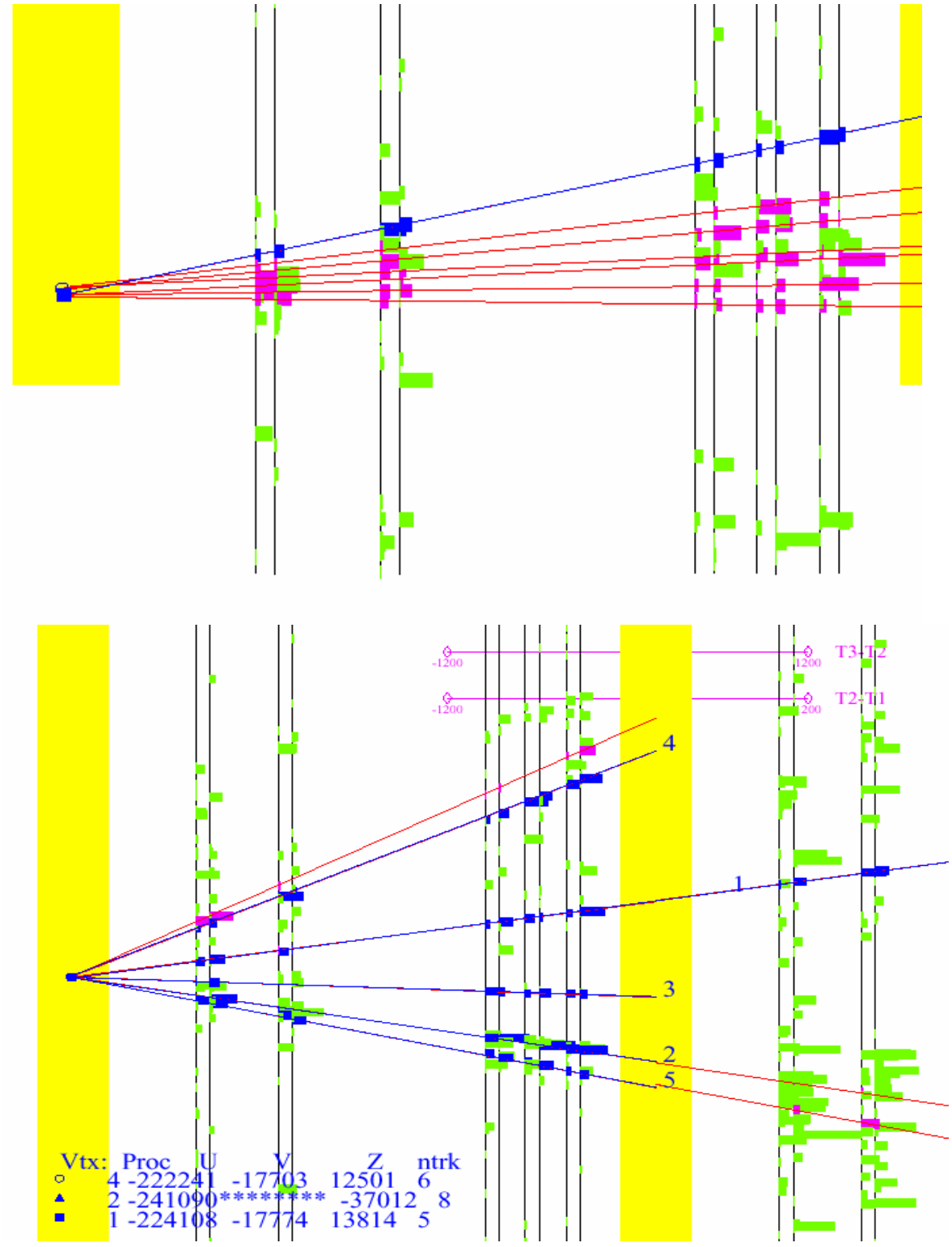

Figure 4-6 In this event the vertex is easily determined in the V view (bottom). In the U view above the vertex is placed on the track at the Z position determined from the V view. This image also shows how isolated hits are used, and on track number 3 some clusters of hits are ignored in planes 3 and 4.

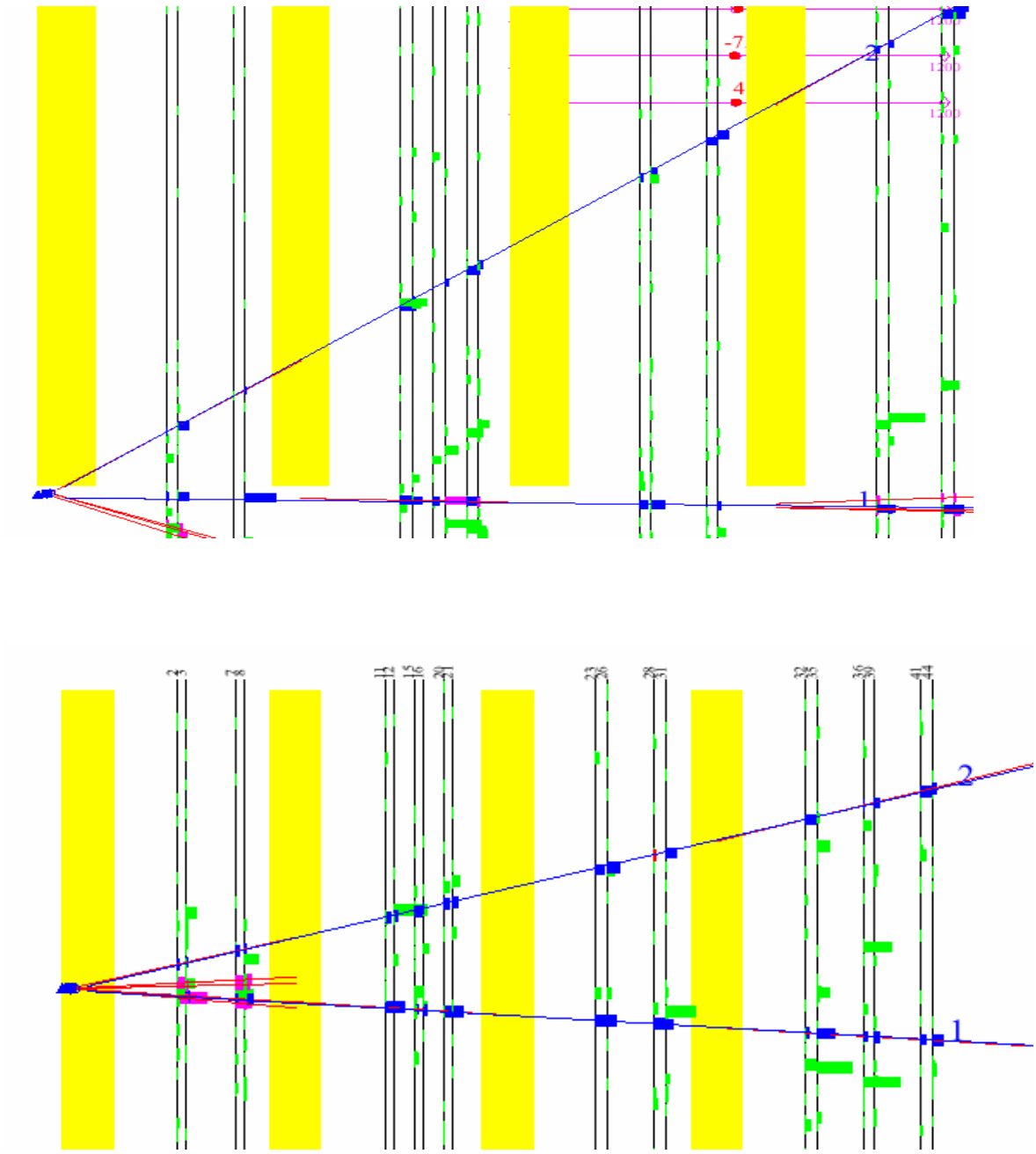

Figure 4-7 Combining 2D tracks: The above graphics show scintillating fiber hits in the U-Z and V-Z planes from the same event. This is a simple event, and while it is clear that there are two tracks which extend beyond the second emulsion module (second rectangle), it is not obvious which line from the U view is associated with which line from the V view. The next figure shows that the ambiguity is resolved using the X view of the scintillating fibers and the vector drift chambers. Also notice the lines on the left which exit the bottom of the detector in the V view (top). The associated lines in the orthogonal view stop at the Z position where those in the top view exit

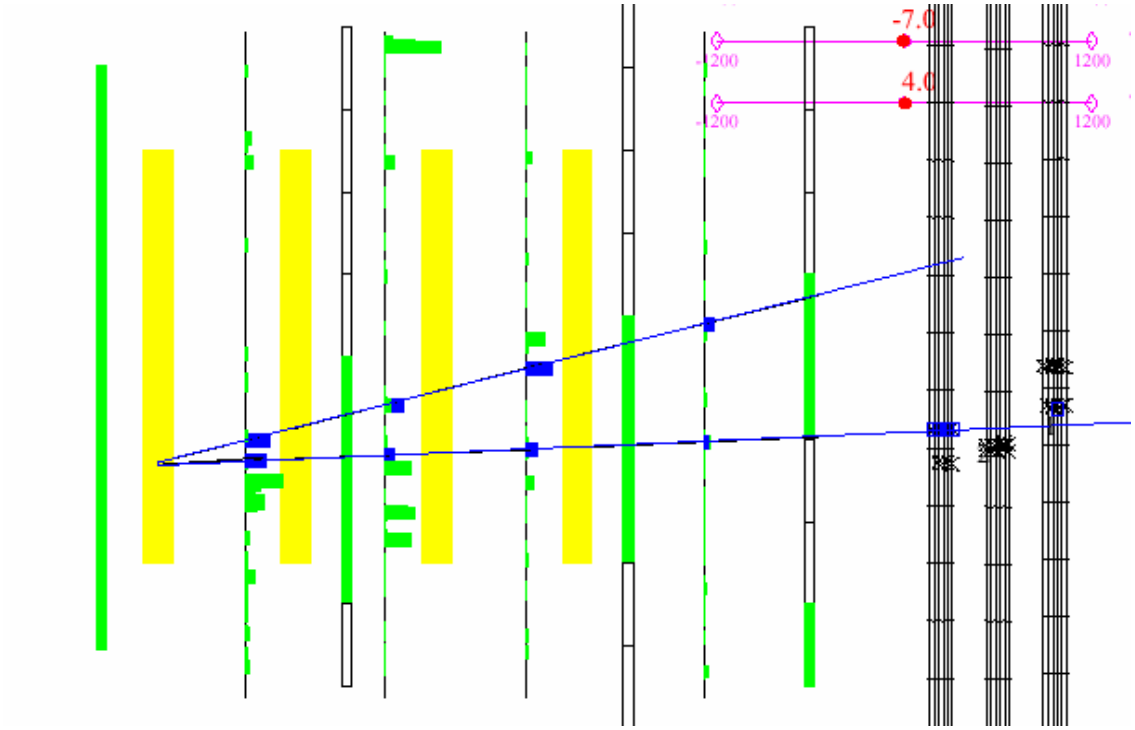

Figure 4-8 This X-Z view of part of the spectrometer confirms that the 2D lines in figure 4-7 were paired correctly to form these 3D tracks. The longer rectangles are the emulsion modules, thin white rectangles are trigger counters, and interspersed vertical lines are x-plane scintillating fibers. The three groups of vertical lines on the far right are the vector drift chamber.

4.1.1.2 Locate One or More Emulsion Tracks From An Interaction

Having selected the spectrometer track(s) the next step is to locate the particular emulsion track(s) which match them. That is, locate the emulsion track left by the same particle which produced the given spectrometer track. This is done by looping over all emulsion tracks and filtering them until only a few (~10) remain as candidates for matching the chosen spectrometer track.

Because of the large muon background there exist approximately 100,000 tracks in a 5mm by 5mm scan area, most of which penetrate all plates of the scan volume. We are not interested in these through-going tracks. We are only interested in tracks which originate at an interaction vertex which is presumed to be inside the scan volume.

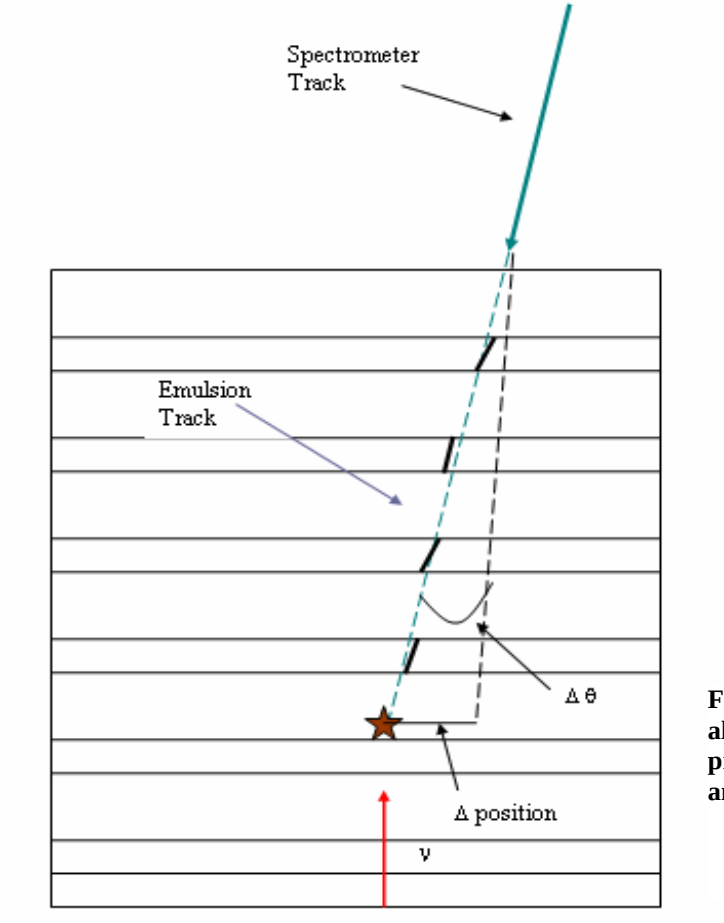

Figure 4-9 Deviations allowed between the projected spectrometer track and an emulsion *match* track.

Therefore, the first filter applied to the emulsion tracks is the requirement that they originate within the scan volume. Call this set the *starting tracks*. Next, the set is further reduced by comparing the angles and positions of each starting track to the spectrometer track we have chosen. If the u or v angle of a starting emulsion track deviates by more than 15mrad from the spectrometer track that track is dropped. (fig 4.9). Similarly, if the projected spectrometer track is more than 1.0mm from the u-v position of the emulsion track at its starting z position that emulsion track is cut from the list of *matched* tracks. The tracks in the match list are further required to consist of two or more segments. Typically three segments are required, but when no vertex is found this constraint is relaxed to allow two segment tracks. Finally, it is required that the standard deviation of segment angles from their parent track be less than 8.5 mrad. This filters out low momentum tracks which would be unlikely to correspond to the chosen spectrometer tracks. Depending on the event all of these criteria are varied as necessary. For example, if there is significant distortion in the emulsion surrounding an event the allowed deviations can be increased for that event.

4.1.1.3 FORM TWO TRACK VERTICIES

The search for interaction vertices is begun by comparing each track from the matched set to each track in the starting track set. First two track vertices are formed and later other tracks are added to these vertices to make up a candidate event. Before beginning the vertex search some single segments are added to the list of starting tracks. Occasionally a short lived particle or the remnant of nuclear breakup will be evident in the form of single segments. These short tracks can be helpful in the event search, especially when the neutrino interaction has low multiplicity. For this reason all single segments which are near the upstream end of each matched track are added to the list of starting tracks. The size of the area included for the single segment search depends on the distance between emulsion plates and is given by Tan^{-1} 0.45 rad = dl / dz . (fig 4.10).

Two track vertices are formed when one of the matched tracks forms a vertex with another starting track satisfying the following criteria:

1) The distance of closest approach is less than (2.5 + r dz) μm, where dz is the distance between the point of closest approach and the starting z position of the matched track. r has the value 1.5μm, but when no vertex is found it can be increased up to 3.5μm

2) The Z position of the vertex is between the most upstream track segment and the preceding emulsion plate. (fig 4-10).

3) The two tracks start within two plates of each other.

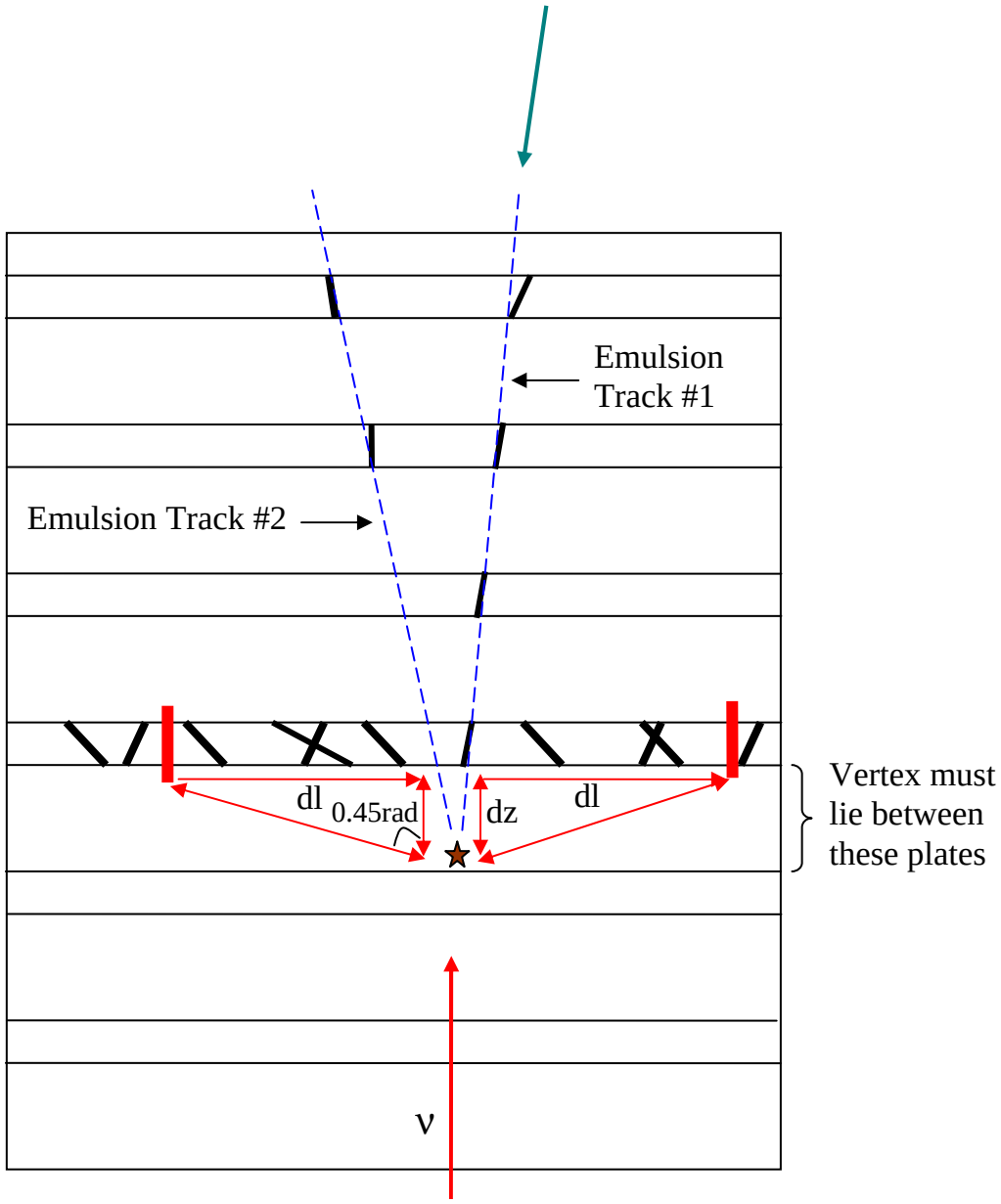

Figure 4-10 Formation of a two track vertex. Track #1 is the emulsion track which matches the spectrometer track. Notice that track #2 has segments missing in the first two plates. Two missed plates are allowed to account for scanning inefficiency. Single segments are considered within the area defined by dl.

After two track vertices have been formed between the matched tracks and the set of starting tracks, a similar procedure is done with the matched tracks and the set of *ending tracks*. Ending tracks are those emulsion tracks which end inside the scan volume rather than exiting the sides or the downstream end. Some neutrino interactions have

backward going tracks so it is useful to include them in the search. Of course this may result in the location of a secondary vertex, but locating a secondary vertex aids in locating the primary vertex.

4.1.1.4 FORM MULTI-TRACK VERTICIES

Having located a set of two track vertices, the next step is to find additional tracks which originate at these vertices. Again, only starting and ending tracks are considered. Before the track search is made, however, another process is applied to the set of all starting tracks. During tracking the parameters of each track were obtained by a least squares fit to all of its segments. In the case of a low momentum track, or any track which scatters, the overall fit to the track will be misleading. Since the purpose here is to locate the interaction vertex we are most interested in the parameters of the beginning of the track, i.e. the parameters of the track as it leaves the vertex. For this reason each starting track is refit to its first three segments. After track refitting a loop is made over all starting and ending tracks searching for additional tracks which have an impact parameter of less than 10 microns to the vertex. The tracks are required to start within two plates of the vertex. Many of the tracks added here will be filtered out in later processes but the aim now is to use a rather loose filter so that the true interaction tracks are not missed in the formation of the vertex.

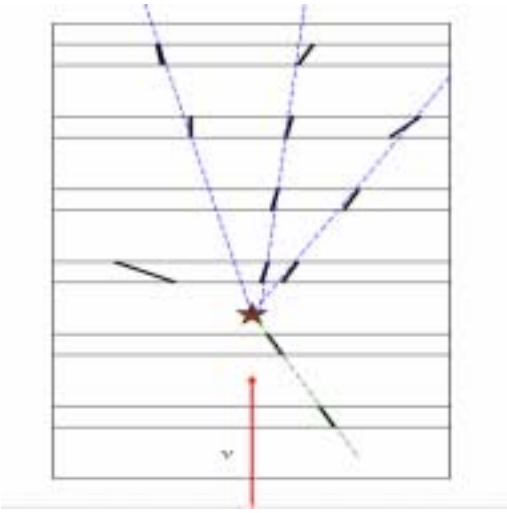

Figure 4-11 Above, vertex tracks include single segment tracks and backward going tracks. Below, vertex tracks are fit to the first 3 segments.

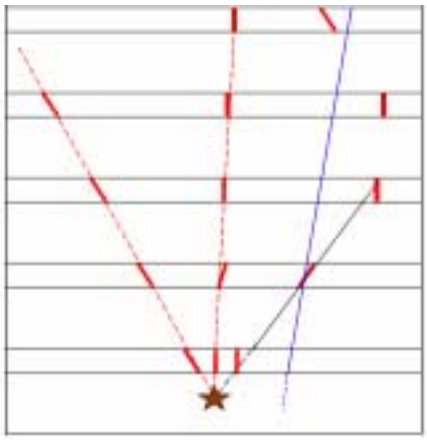

From the set of multi-track vertices the goal is to eliminate the background and to identify the true neutrino interaction vertex. Before attempting to select the true vertex all vertex candidates are refined. The first step in refining the vertices is to fit each vertex position to its current list of tracks. Up to this point the vertex position was taken to be the point of closest approach of the matched track and the first added starting track. That is, the original two track vertex position. Now a more sophisticated fit is done using information from all tracks. The position of closest approach of each pair of tracks in the vertex is found. These positions, weighted by χ^2 of the two tracks being considered, are averaged and the result is defined as the vertex position.

After refitting, the vertices are further refined by looping over the tracks and dropping those which do not point close enough to the new vertex position. For each vertex this is done by finding the median value of the impact parameters of all tracks belonging to that vertex. A loop is then made over the tracks and those with impact parameters greater than 2.2 times the median value are eliminated. Using the median value rather than the average is a more effective way of eliminating stragglers while still allowing for poor emulsion quality. With the reduced set of tracks the vertex position is fit again as described above. The fitting and track dropping cycle is continued until no tracks are dropped or until only two tracks remain in the vertex. What remains after applying this procedure to all vertices is a set which should include the true vertex formed by the neutrino interaction. The size of the final set varies depending on the size and position of the scan volume, among other things. Typically about 15 vertices remain. Those which remain will be evaluated automatically and manually to determine which one is most likely the true interaction vertex. The evaluation process is described in section 4-2.

4.1.2 Other Location Methods Using Spectrometer Tracks

Another related method of event location involves the use of *phantom tracks* rather than real three dimensional spectrometer tracks. If there are multiple clear 2D lines visible in both the u and v views of the spectrometer, but there is no further evidence of which tracks should be paired to form three dimensional tracks, it is useful to pair all possible permutations of the 2D lines. These associated pairs, which may not represent the actual trajectories of particles, form what are called phantom tracks. Phantom tracks are then used in an analogous manner as the matched tracks described above. Usually at least one of the phantom tracks is a real 3D track so an interaction track from the emulsion can be matched to it. As in the track matching method described above, the idea here is to use the constraints provided by the phantom track parameters to reduce the number of background events. Figures 4-12 and 4-13 show the scintillating fiber images for event 3299_09040, which was located by this method.

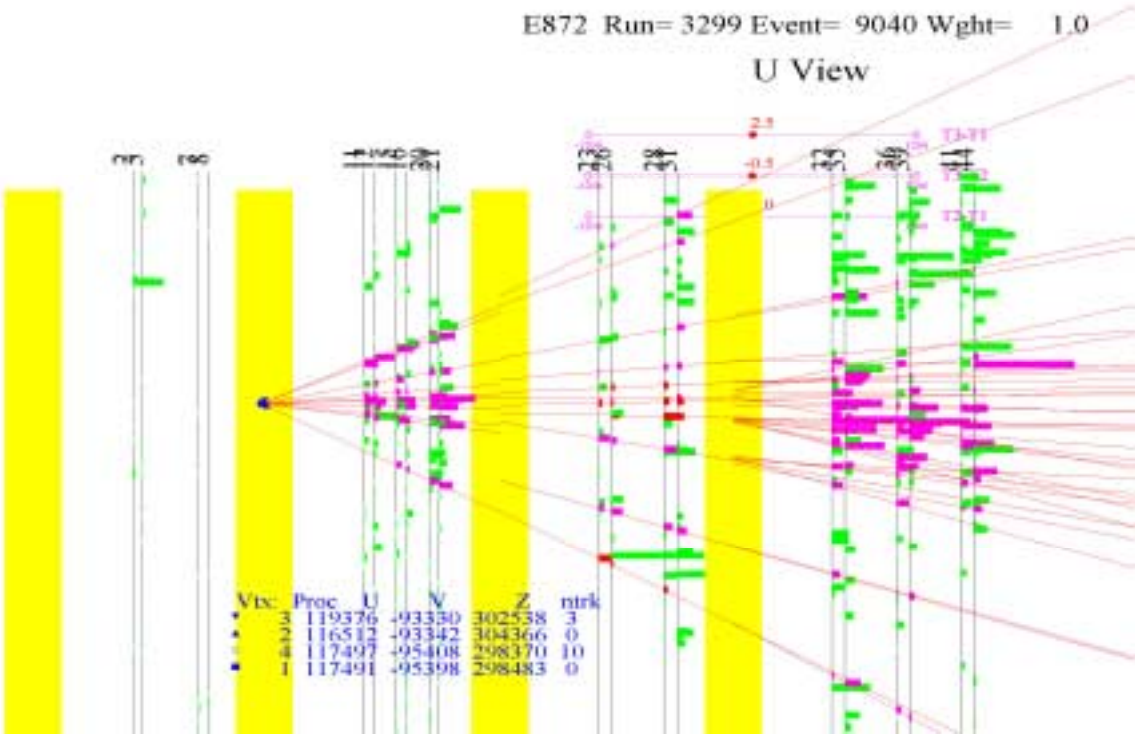

Figure 4-12 This image and the next show that there are clearly defined lines in both views of the SFT, but it is not clear which lines should be combined to form 3D tracks. In this case phantom tracks can be made. The full length of the SFT is shown here with the 4 emulsion modules (rectangles).

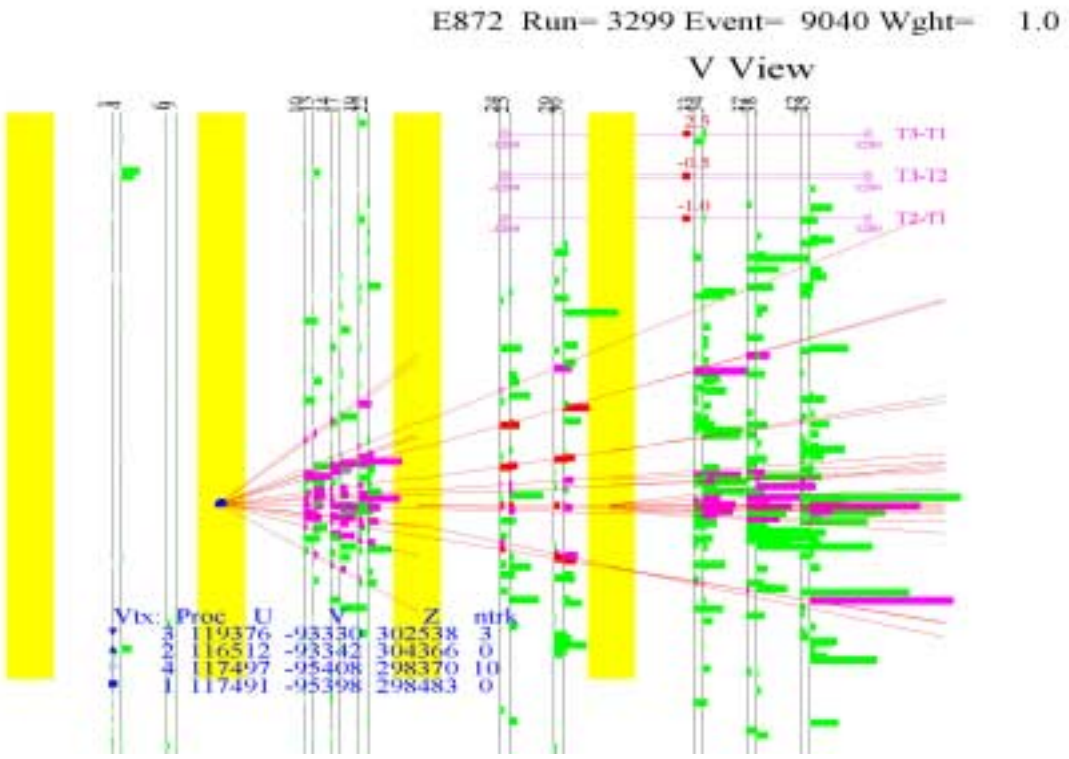

Figure 4-13 Here is the V view of the SFT data for the same event shown in figure 4-11.

.

In some events a useful method of event location utilizes the spectrometer information left by an electromagnetic shower. For some showering events it can be difficult, if not impossible, to identify the individual tracks in the scintillating fibers and in the rest of the electronic detector. If tracks can be identified it may be difficult to determine whether or not they are primary tracks. In these cases it is useful to form a three dimensional spectrometer track along the direction of the shower core. The track is formed by selecting hits along the core in each two dimensional projection. The track direction is refined by forcing it to match the point in the electromagnetic calorimeter where the largest amount of energy was deposited. (fig 4-14, 4-15). The core track is

then projected backward to the emulsion and a search is made for emulsion tracks which match it.

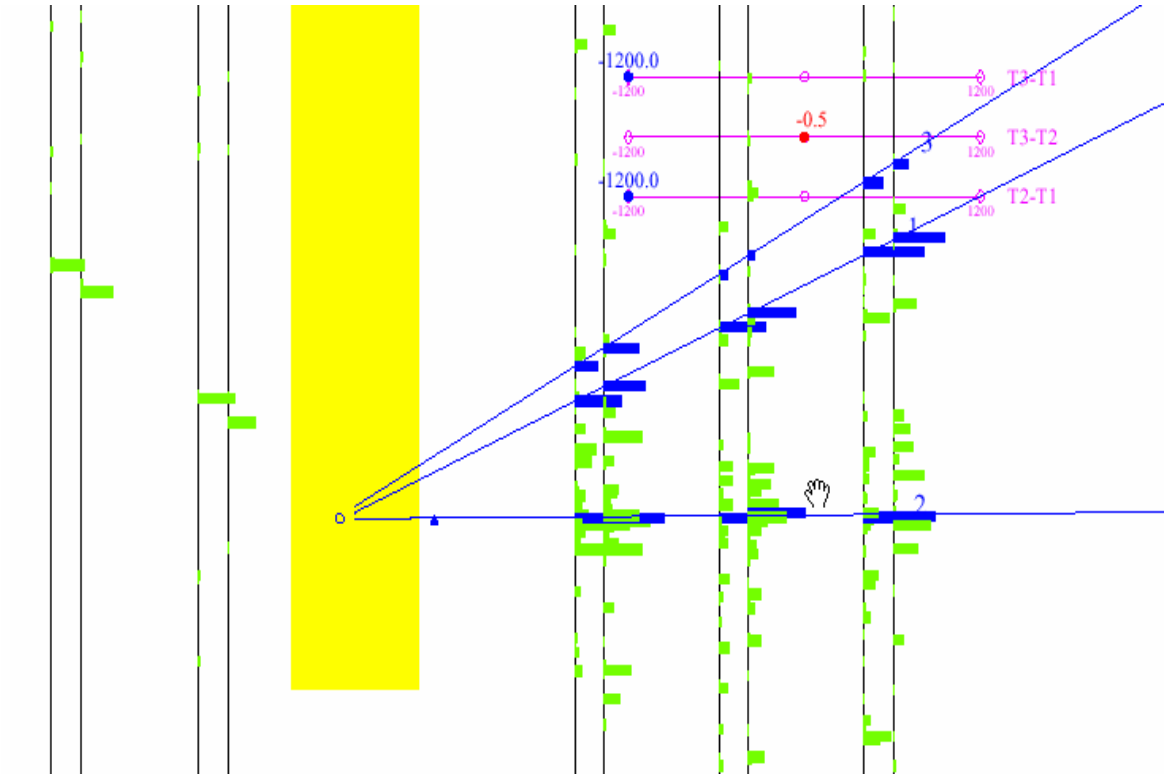

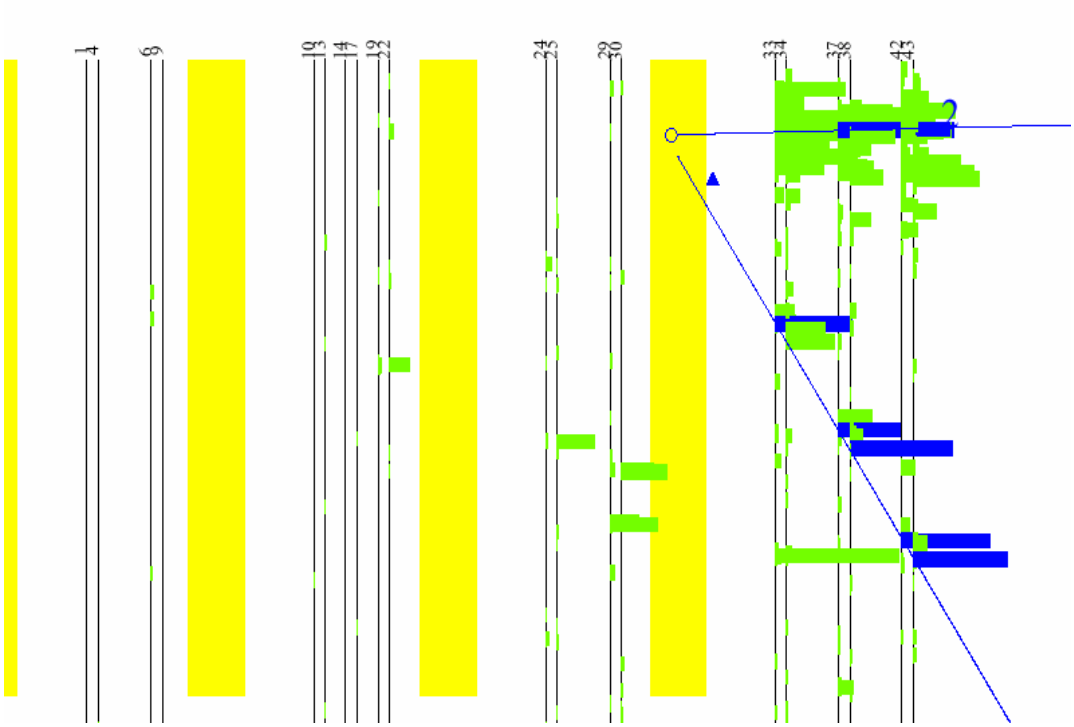

Figure 4-14 Track #2 is not well defined by isolated hits. It is made by selecting hits along the core of the shower.

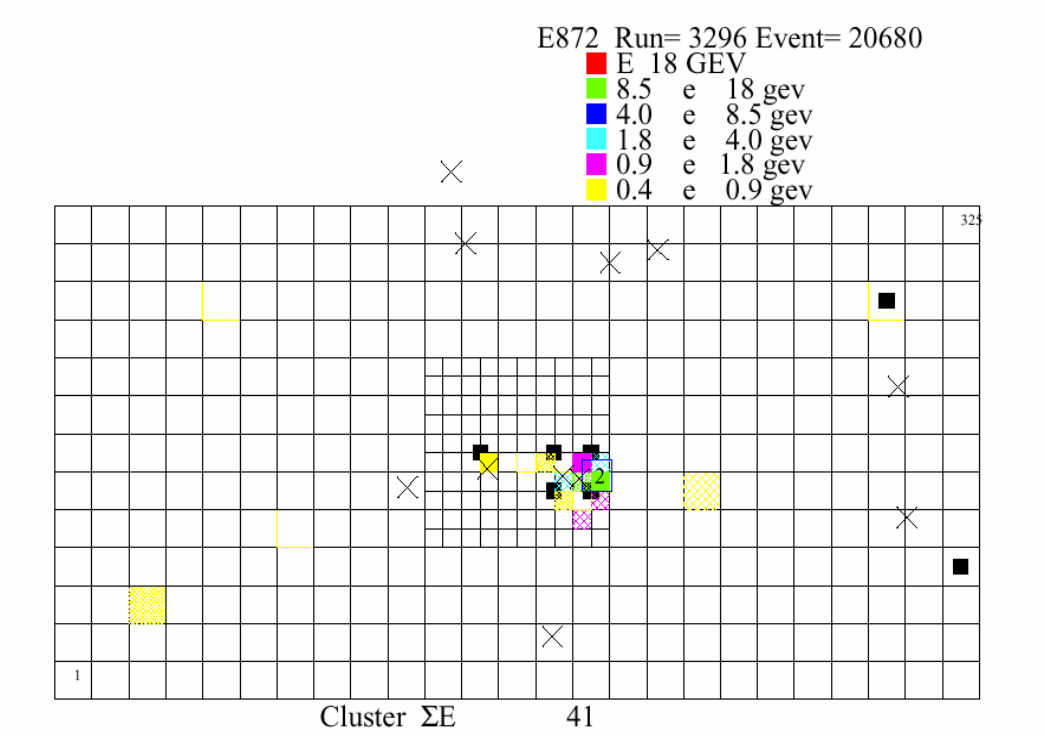

Figure 4-15 In this image of the calorimeter the number 2 marks the position of the *core track*. The core track is constrained to point to the position in the calorimeter where the largest amount of energy was deposited, indicated here by the center left box.

4.1.3 LOCATE NEUTRINO INTERACTION USING ALL EMULSION TRACKS

A more general method for locating neutrino interactions in the emulsion consists of a comprehensive search for any tracks which form vertices with other tracks. This method produces more background candidates but it is simpler in the sense that matched tracks need not be found in either the spectrometer or the emulsion prior to the vertex search.

In this method vertices are formed in a similar manner as in the matching method. Two track vertices are formed first with a maximum impact parameter of 2.5 microns. The impact parameter criterion is then relaxed and a search is made for other tracks which originate at the two track vertices. Track fitting and vertex fitting are done in the same manner as described above. The procedure is repeated until all tracks have impact parameters of less than 2.2 times the median value or until only two tracks remain from

the vertices. There are a few slight differences between this method and the spectrometer track matching method. In general, the selection criteria are kept tighter in this method to avoid the large background which would otherwise result from using all emulsion tracks. The tighter criteria include an increased number of segments, usually 3, required in the vertex tracks. Also, the first two vertex tracks must begin in the same emulsion plate and skipped plates are not allowed during the two track vertex formation stage. Single segments are not added to the vertices in this method unless no viable candidates are found. Although the background level is higher for this method it is frequently adequate for event location. In particular, this is the most straight forward method of locating high multiplicity events. This method is required when the other methods fail. This is the case for events which have produced so many hits in the scintillating fibers that tracking is next to impossible such as the event shown in figures 4-16 and 4-17.

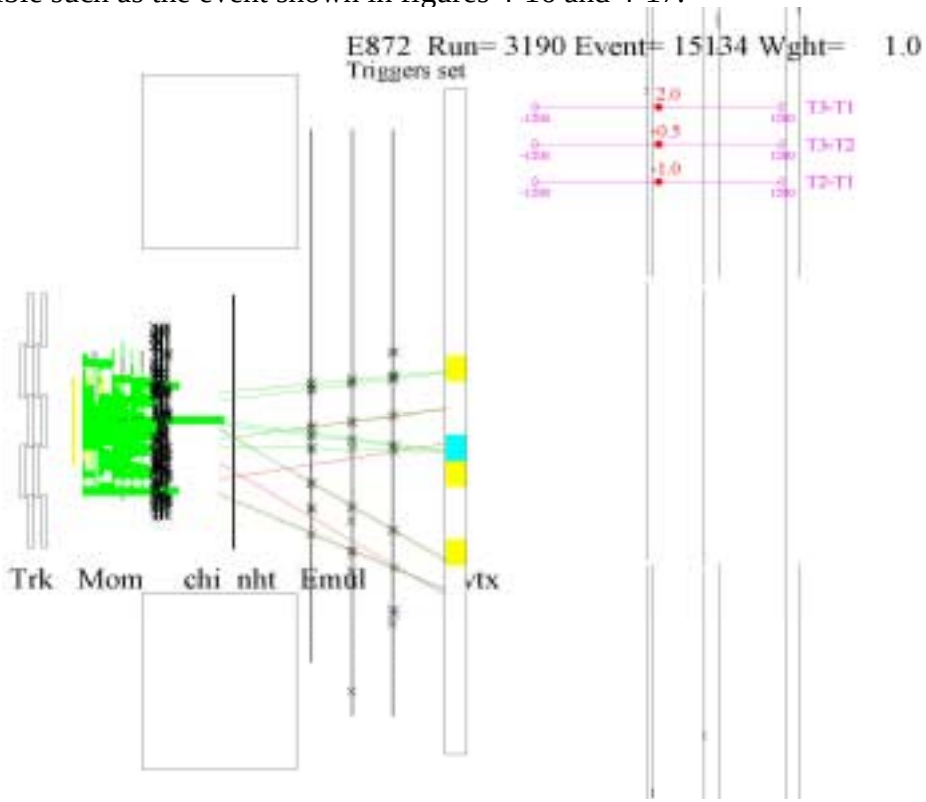

Figure 4-16 Shown here is the X-Z plane of the spectrometer for event 3190_15134. In this event individual lines and tracks are difficult to isolate. This is seen clearly in this image and also in the scintillating fiber tracker displays on the next page. From left to right, hits are shown in the scintillating fiber tracker, drift chambers (thick black and following three thin black planes), calorimeter, and on the far right the three lines represent the muon ID.

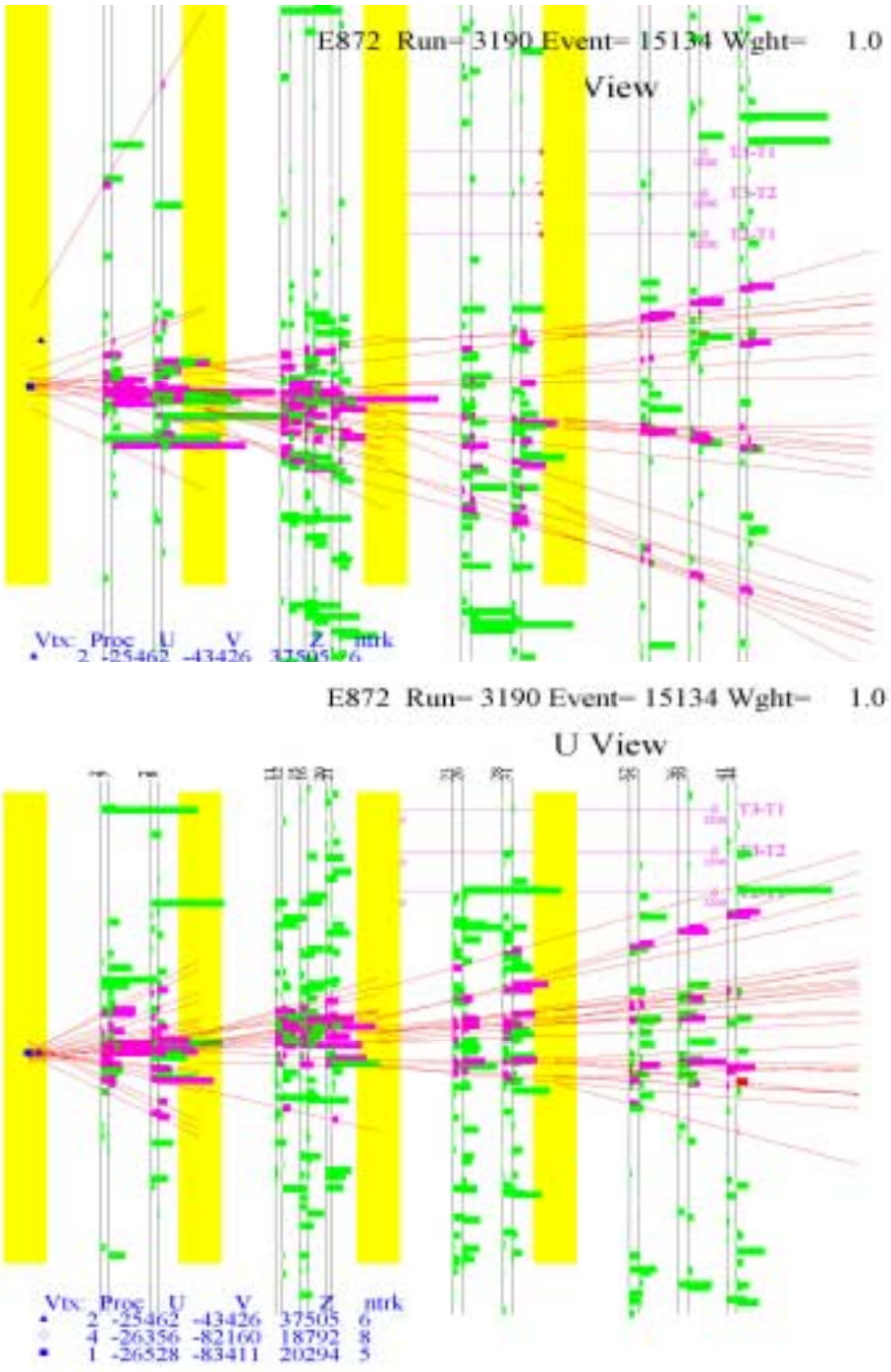

Figure 4-17 Scintillating fiber hits in event 3190_15134 are numerous and close together, making tracking very difficult.

4.1.4 LOCATING EVENTS USING SINGLE SEGMENTS

A final method of locating events involves using only single segments to find the neutrino interaction vertex. In the other methods single segments, or tracks which traverse only one emulsion plate, are used only to augment vertices formed from longer tracks. In the single segment methods it is the impact parameters of *projected segments* which are considered in vertex formation. There are several reasons why all of the previously described methods might fail. One reason the longer tracks may fail to produce a candidate vertex is that an event might have only one or two tracks. Most two track vertices are located using the other methods, but if one of the tracks has low momentum or if there is some other reason the track does not point to the vertex with a small impact parameter the vertex may be missed. An event consisting of one long track and one or more single segments may be found, and frequently is, using the track matching method. However, if the longer track has not been identified as a matched track that method will fail.

A more typical reason for failing to identify the event using longer tracks is that the emulsion quality is poor. If there is missing data because of distortion or poor development, the tracks will be incomplete. If this happens within one plate of a vertex, the long tracks probably will not form a vertex with the requisite precision but the single segments may still produce a vertex. Figure 4-18 shows the image of an event where the single segment method was required because of poor emulsion quality.

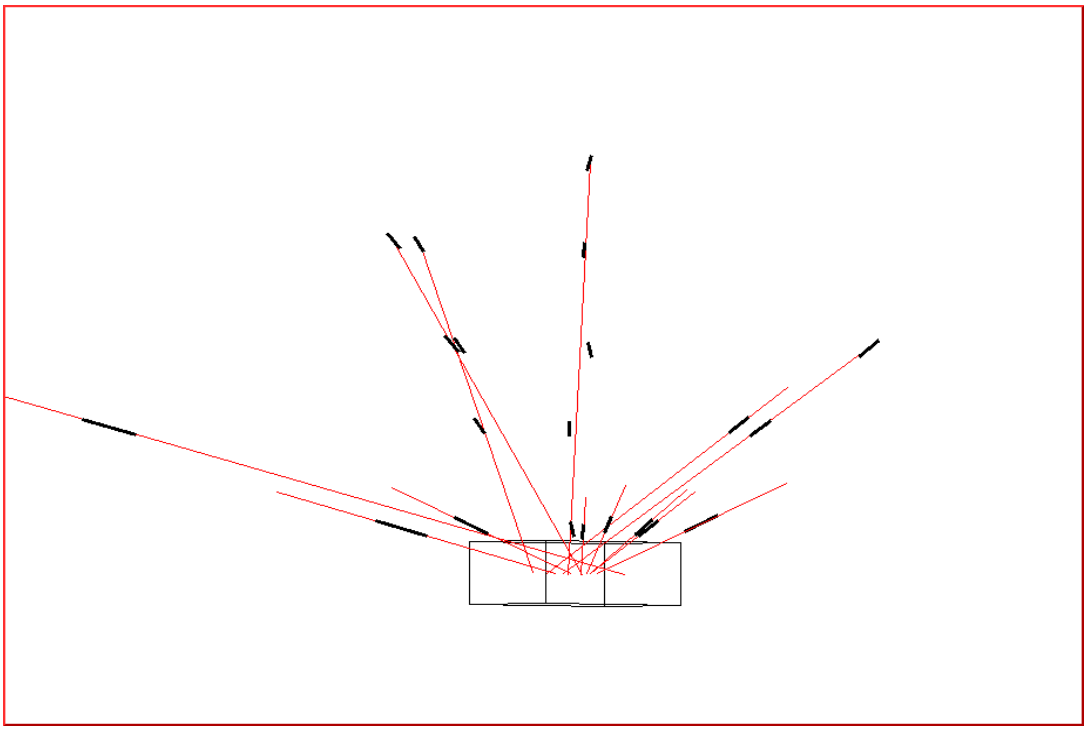

Figure 4-18 Even though event 3004_35680 has 10 primary tracks it was not located until single segment algorithms were employed. The problem with this event is plate slipping, which causes segments to be either mislinked or not linked at all. Shown above is the event as it appeared after the single segment location program was run. The event is shown below after being reconstructed using the emulsion display.

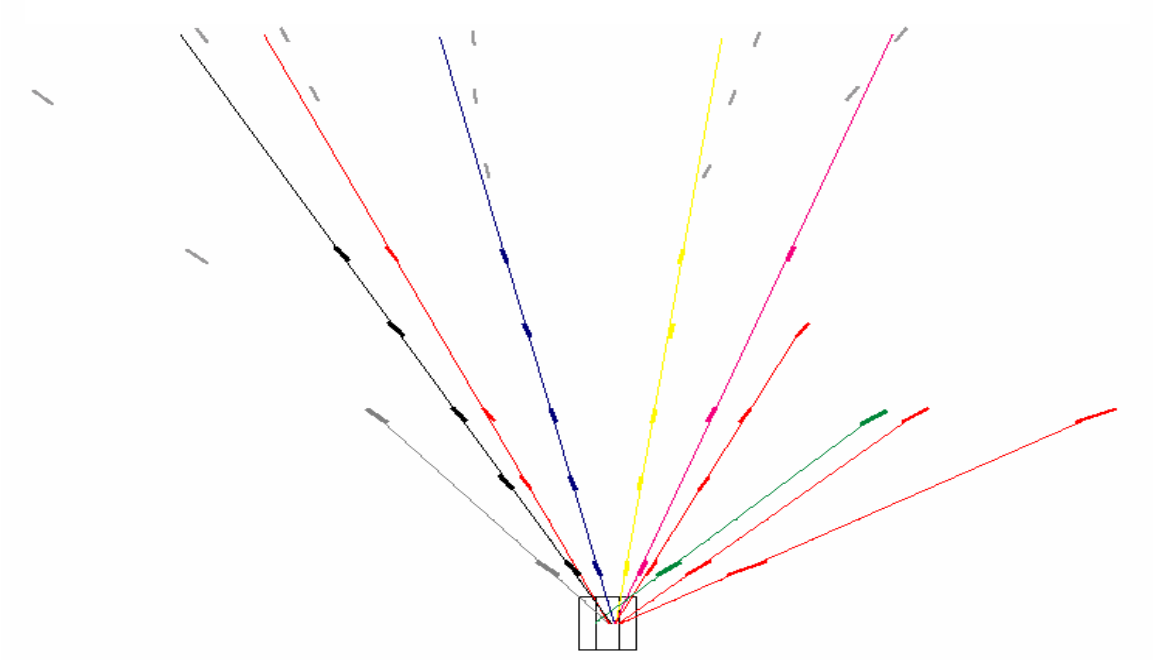

The single segment vertexing algorithms are largely the same as those previously described. Segments are used in lieu of tracks in the spectrometer track matching method, the phantom track method, and the general method which uses all starting tracks within a scan volume. There are a few differences due mainly to the larger background that would result without tighter selection criteria. If a particular event file is larger than 25 megabytes, which typically means that the scan volume contains more than 250,000 segments, that file is divided. The number of divisions obviously depends on the original size of the file. The divisions are made so that the edges of the smaller volumes overlap one another. The single segment methods also differ in that the segments are first sorted according to their plate number and u-v positions. Only segments from the same or neighboring region are paired with each other in search of vertices. Limiting the number of segment pairs to check usually allows the program to complete in less than one hour. Another difference in the programs is that, because of the larger uncertainty in angle for a single segment, the impact parameter between two segments is weighted more heavily by the distance between the segments and the vertex than in the longer track methods. With single segment vertexing usually three or more segments are required to form a vertex. This criterion is relaxed to two when no candidates are found.

There is an extension of the phantom track method which can be helpful when using single segments to locate events. Recall that in that method only the first emulsion vertex track was required to match the phantom spectrometer track. That emulsion track was called the matched track. A set of matched tracks was obtained and each one was compared to all other starting tracks in an attempt to form two track vertices. In this revised method only single segments which match the phantom spectrometer tracks are compared to each other in search of vertices. This greatly reduces the background and speeds up the processing time.

The single segment methods are quite successful, but they do require more computer time and human interaction. Therefore they are left as the last option to event location. Regardless of which location method has been used to identify candidate events there is one last process applied to the tracks of all vertices. That process is to link the tracks or single segments, if possible, both upstream and downstream. During track

formation the track forming criteria were such that many of the tracks were disjoint rather than being linked all the way through the scan volume. When tracking criteria are looser lower momentum tracks or scattered tracks can be linked through to the end of the scan volume. In this case the parameters of the tracks will represent an average fit of the segments, but will not represent any one portion of the track very well. After the vertices have been formed, however, it is better to have the tracks fully linked. The total number of segments and knowledge of a tracks exiting status are information that can be used to evaluate the quality of a vertex.

The creation of the above location methods was an iterative process. The general routine that uses all emulsion tracks and no spectrometer data was used first. (Section 4.1.3). Although that algorithm worked for most events it produced overwhelming background for other events. The 3D spectrometer track matching routine was used next to eliminate some of the background vertices by requiring vertex emulsion tracks to match the spectrometer track(s). That proved to be very effective except when no reliable 3D spectrometer tracks could be identified. At that point phantom spectrometer tracks were used to constrain the emulsion vertex tracks since that procedure would still produce less background than the general method. Single segment data were used from the beginning in all algorithms, but the purely single segment methods were not used until most of the events had already been located. At that time many events that were left were problematic because of slipping or distortion, the cases where single segment methods are necessary.

Work continues on event location with a goal of developing a set of techniques that give 100% efficiency. Since the time of this analysis other location techniques have been developed. The most promising of these is the use of the changeable sheets to link spectrometer tracks to emulsion tracks. Changeable sheets were single emulsion sheets placed on the ends of the emulsion modules. These sheets were changed frequently, approximately each week, so that the background of ionizing tracks penetrating them was much lower than the background of tracks through emulsion modules themselves. Using these as very high resolution detectors immediately in front of the emulsion modules allows for the matching technique described in section 4.1.1 to be used more effectively.

The software for another changeable sheet method has not been tested because the necessary data has not been collected. This method is almost identical to the single segment methods described in section 4.1.4 except that changeable sheet data would be used instead of normal emulsion plate data. Depending on the distance of the predicted vertex position from the changeable sheet as much as 6cm x 6cm of the changeable sheet would have to be scanned. Considering the success of the other single segment methods and the low density of segments within a changeable sheet I believe this method would be effective in some events.

4.2 EVALUATION OF CANDIDATES: SELECTING THE TRUE INTERACTION VERTEX

After running the location routines there remains a set of candidate events which must be evaluated for their likelihood of being the true neutrino interaction. The evaluation of the candidates is first done automatically and then manually.

4.2.1 AUTOMATIC EVALUATION

There are a number of characteristics of a vertex which are quantifiable and which are useful in determining a vertex's likelihood of being an actual interaction vertex. These characteristics include the following

- Multiplicity, or number of primary tracks in the vertex
- Fraction of vertex tracks exiting scan volume
- Fraction of emulsion vertex tracks matching spectrometer tracks
- Angular difference between spectrometer track and matched emulsion track
- Position difference between spectrometer track and matched emulsion track
- Average first segment impact parameters to vertex
- Average track impact parameters to vertex
- Vertex position difference from predicted position
- Emulsion quality

Figures 4-19 and 4-20 show the distributions of these parameters for both true and fake interaction vertices. None of these parameters are used individually to select or reject a vertex. Rather they are combined and the result is used to rank the candidates for their likelihood of being true interaction vertices. The procedure for ranking the candidates is described below. Most of the parameters listed above are self explanatory, but two require further explanation. The fraction of emulsion vertex tracks matching the spectrometer depends on what is meant by *match*. An emulsion track is said to match a

spectrometer track if, when the emulsion track is projected to the position of the spectrometer track, the two tracks differ in angle and position by no more than 0.03 radians and 1.5 mm. Furthermore the spectrometer track should contain more than 3 scintillating fiber hits.

The other parameter which requires further explanation is emulsion quality. Emulsion quality at the location of a vertex can be quantified in part by considering track characteristics in that vicinity. A large fraction [more than ~ 15 %] of neighboring tracks which begin in the vertex plate is an indication of a problem in the emulsion. The trouble could be plate slipping, emulsion distortion, low grain density, or some other tracking or scanning problem. If plate slipping is the cause of the large number of starting tracks, there should be an approximately equal number of ending tracks in the previous plate. If the actual emulsion quality is poor there may be segment data missing from the previous plate. In that case there would be a large number of tracks ending two plates upstream of the vertex plate. Or, since skipped plates are allowed in track formation, there would be tracks which span the plates but have segments missing from the damaged plate. Because of these problems, we quantify emulsion quality near a vertex by finding the fraction of neighboring tracks which either start in the vertex plate or have missing segments in the previous plate. If the emulsion quality is poor in a particular area, there may be a high level of background vertices due to the larger number of starting tracks.

The vertex characteristics listed above are quantified and used as parameters in determining which vertices are the best candidates within a given event. The quantified result is also used to determine how likely it is that any given vertex is a true interaction vertex. The procedure for doing this is as follows. First, the mean and standard deviation of each parameter distribution is determined for true interaction vertices by using a set of known located events. The z-score, for a particular parameter of a particular vertex, is defined as the difference between the mean and the measured value in units of the standard deviation for that parameter. The final score for one vertex is the sum of the individual parameter z-scores for that vertex. For a given event this procedure results in each candidate vertex being ranked within the event. The resultant score also reflects the likelihood that each candidate vertex is an interaction vertex.

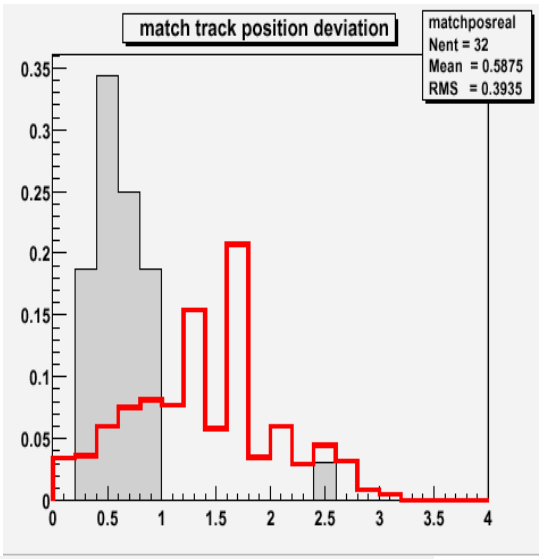
match track position deviation
matchposreal
Nent = 32
Mean = 0.5875
RMS = 0.3935
0.35
0.3
0.25
0.2
0.15
0.1
0.05
0
0
0.5
1
1.5
2
2.5
3
3.5
4

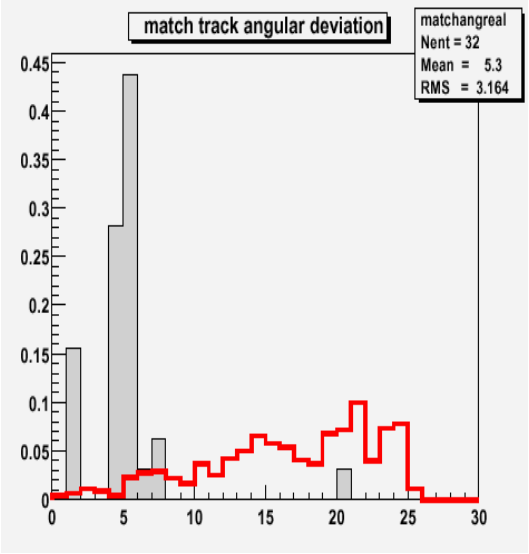
match track angular deviation
matchangreal
Nent = 32
Mean = 5.3
RMS = 3.164
0.45
0.4
0.35
0.3
0.25
0.2
0.15
0.1
0.05
0
0
5
10
15
20
25
30

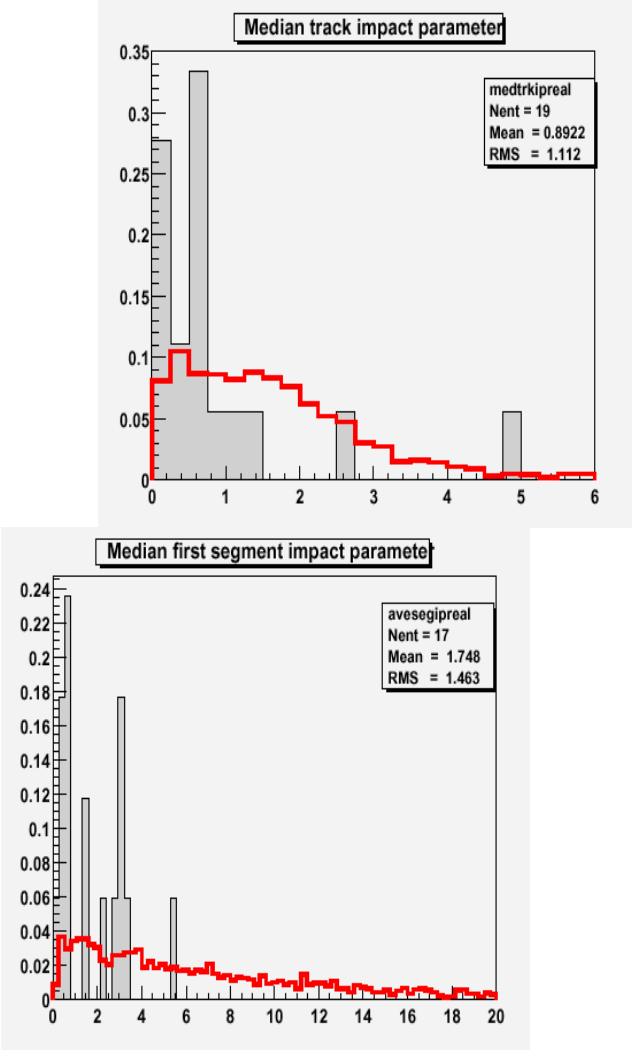

Figure 4-19 Shown are distributions of four parameters used in the automatic evaluation of candidate vertices. These distributions were produced using results from the application of location methods to known, located events. The values of true interaction vertices fill the grey histograms and the distributions of fake vertices are represented by the jagged vertical line. The parameters are, clockwise from upper left, 1) the position difference between the chosen spectrometer track and the matching emulsion track in mm. 2) the angular difference between the spectrometer track and the matching emulsion track in mrad. 3) the median value of first segment impact parameters to the vertex (μm). 4) The median impact parameters of tracks to the vertex (μm). The distributions of four more parameters are shown in figure 4-20.

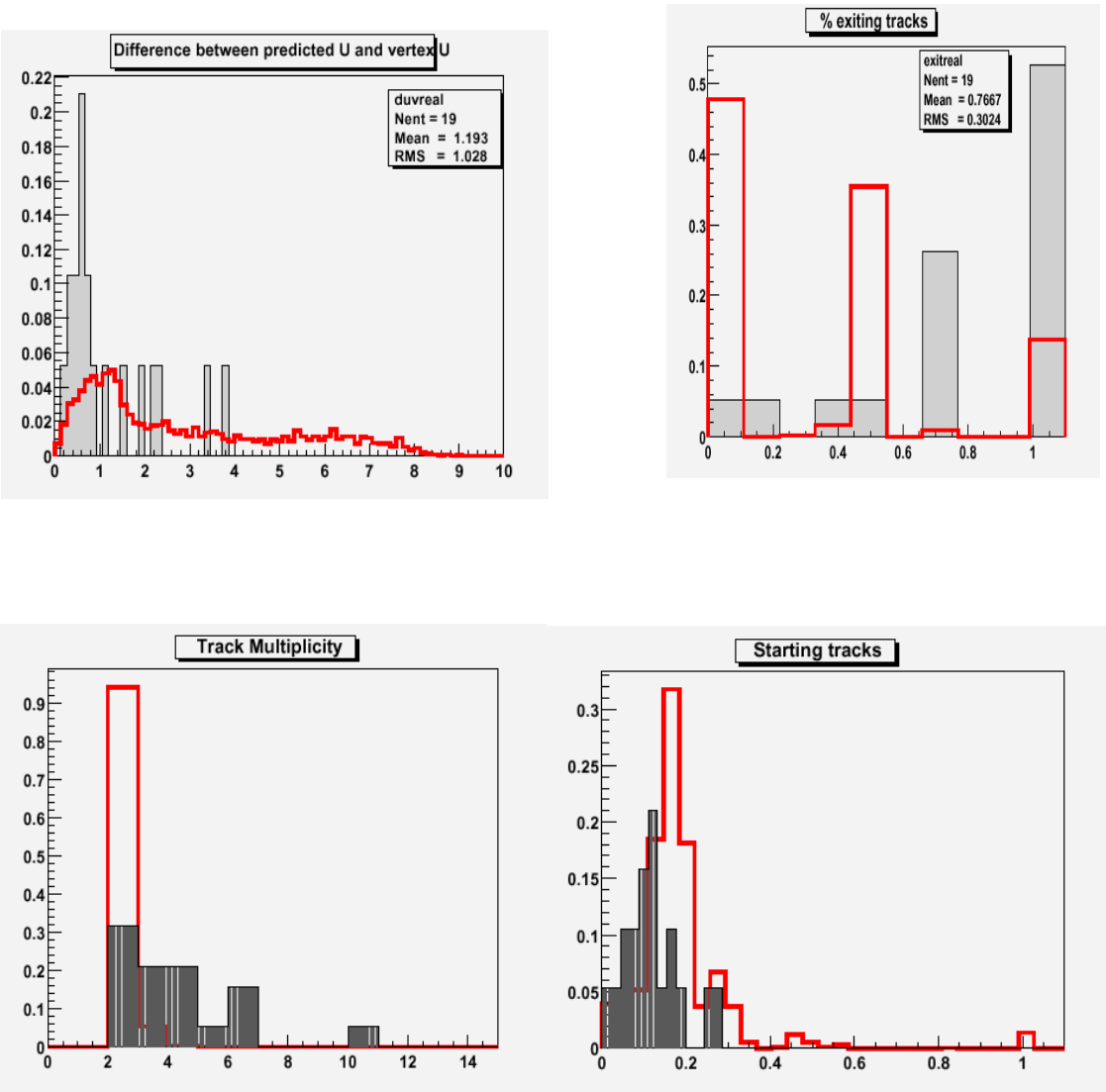

Figure 4-20 the distributions of four more parameters used to evaluate vertex candidates are shown, with the true vertices represented in grey histograms and the fake vertices shown by the line. clockwise from the upper left they are 1) the difference in mm between the vertex position and the predicted vertex position, 2) the fraction of vertex tracks which exit the scanned volume of emulsion, 3) the number of primary tracks in the vertex, and 4) the fraction of tracks which originate within a small radius of the candidate vertex. The last parameter relates to emulsion quality and is only used to reject candidates when the value is greater than 0.6. It is not used to calculate the z-score that is used for ranking or scoring.

4.2.2 MANUAL EVALUATION

Although the automatic evaluation process is efficient at selecting the true vertex manual evaluation is still required to confirm the selection. Manual evaluation is done by viewing the events electronically using the 3D display and also by physically viewing the emulsion through a microscope. The three dimensional display that was developed for DONUT emulsion data uses CERN ROOT libraries[26]. The 3D display is in some ways more useful than actually looking at the emulsion through a microscope. First, multiple plates can be viewed simultaneously so that entire tracks can be seen rather than only single segments. In the display, the image can be rotated in any direction which is very useful when attempting to reconstruct an event or a single track. The variable characteristics of emulsion make this tool particularly useful. Figure 4-21 shows a slipping event where the 3D display is used to decipher the problem. The display has limitations, however, because all emulsion information is not present in the digitized data. As stated in chapter 2, the hardware track selector is 97% efficient so that 3% of the segment data are not present in the files. Furthermore, tracks with angles > 450mrad, are also not detected by the track selector. For these reasons, it is necessary to use both the graphical display and visual emulsion examination to evaluate the candidate events.

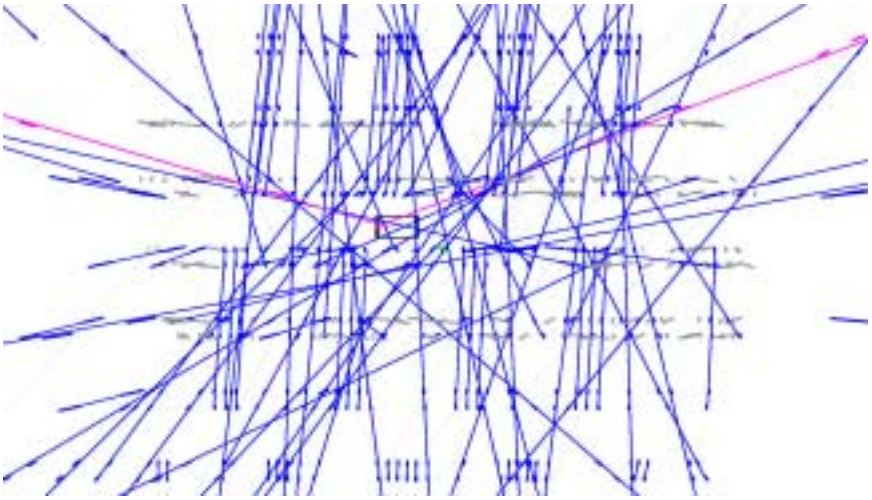

Figure 4-21 In this image you can see that while a few tracks link all the way through the plates many tracks are broken and shifted between the bottom two plates, and again near the middle plates. The vertex formed by the tracks, shown as a box near the center of the image, is most likely a fake since most of the "starting tracks" in that plate should not actually start there.

The first step in the event verification procedure is to view the candidate vertices interactively using the 3D display. For each candidate the vertex tracks and their associated segments are displayed. The vertex is rotated about its axis to see if the tracks form a vertex in all projections. Frequently fake vertices are eliminated during this step because, even though the distance of closest approach may be small, the tracks are seen to be parallel and separate in some projection. Figures 4-22 - 4-23 show images of fake vertices and the actual interaction vertex for event 3235_11264.

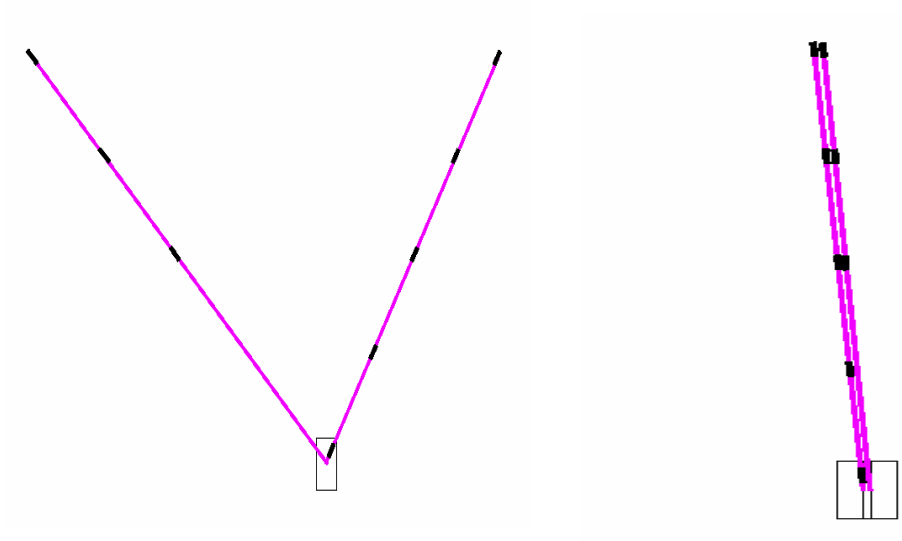

Figure 4-22 Event 3235_11264. This vertex looks plausible on the left, but the orthogonal view on the right reveals that the tracks are parallel and separate (in this 2D projection). In the left-hand picture the vertex is also suspect because of the missing segments in the first two plates.

The next step is to add neighboring tracks and segments to the display. If something is wrong with the emulsion near a vertex, it is often noticeable from this view. For example, it might be that a blank area with no segments is seen just upstream of a vertex, or that the vertex is very near the edge of the scan volume. It may be that other tracks

reveal that there was slipping. In these cases the viewer will be suspicious that the vertex is fake.

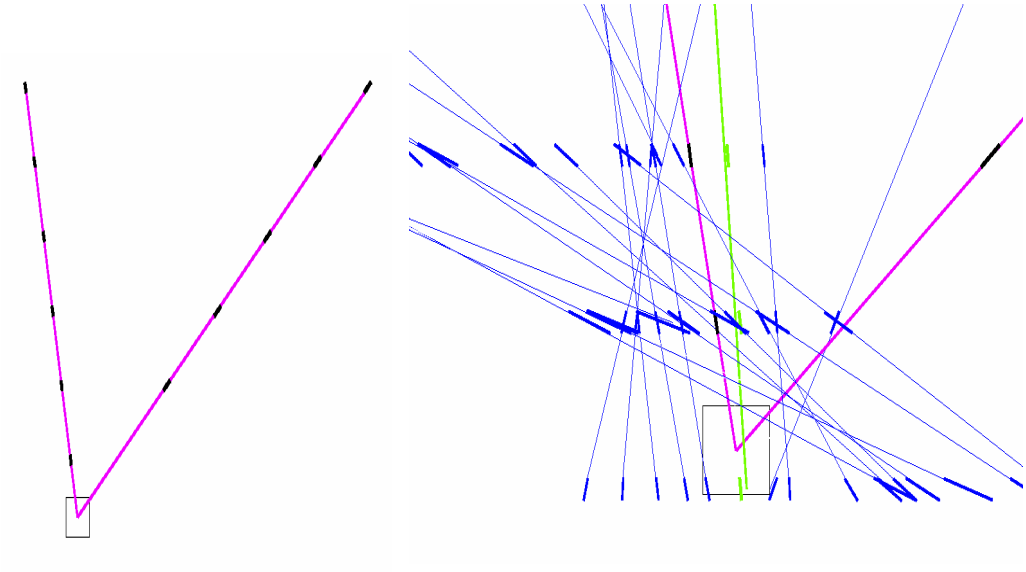

Figure 4-23 A different vertex from event 3235_11264 looks plausible on the left but the view of neighboring tracks on the right shows why it is fake. A probable low momentum track, was mislinked in the first plate. The segment shown at the center of the bottom of the box should have been linked to the other vertex track on the left. Then the two tracks would no longer form a vertex. Single segments are not displayed for the purpose of clarity. Note that in these and the following images of emulsion data the vertical distance displayed is about 50 times the horizontal distance shown, so the track angles appear much larger than they are.

If a vertex looks plausible after these observations have been made, there are two more steps to this portion of the evaluation. First, each track in the vertex is projected upstream and the tracks and segments in the area surrounding the projection are viewed. A visual check is made to determine whether or not any segments in this area should have been connected to the track. If a track links to a segment or to another track upstream of a vertex then it can not be part of that vertex. Each vertex track is viewed one, two, and three plates upstream in this fashion. Finally, the projections of the emulsion tracks are viewed in the spectrometer event display to see if they match any spectrometer tracks. It

is possible that a match was not automatically made because of inefficiency in the spectrometer tracking but that visually one can see that a match is plausible.

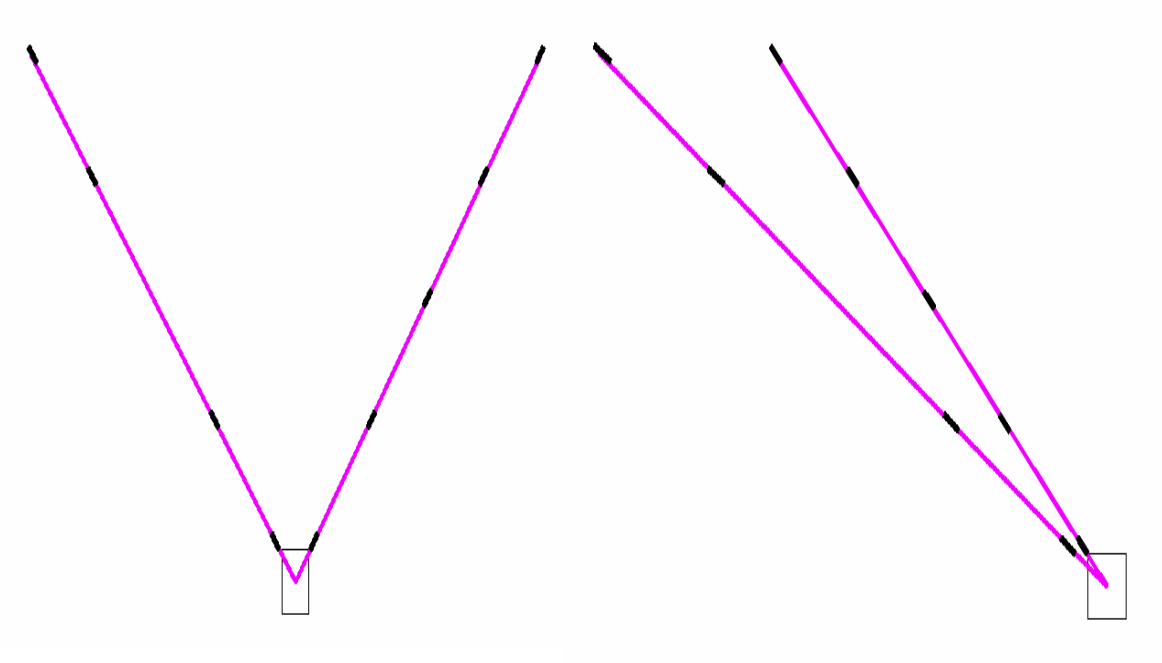

Figure 4-24 Above, the true vertex for event 3235_11264 is displayed in orthogonal views. The tracks form a vertex in all 2D projections. Below, a close-up view of the beginning of each track is shown, along with surrounding tracks and segments. The projection of each vertex track is shown in the two plates preceding the vertex. There appear to be no tracks or segments which could link to the vertex tracks, so the tracks truly are starting tracks. Also, the emulsion and tracking quality here are good as indicated by the blue tracks that link through all plates. The dark segments line up well with the tracks and there are no slipping plates. The light segments shown are not associated with any tracks.

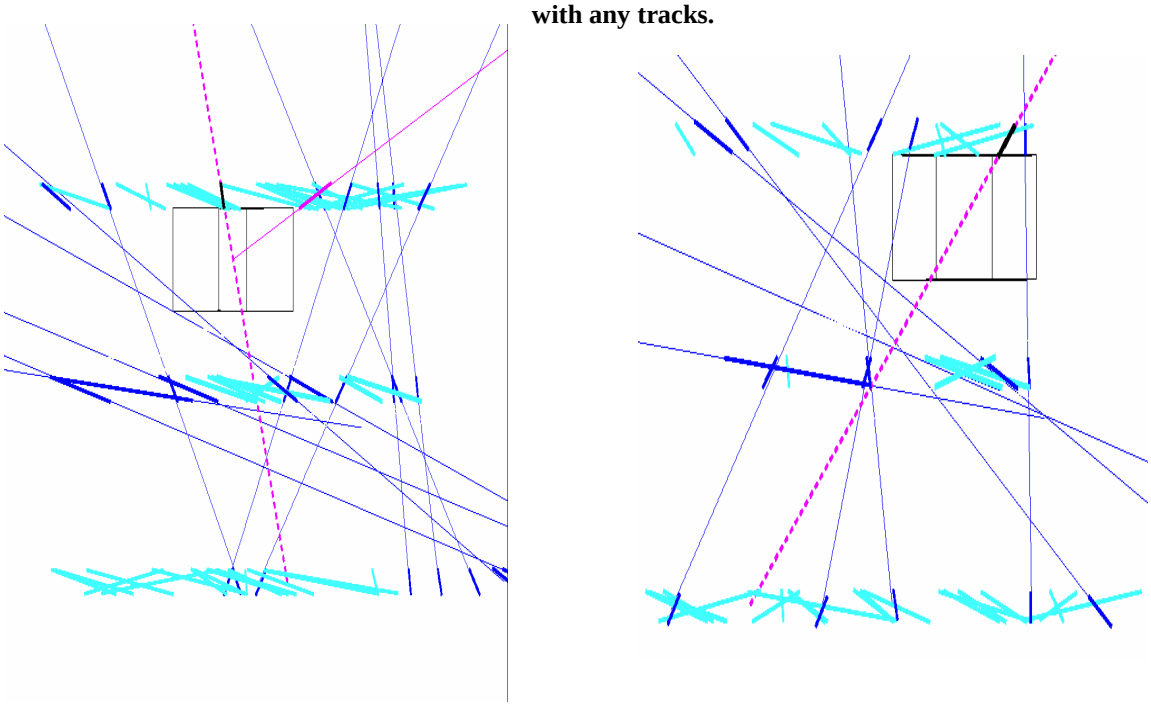

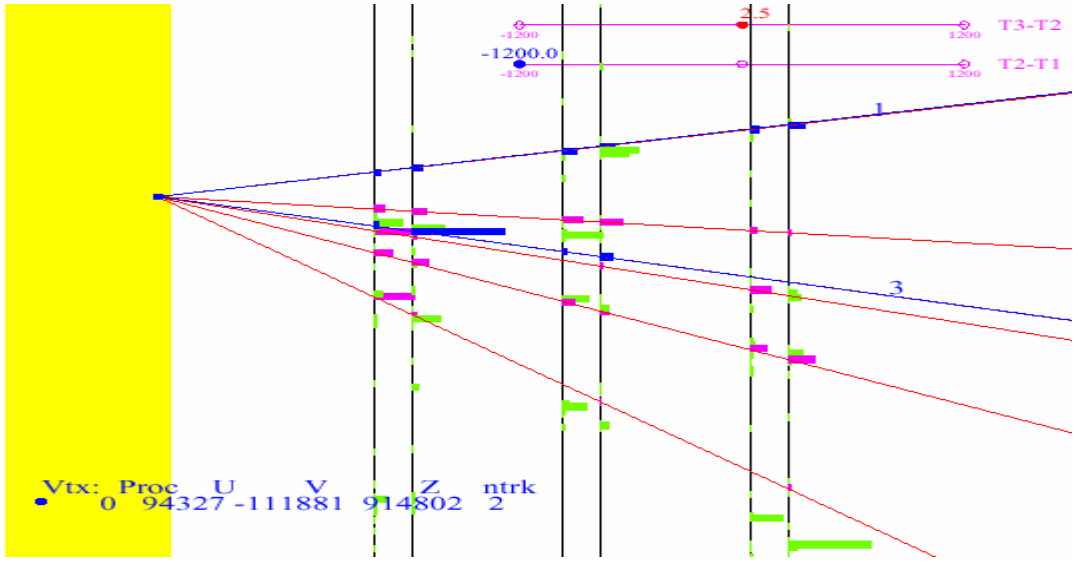
2.5
-1200
1200
T3-T2
-1200.0
-1200
1200
T2-T1
1
3
Vtx: Proc U V Z ntrk
0 94327 -111881 914802 2

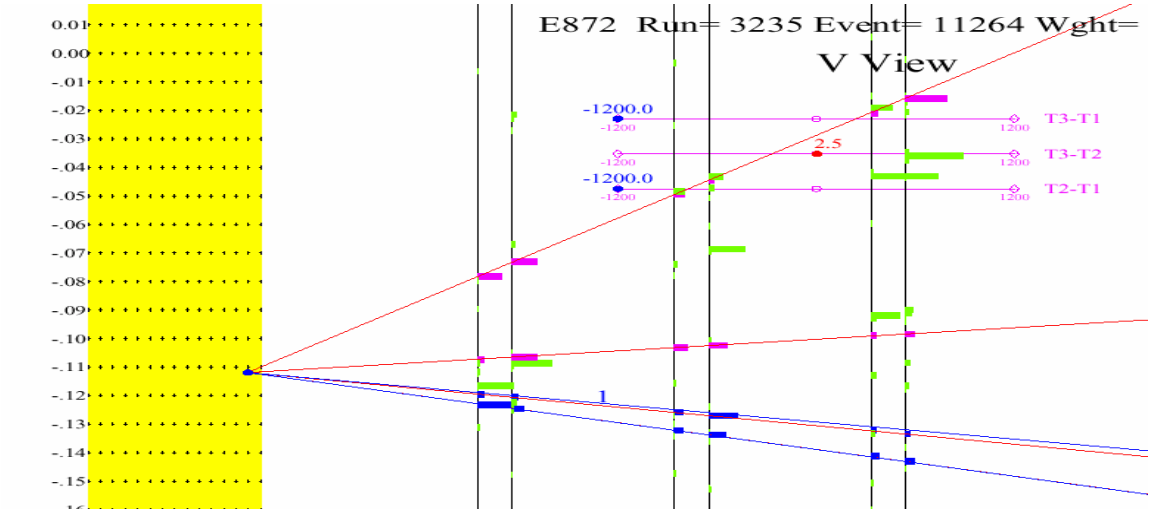
E872 Run= 3235 Event= 11264 Wght=
V View
0.01
0.00
-.01
-.02
-.03
-.04
-.05
-.06
-.07
-.08
-.09
-.10
-.11
-.12
-.13
-.14
-.15
-1200.0
-1200
1200
T3-T1
2.5
-1200
1200
T3-T2
-1200.0
-1200
1200
T2-T1
1

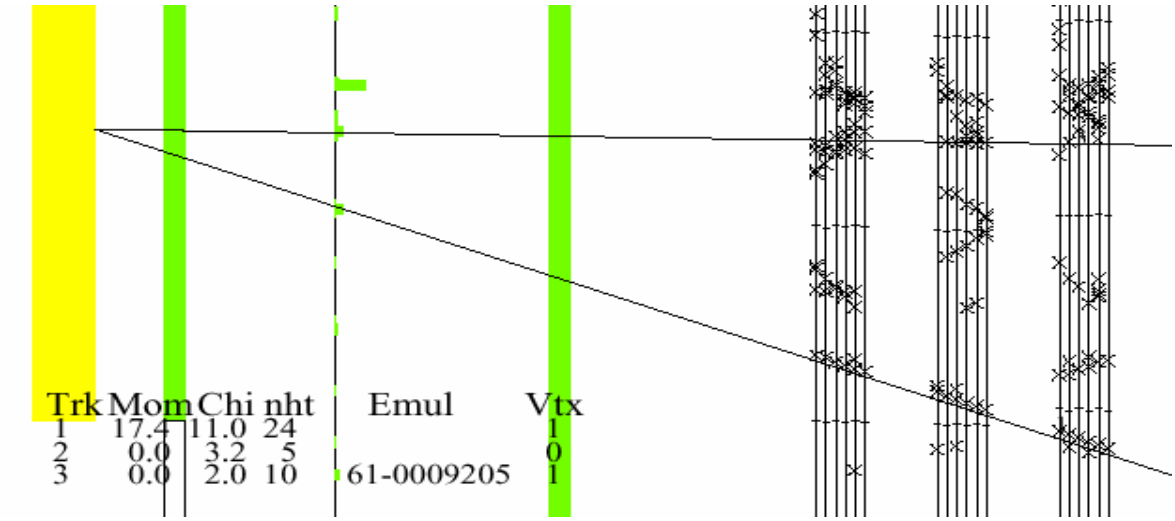

Figure 4-25 The true vertex for 3235_11264 matches the spectrometer well. Scintillating fiber tracks in the U and V views are shown above, with the projected emulsion tracks as lines. Beneath them the X view of the scintillating fiber tracker is shown as well as the vector drift chamber. The projected emulsion tracks are shown.

4.2.3 Location Efficiency

To calculate the efficiency of the location methods described in this chapter 30 randomly selected events were examined in great detail as described below.

The first step in the process is to run the general location routine described in section 4.1.3. Since this method does not require the input of selected spectrometer tracks it is the easiest way to begin. The automatic evaluation code is then run on the resultant set of candidate vertices for each event. The goal here is to pick out the easy events; that is, those whose true vertex has high multiplicity (>=4 tracks) or those with high automatic evaluation scores relative to other events as described in sect 4.1.3. The top 5 candidates from automatic evaluation, any candidates that set the likely flag, or those with scores > -1.5 are further evaluated using the 3 dimensional display. If a vertex is selected as the true vertex, the position and track information is sent to Nagoya where that location in the emulsion is examined under a microscope.

The next method, applied to the remaining unlocated events, is the spectrometer track – emulsion track matching method. Each event is viewed in the spectrometer display and 3D tracks are selected for the purpose of an emulsion search for the matching track. If it is too difficult to associate a pair of 2 dimensional projections to form a space track, all permutations are used to make phantom tracks. Or, in the case of an electromagnetic shower, a core track is selected as the spectrometer track to match to the emulsion data. The selected 3D track or tracks are then input into the location routine which looks for matching emulsion tracks. Automatic evaluation is run on this set and plausible candidates are selected or rejected using the 3D display. Selected events are sent to Nagoya for an evaluation of the emulsion location under a microscope. In this process the search for a given event is not exhaustive because the search is ended when an acceptable candidate has been located.

If no plausible candidates have been located after these steps, the selection criteria are loosened and the routines are run again. Events which remain unlocated after these steps are examined more closely in both the spectrometer and emulsion displays. If the vertex prediction and track selections were ambiguous the alternative choice is made for

the event location and the location routines are run again on the events. The emulsion tracks are scrutinized for slipping or other potential causes of trouble. Several areas of the scan volume are viewed to determine the quality of the emulsion and tracking. Segment density, alignment corrections, and segment pulse heights can be checked for signs of missing or distorted data. If nothing is revealed the location routines may be run again with even looser selection criteria. Finally, if there are still no credible candidates, an attempt is made to locate the event using the single segment code.

4.2.4 DATA

The event numbers from the sample data set are listed in the first column of table 4-1. The event type abbreviations listed in column 2 have the following meanings:

CCmu	muon neutrino charged current interaction
CCe	electron neutrino charged current interaction
NC	neutral current interaction

Module numbers and emulsion types listed in the table refer to the definitions given in chapter 2, table 2-2 and figure 2-7. Table 4-1 also lists the number of emulsion plates scanned in the volume surrounding the vertex, and the density of segments near the vertex. Location results of this sample study are given in the next chapter.

Table 4-1 Event numbers and characteristics of the sample set of 30 events. The columns are explained above.

EVENT NUMBER	EVENT TYPE	MODULE	EMULSION TYPE	NUMBER OF PLATES SCANNED	SEGMENT DENSITY (seg/mm^2)x10^4
2879_12293	CCmu	3	ECC 200	23	6.9
2884_14149	CCmu	3	ECC 200	20	9.6
2892_02649	CCmu	1	ECC 200	44	9.9
2893_07799	CCe	1	ECC 200	45	9.7
2907_12929	CCe	1	ECC 200	24	9.5
2929_20792	CCmu	1	ECC 200	22	6.7
2934_00494	CCmu	1	ECC 200	22	10.0
2991_07358	CCe	1	ECC 200	20	8.2
2996_01287	NC	4	ECC800	13	14.1
3000_17634	CCe	3	ECC 200	22	6.4
3004_35680	CCmu	4	BULK	14	7.0
3008_29159	CCmu	1	ECC 200	22	7.3
3024_08169	NC	3	ECC 200	16	7.5
3059_01284	CCe	2	BULK	9	10.3
3073_22977	CCmu	7	ECC800	18	15.2
3096_05346	NC	4	BULK	27	15.3
3111_03598	CCe	2	BULK	20	10.9
3190_04273	CCmu	1	ECC 200	42	7.5
3190_06547	CCe	4	BULK	18	13.5
3190_15134	CCe	1	ECC 200	22	6.8
3191_03827	CCmu	2	BULK	18	14.5
3235_11264	NC	8	BULK	7	18.5
3254_01397	CCmu	8	BULK	17	20.8
3287_24160	CCe	2	ECC800	16	9.2
3299_09040	NC	2	BULK	26	9.3
3336_11582	CCe	2	BULK	19	23.0
3350_17729	CCe	7	ECC800	24	8.1
3352_26934	CCmu	7	ECC800	16	7.2
3356_03543	CCmu	7	ECC800	18	6.9
3358_14209	NC	7	ECC800	15	9.6

5 Results

5.1 Results of 30 event set

From the sample set of 30 events presented in the last chapter 26* events were located using the methods previously described. From these data a location efficiency of 87% is calculated. This is an improvement from the 58% efficiency documented in the DONUT paper published in Nuclear Instruments Methods in 2002[23]. Tables 5-1 and 5-2 list results and event characteristics of the 30 events. Among the located events the automatic evaluation routine selected the true vertex as the most likely candidate 71% of the time. In 21% of the cases the true vertex was selected automatically as the second most likely, and 4% were selected as the third most likely. Evaluation of vertex candidates using the three dimensional emulsion display provided correct selection of the true neutrino interactions and rejection of fake interactions with 100% efficiency. The remaining 4 unlocated events produced no credible candidates after examining the 3D display and the spectrometer display.

Figure 5.1 shows that the location efficiency decreases as the depth of the vertex position within an emulsion module increases. The cause of this trend is twofold. Particles from interactions which occur near the upstream side of a module traverse more material and therefore produce more showering before reaching the scintillating fiber planes. Showering subsequently confuses the spectrometer tracking software and obscures the vertex position. Since only a small volume of emulsion is scanned near the vertex prediction, this showering makes it more likely that the scanned volume does not actually contain the true interaction vertex. Similarly, as more material is traversed the effect of multiple scattering on the particle trajectories makes an accurate prediction of vertex position more difficult. By the time the particles have reached the spectrometer their directions may have changed enough so that the spectrometer tracks no longer point to the true primary vertex position.

* One event is pending confirmation from Nagoya.

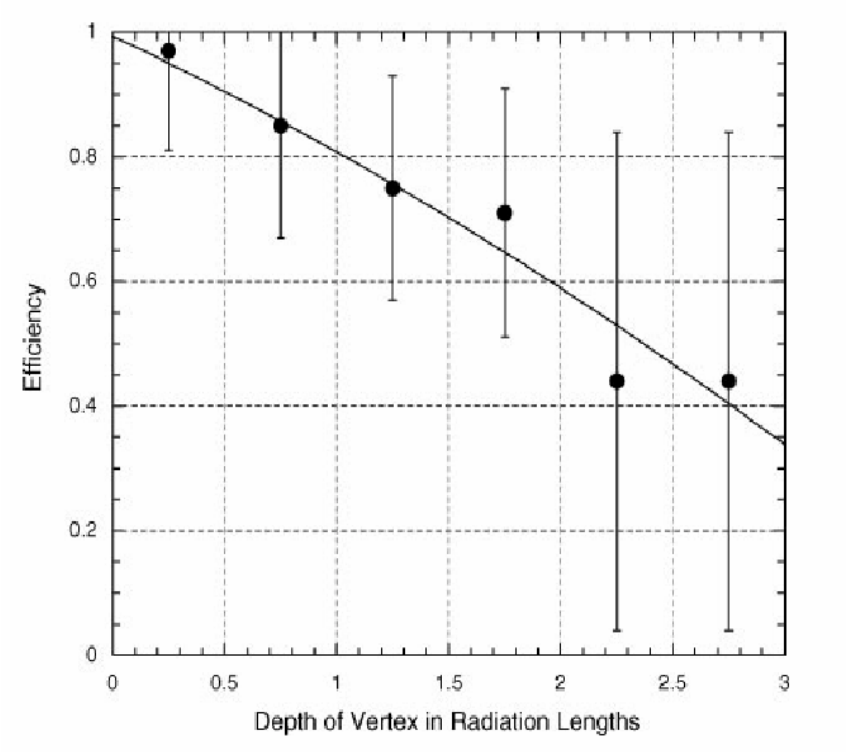

Figure 5-1 Vertex location efficiency is shown here as a function of the depth, in radiation lengths, of the vertex prediction within an emulsion module. The diminishing efficiency is evident in the 30 event set as well as the complete set of DONUT data, which is shown here because of the higher statistics. [27].

Table 5-1 Results of the 30 event set. The entries refer to the values of the true interaction vertices, except those in column 7. Column 7 gives the total number of vertices located in the event, including background vertices, divided by the scanned volume (i.e. the vertex density). Further explanation of the columns is given after the table.

EVENT NUMBER	Located	Location method	Place in Automatic evaluation	Z-Score	Likely Flag	Vertices/ Cm^3	Number of primary vertex tracks
2879_12293	Y	1	1	3.10	N	22	3
2884_14149	N	-	-	-	-	42	-
2892_02649	Y	2	-	-	N	4	1
2893_07799	Y	2	-	-	N	3	1
2907_12929	N	-	-	-	-	83	-
2929_20792	Y	2	1	3.7	N	30	3
2934_00494	Y	2	1	-1.58	N	31	3
2991_07358	Y	2	1	0.49	N	8	2
2996_01287	Y	1	1	4.70	Y	20	4
3000_17634	Y	3	1	0.5	Y	32	4
3004_35680	Y	5	2	2.3	Y	1714	10
3008_29159	Y	1	5	-4.0	Y	200	6
3024_08169	N	-	-	-	-	17	-
3059_01284	Y	2	1	3.1	Y	7	7
3073_22977	Y	2	2	1.1	N	56	2
3096_05346	Y	5	1	1.9	N	104	
3111_03598	Y	5	1	-.8	N	160	3
3190_04273	Y	1	1	-12.1	Y	6	5
3190_06547	Y	1	1	4.6	Y	20	4
3190_15134	Y	1	2	-2.12	N	33	2
3191_03827	Y	1	1	4.65	N	25	2
3235_11264	Y	2	2	-1.91	N	104	2
3254_01397	Y	1	1	3.15	Y	133	4
3287_24160	Y	4	2	-3.9	Y	191	4
3299_09040	Y	3	1	2.1	Y	52	6
3336_11582	Y	3	1	1.6	Y	98	6
3350_17729	N	-	-	-	-	32	-
3352_26934	Y	5	3	-4.1	Y	31	15
3356_03543	Y	2	1	0.43	N	42	2
3358_14209	Y	2	1	1.2	N	213	2

The key to the location methods listed in table 5-1 is

1= general method (comprehensive search, section 4.1.3)

2 = 3D track match (4.1.1)

3 = Phantom track match (4.1.2)

4 = Core track match (4.1.2)

5 = Single segment methods (4.1.4)

The fourth, fifth and sixth columns of table 5-1 refer to the automatic evaluation process described in section 4.2.1. The last column of table 5-1 gives the number of primary tracks in the true vertex. Events 2892_02649 and 2893_07799 are listed as located but no z-score or ranking by the automatic evaluation process is given. These events have only one primary track therefore the normal vertex measurements are not obtained. Using the spectrometer-to-emulsion track matching functions these single track events were identified after no viable vertex candidates were located using the methods of chapter 4. The fact that the single track in these events originates within the scanned volume was confirmed manually under a microscope in Nagoya.

Table 5-2 lists additional results of the 30 events which reflect properties of the emulsion and tracking for each event.

Table 5-2 Properties of the emulsion and tracking for 30 events. All columns pertain to the scanned emulsion volume surrounding each event.

EVENT NUMBER	Scanning Efficiency (%)	Angular segment-to-track deviations (mrad)		Position segment-to-track deviations (μm)		Segment Density (seg/cm^2)x10^5		Average Segment Pulse Height	Starting Tracks (%)
		Mean	RMS	Mean	RMS	Mean	RMS		
2879_1229	97	5.6	1.1	1.0	0.3	0.67	0.17	11.2	12
2884_1414	96	4.2	0.6	1.1	0.2	0.96	0.41	11.6	12
2892_0264	96	4.5	0.6	1.0	0.3	0.80	0.45	10.6	11
2893_0779	95	4.5	0.6	0.4	0.1	0.71	0.41	11.9	11
2907_1292	96	4.4	0.7	1.1	0.2	0.95	0.40	12.2	13
2929_2079	97	4.1	0.6	1.2	0.4	0.66	0.09	13.1	18
2934_0049	95	4.7	0.7	1.1	0.4	0.99	0.11	12.8	12
2991_0735	96	4.1	1.0	0.4	0.2	0.82	0.27	13.2	13
2996_0128	97	4.1	1.0	1.2	0.4	1.44	0.28	12.9	10
3000_1763	98	7.3	1.1	1.2	0.4	0.63	0.09	11.3	15
3004_3568	98	8.1	1.3	1.1	0.5	0.68	0.24	12.2	29
3008_2915	95	6.5	1.0	1.2	0.4	0.71	0.18	12.9	10
3024_0816	95	5.2	0.5	1.3	0.4	0.74	0.15	12.2	15
3059_0128	97	3.9	0.6	0.9	0.2	1.03	0.13	13.3	13
3073_2297	97	1.0	0.8	0.3	0.2	1.51	0.55	12.2	13
3096_0534	96	5.0	0.9	1.1	0.3	1.53	0.51	12.5	18
3111_0359	94	4.5	0.7	1.2	0.2	1.04	0.14	11.9	25
3190_0427	97	4.2	0.8	1.3	0.4	0.62	0.3	11.6	14
3190_0654	98	3.6	0.6	0.9	0.2	1.32	0.36	12.3	8
3190_1513	96	5.9	0.8	1.3	0.3	0.66	0.08	12.8	7
3191_0382	98	3.2	0.4	0.7	0.2	1.44	0.29	12.9	7
3235_1126	98	4.3	0.6	0.8	0.2	1.83	0.19	13.2	13
3254_0139	98	7.0	0.6	1.2	0.3	2.01	0.59	12.5	20
3287_2416	95	4.6	0.6	0.7	0.2	0.91	0.13	12.4	13
3299_0904	94	4.7	0.7	1.2	0.5	0.92	0.14	12.2	30
3336_1158	98	3.0	0.5	0.7	0.2	2.24	0.83	11.6	8
3350_1772	97	3.9	0.4	0.9	0.4	0.82	0.30	12.3	13
3352_2693	94	4.1	1.2	0.8	0.4	0.66	0.36	12.6	24
3356_0354	96	3.3	0.5	1.1	0.3	0.69	0.12	12.3	8

5.2 Two Events

In this section two events will be discussed in more detail. They exemplify the effectiveness of software techniques presented in chapter 4 and the usefulness of the three dimensional emulsion display.

Event 3352_26934 is a charged current muon interaction which occurred in ECC type emulsion in station 3. This event was located using the general location routine which searches all emulsion tracks regardless of spectrometer information (section 4.1.3). The true interaction vertex was selected from 16 candidate vertices by visual inspection in the emulsion event display. In this case the only two multi-segment tracks in the vertex have an impact parameter of ~10μm, which would normally eliminate this vertex from consideration. (fig 5-2). There is significant plate slipping and distortion in this event and so most tracks, including the vertex tracks, are not fit very well. The z score for the actual interaction vertex was -4.1 and this vertex was selected by the automatic evaluation as being the third most likely to be the true vertex. That means the real vertex neither appears to be the best candidate in this event nor does it even look like a real neutrino interaction vertex. The vertex was flagged in software as likely because it contains 13 single segments. Examination in the 3D display revealed the event to be a viable neutrino candidate and its validity was confirmed by a manual scan in Nagoya. This neutrino interaction would likely not have been found without the use of single segments.

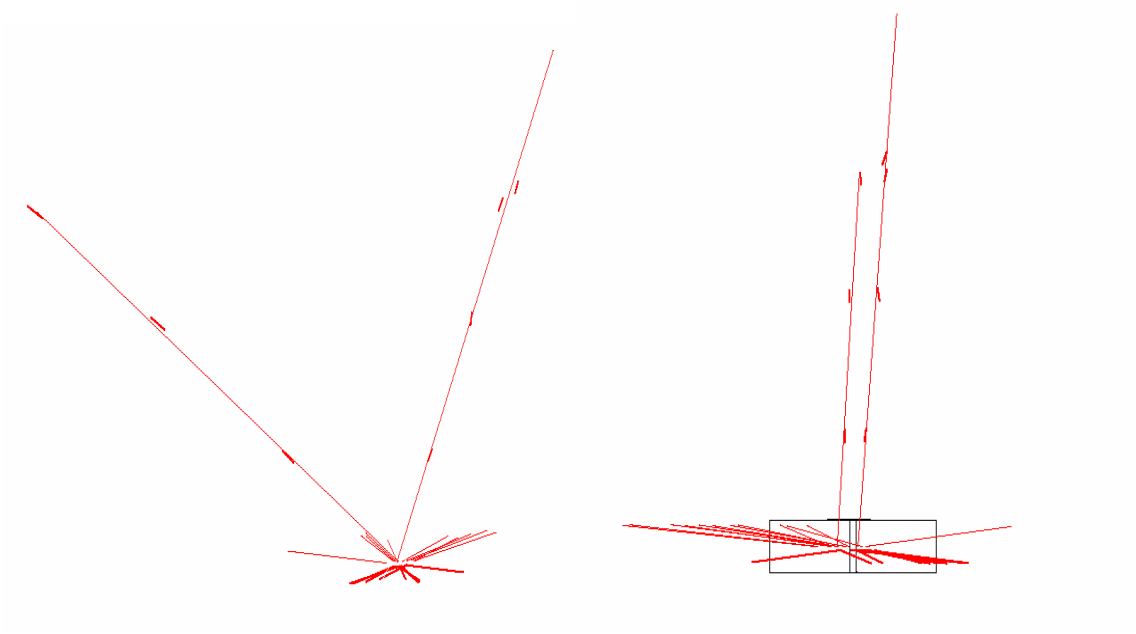

Figure 5-2 Event #3352_26934. Poor emulsion quality and low multiplicity made this event difficult to locate. The two multi-segment tracks do not form a vertex in the view on the right, but 13 single segments associated with the vertex flagged it for observation.

Event 3334_19920 is a charged current tau neutrino interaction that was located using the general location routine described in section 4.1.2. This event was identified as a tau neutrino interaction candidate while being observed in the three dimensional emulsion display. That observation was an unusual occurrence because the display was not typically used for that purpose. In general it was more efficient to use decay search algorithms to find ν_τ candidates. The other tau neutrino events were found in that way or by manually following each track in the emulsion using a microscope. In this case, however, it was noticed while inspecting the primary vertex that there appeared to be no lepton connected to the vertex. Inspection of the spectrometer display did not indicate a neutral current event and yet in the emulsion display no charged lepton was apparent. The missing lepton was evident in that there was no visible track to balance the momentum carried by all the other tracks (fig. 5-3).

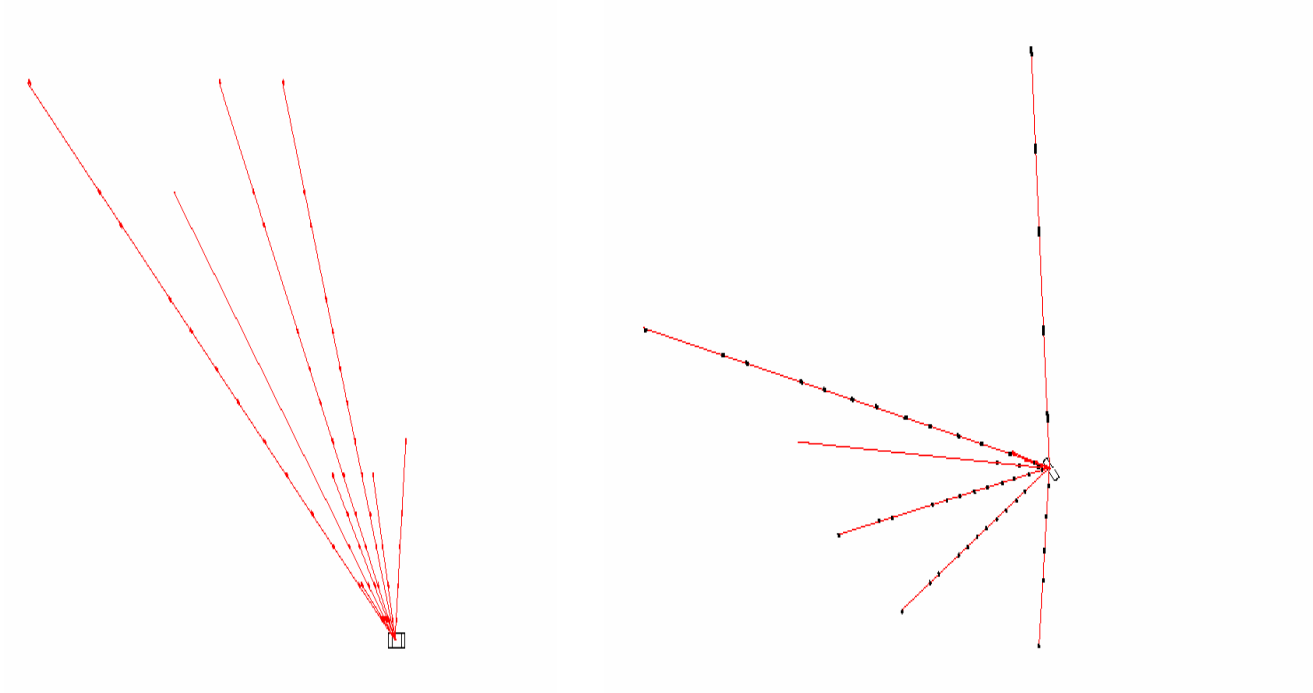

Figure 5-3 Event 3334_19920 shown as it appeared upon first observation in the U-Z view on the left and along the beam direction on the right.

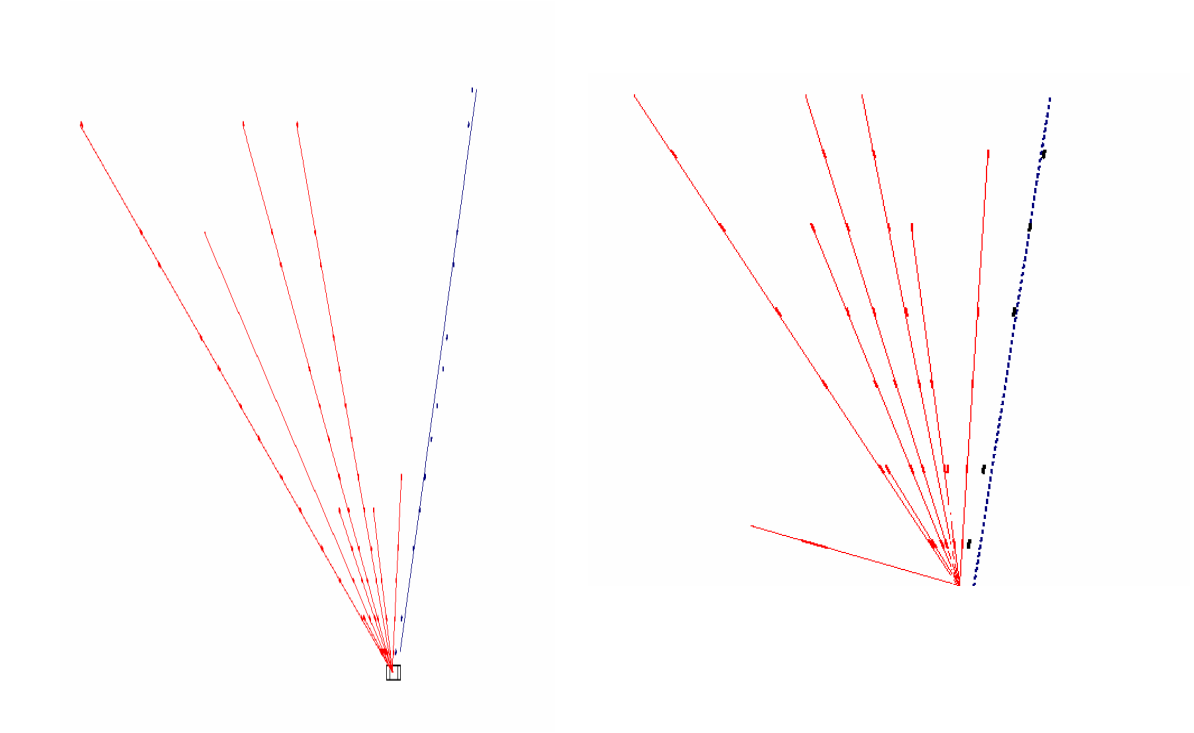

Figure 5-4 After a closer look in the emulsion display the track on the far right was found, but it did not point precisely to the primary vertex.

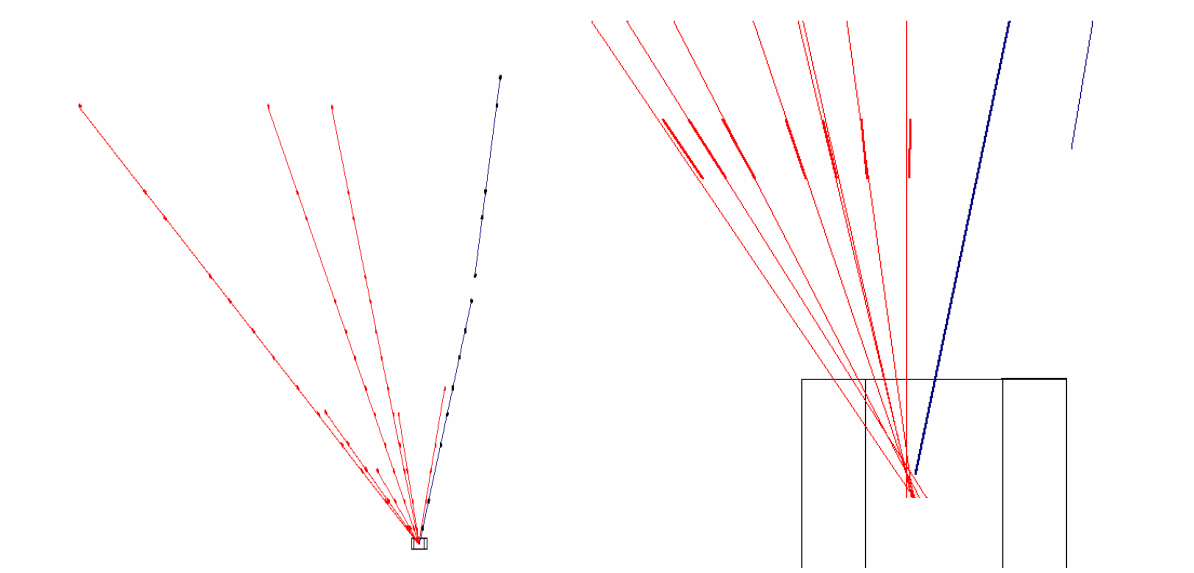

Figure 5-5 After the new track was divided the upstream portion pointed to the primary with an impact parameter of 0.6 microns. The enlarged image on the right shows the vertex tracks with their first segments. The thick line on the right is the projection of the first segment of the new track. The thin line in the upper right is just the end of the track while it was still mislinked.

A close-up view in the display revealed that another track started near the vertex but with an impact parameter of 18.9μm, much greater than the 3.5 μm cut for vertex tracks. (fig. 5-4). Examination of that track showed that it was not a single track but rather two tracks connected together with a kink angle of 10.2 mrad. (fig 5-5). The first 9 segments formed a track which pointed perfectly to the primary vertex and also pointed in the correct direction to be the primary lepton. Inspection of the region near the kink revealed two additional tracks which also pointed to the end of the primary track. Those two tracks, in addition to the second portion of the original track, formed a secondary vertex (fig 5-6). It was unlikely that this vertex was due to a secondary interaction since its location was in the plastic part of the emulsion plate. It also was unlikely that the decaying particle was a charmed hadron since no other lepton was observed to emerge from the primary vertex and because of its angle relative to the other tracks. These potential sources of background are examined in section 5.3 as an example of the DONUT analysis.

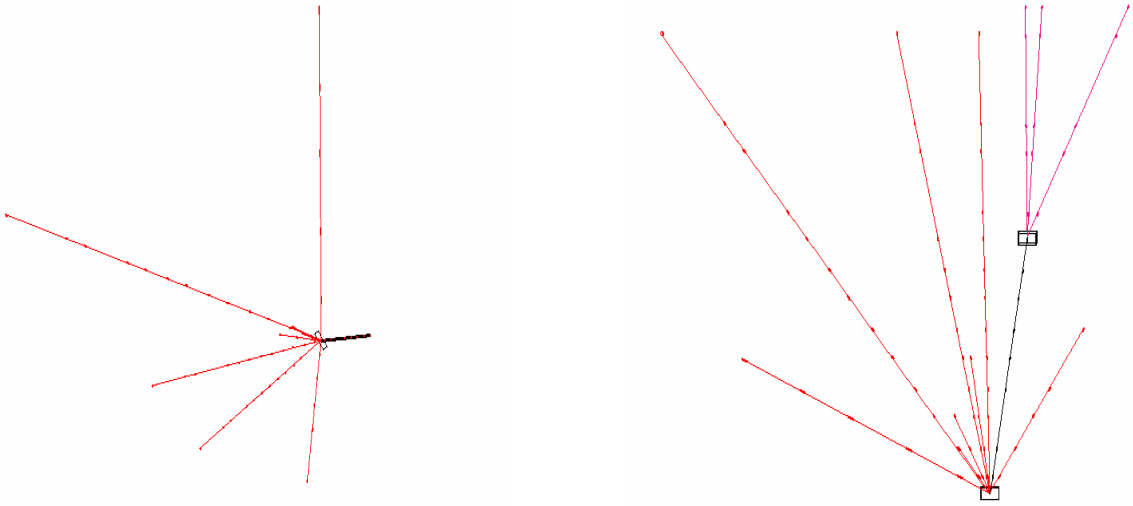

Figure 5-6 The beam's eye view on the left shows that the new track, the dark track pointing to the right, could be the missing lepton since it is pointing in the correct direction for transverse momentum conservation. On the right, two additional tracks are seen to form a secondary vertex with the downstream portion of the original track.

5.3 DONUT Results

Out of 6.6 x 10^6 experimental triggers recorded during the E872 data run 1020 neutrino event candidates were identified after software filtering (chapter 2). This number compares well to the expected number of 1100 $\pm$ 200[27]. Among this set 197 were rejected because they were either not within the fiducial volume of the emulsion, they were secondary interactions of events where the primary was out of the fiducial volume, or there was an irreparable problem such as emulsion damage. At the present time 564 neutrino events have been located and 259 remain unlocated. The set of located neutrino events includes 9 tau neutrino interaction candidates including one which will be discussed in detail in this section. The first results of four tau neutrino events were published in Physics Letters B in 2001[28]. More recently the ν_τ cross section was calculated using DONUT data to be $\sigma_{\upsilon_\tau N} = 45 \pm 21 \times 10^{-38} cm^2$, in agreement with the standard model prediction calculated to be[29] $\sigma_{\upsilon_\tau N} = 48 \pm 5 \times 10^{-38} cm^2$. DONUT data were also used to calculate an upper limit on the ν_τ magnetic moment of[30] $\mu_{\upsilon_\tau} \leq 4.2 \times 10^{-7} \mu_B$. Table 5-3 lists the composition of the (564) located events

Table 5-3 Composition of events located in DONUT

Composition of Data Set			
Neutral Current			174
Charged Current			376
ν_μ		232	
ν_e		159	
ν_τ		9	
ν_τ long	7		
ν_τ short	2		
Charm		10	
Charged	4		
Neutral	6		
Total			564

Event 3334_19920 is analyzed here as an example of the identification analysis of located neutrino interactions. Determining the probability that this event was a tau neutrino interaction requires essentially three things. First, all background processes

which could potentially mimic this event need to be identified. Second, the expected frequencies of these processes, both background and ν_τ interactions need to be found. Third, measurable characteristics of tau decays and background processes need to be evaluated so that measurements of these properties can be used to determine the likelihood of such an event. This statistical analysis has been the subject of other theses from which a summary of results is given here[31],[29]

The relative probability that event 3444_19920 was a ν_τ interaction rather than a background event can be written as

$$P(\nu_\tau \mid \vec{x}) = \frac{\Pi(\vec{x} \mid \nu_\tau) A_{\nu_\tau}}{\Pi(\vec{x} \mid \nu_\tau) A_{\nu_\tau} + \sum_{bkg} \Pi(\vec{x} \mid bkg) A_{bkg}}$$

5.1

.

In this equation, which is Bayes theorem, A_{ν_τ} is the prior probability of a ν_τ interaction and A_{bkg} is the prior probability of a particular type of background event[32]. The prior probability of an event type is given by the fraction of times one would expect to see that type of event out of the total number of events. For a given process it depends on the neutrino fluxes, the neutrino cross-sections, the trigger and location efficiencies, and the probability that an event of that type passes the tau selection criteria. The tau selection criteria are listed in table 5-4[*]. A Monte Carlo simulation was used to determine that the background processes to the ν_τ interaction signal are either charm particle decays where the primary lepton is lost, or secondary hadronic interactions resulting in 3 charged daughters[28].

[*] Note that this is a significant simplification of the situation, since each of these variables depends on a number of other variables. For example, the prior probability of a muon neutrino interaction which produces a D^+ meson to appear like a tau trident interaction depends on the branching ratio of the D^+ to 3 charged daughters. It also depends on the experimental efficiency of detecting muons, since such an event will only be a background to the tau signal if the primary muon goes undetected. For a full description of this analysis see reference 28 or 30.

Table 5-4 Tau selection criteria

Primary lepton	No electron or muon may originate at the primary vertex	trident and kink
Decay length	The distance between the primary and secondary vertices must be < 10mm	trident and kink
Kink angle	The angle of the daughter track relative to its parent track must be > 10mrad	Kink
Impact parameter	The impact parameter of the daughter to the primary vertex must be > 500μm	Kink
Daughter momentum	The momentum of the daughter track must be > 1GeV	Kink

All simulations were done using a Monte Carlo program created for the DONUT experiment. The Monte Carlo was comprised of a neutrino generator representative of the e872 neutrino beam, a neutrino interaction generator, and a detector simulator representative of the DONUT detector. Neutrino interactions were simulated using the LEPTO[33] program package and the resultant particles were propagated through the detector using GEANT[34]. For a detailed description of the e872 Monte Carlo, including values used for input parameters and tests that were done to verify the validity of the program see reference 13[13].

In equation 5-1 the quantities $\Pi(\vec{x}\,|\,\nu_\tau)$ and $\Pi(\vec{x}\,|\,bkg)$ are probability density functions for ν_τ interactions and background processes, respectively, evaluated at $\vec{x}$, where $\vec{x}$ is an n-dimensional vector of n measurable properties of the events. The four properties used in the DONUT trident analysis were: 1) decay length 2) primary lepton angle 3) azimuthal angle imbalance and 4) daughter track impact parameters to the primary vertex. These parameters are illustrated in figures 5-7 and 5-8 and defined in table 5-5. The probability density functions reflect the likelihood that the particular event type yield the measured value of $\vec{x}$. Essentially they provide the fraction of events of a particular type which are less likely than the event being analyzed to have the measured value of a given parameter. The probability density functions for each of the four

parameters were derived from distributions of a large number of simulated events. Distributions of these parameters are shown in figures 5-9 and 5-10.

Table 5-5 Parameters for probability analysis.

Parameter	Definition
L	The decay length of the τ or charm particle or the distance between the primary vertex and the secondary interaction point for other hadrons. (fig 5-7)
θ	The angle of the τ, charm or interacting hadron relative to the incoming neutrino. (fig 5-7)
$\Delta\Phi$	This is the angle between the projection of the τ, charm or interacting hadron displacement onto the x-y plane, and the average of all other primary tracks projected onto the x-y plane (fig 5-8).
ΣIP	Sum of daughter impact parameters to the primary vertex (see figure 5-7).

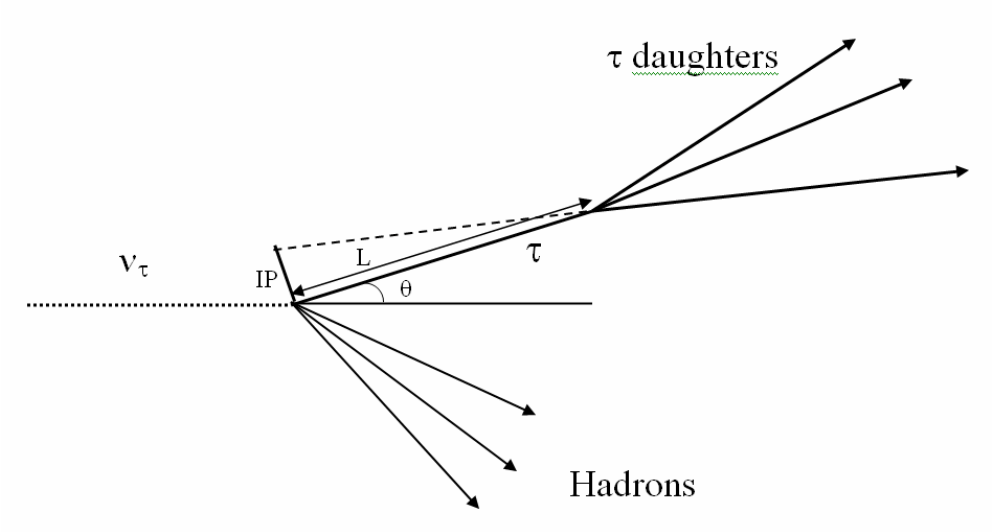

Figure 5-7 The parameters L, θ and IP used for probability analysis are illustrated in this image. For the purpose of clarity only one of the daughter impact parametes to the primary vertex is shown. The sum of all three daughter impact parameters is used in the analysis.

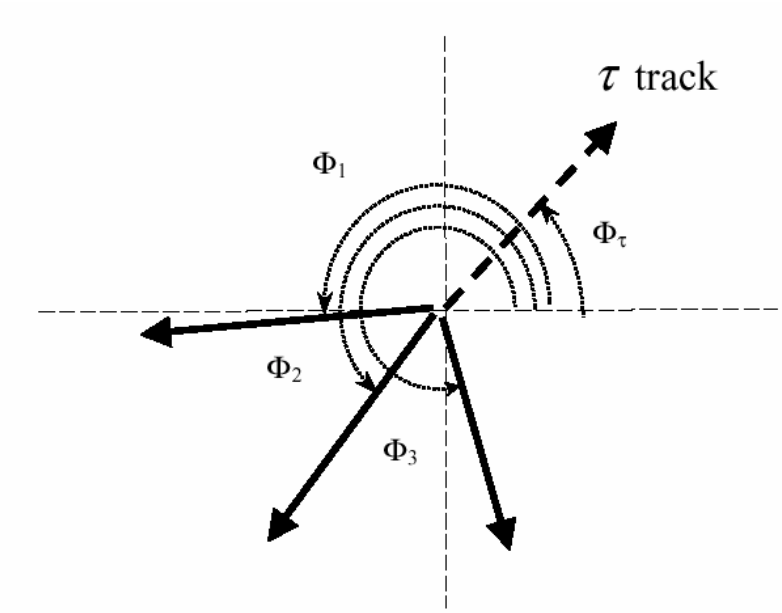

Figure 5-8 Looking along the beam direction, the azimuthal angles of a tau track and three other primary tracks are shown. $\Delta\Phi$ is given by the difference between Φ_τ and the average value of the other Φ angles. For a tau neutrino interaction this value should be near π, reflecting conservation of transverse momentum.

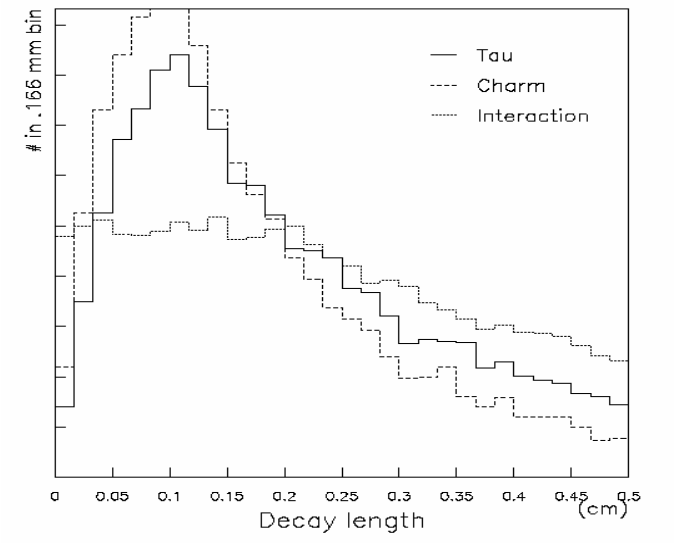

Figure 5-9
Monte Carlo distributions of the parameters L, θ, and ΔΦ for tau neutrino interactions and background processes. [30]

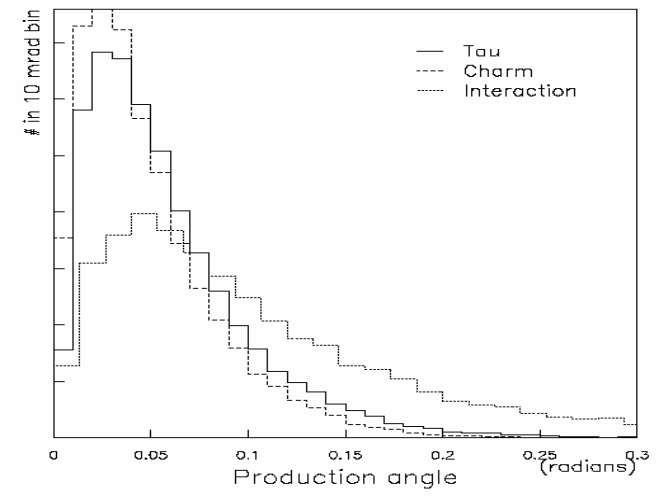

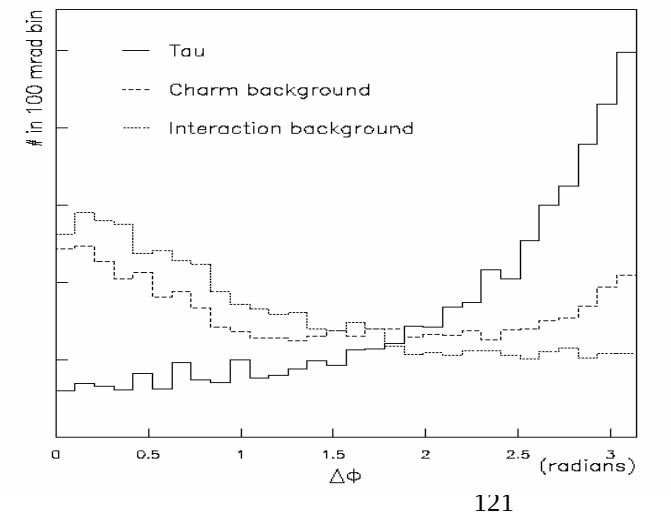

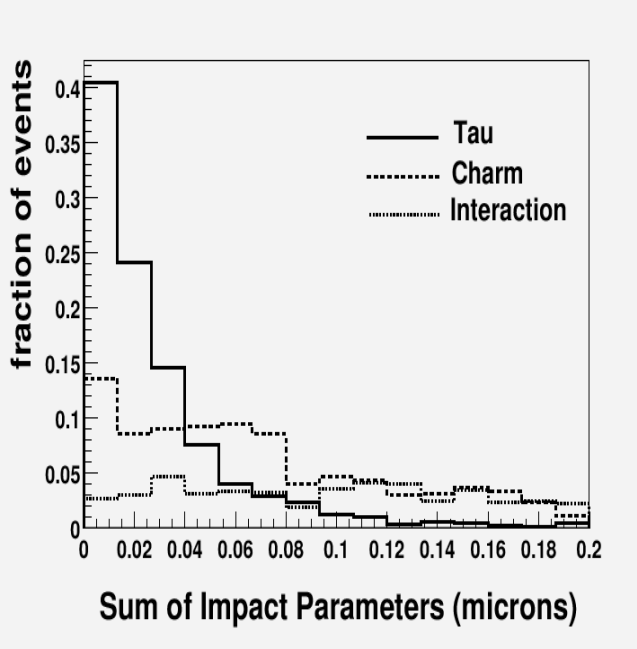

Figure 5-10 Distributions of parameter ΣIP. [28]

Prior probabilities and probability density functions for ν_τ events, hadronic interactions, and charm particle decays have been calculated for all tau neutrino candidates in the DONUT data and are listed in table 5-6 [28]. Substituting values from table 5-6 into equation 5-1 give the relative probabilities that the tau neutrino candidates in DONUT are charged current ν_τ interactions as opposed to background processes. The result for event 3334_19920, to three significant figures, is that the probability of it being a ν_τ interaction is 1.00 vs. 0.00 probabilities that the event is either a charm decay or a hadronic interaction. This event is most likely a tau neutrino interaction.

Other kink and trident events located in the experiment were analyzed in a similar manner[28] and the results of that analysis are listed in Table 5-6. Of the 7 long tau neutrino candidates 6 of them are most likely tau neutrino interactions. Event 3263_25102 has a relative probability of 0.57 of being a hadronic interaction and is therefore most likely not a tau neutrino interaction.

Table 5-6 DONUT result for kink and trident tau neutrino candidates, and for charm particle candidates.

Relative Probabilities for Each Candidate						
Event	**Material**	**Topology**	**Tau**	**Charm**	**Interaction**	**Overall**
3024_30175	Plastic	kink	0.64	0.36	0.00	Tau
3039_01910	Plastic	Kink	0.96	0.04	0.00	Tau
3140_22143	Steel	Kink	0.97	0.03	0.00	Tau
3263_25102	Steel	Kink	0.15	0.28	0.57	Interaction
3296_18816	Emulsion	trident	0.71	0.29	0.00	Tau
3333_17665	Plastic	Kink	0.99	0.01	0.00	Tau
3334_19920	Plastic	trident	1.0	0.00	0.00	tau
2846_09042	Steel	Kink	0.00	0.87	0.13	Charm
3065_03238	Steel	Kink	0.00	0.91	0.09	Charm
3227_03420	plastic	Kink	0.00	0.99	0.01	Charm
3245_22786	Emulsion	trident	0.00	0.99	0.01	Charm

6 Conclusions

Nuclear emulsion was the heart of the DONUT detector. Therefore emulsion analysis techniques such as those presented in this thesis were important for mining the large amount of emulsion data obtained in the experiment. While most particle physics experiments have this common task of deciphering large amounts of data, the challenges associated with an emulsion detector are unique. Distortions within emulsion vary greatly because emulsion is a gel and also because of the nature of emulsion processing (section 2.3.2). For this reason emulsion analysis requires a multi-pronged strategy of pattern recognition to remove the distortions and restore the sub-micron resolution of the detector. Successful techniques for accomplishing this have been presented in this thesis. Specifically, methods for improving emulsion tracking and event location are detailed in chapters 3 and 4. The results from chapter 5 show that by applying these methods location efficiency can be improved from 58% to 87%.

The key elements to improved tracking are:

1. Using iterative tracking algorithms with progressively weaker selection criteria. This allows the high momentum and straightest tracks to be established first while still allowing the formation of lower momentum tracks. Tracking procedures are described in section 3.2.2.
2. Initiating track formation from both the upstream and downstream ends of a scan volume. This procedure improves tracking by taking into account potential non-uniform areas of emulsion where tracks may link easily in one direction but not in the other.
3. Using both single segment and track projections to search for connecting track segments. As explained in section 3.2.2, a matching segment should be near the position of a track's projection in the following plate for high momentum tracks. However, a matching segment's position may be more

precisely predicted by a single segment's projection for lower momentum tracks.

4. Performing fine local alignment on all segments. Emulsion distortions cause track segment data to be skewed. This non-uniform effect is corrected locally on a sub-micron scale by the method described in section 3.2.3.
5. Correcting misaligned or disconnected tracks resulting from plate slipping. This problem occurred when adjacent emulsion plates, or groups of plates, shifted transversely with respect to each other during exposure. A method for realigning track data was explained in section 3.2.5.

Event location efficiency is improved by:

1. Using single segments in addition to multi-segment tracks for vertex formation and evaluation. Treating single segments as tracks often illuminates a true interaction vertex. This may happen because adding single segments increases the total number of primary vertex tracks, which is an important selection criteria. Or, adding single segments may increase the number of vertex tracks that match the spectrometer. Single segments are also used in place of tracks in events with large distortion or plate slipping. These methods are discussed in sections 4.1.1.3 and 4.1.4.

2. Reducing the number of background vertices by requiring that at least one emulsion vertex track match a spectrometer track. Sections 4.1.1 and 4.1.2 describe how the spectrometer track can be either a real three dimensional, phantom, or shower core track.

3. Utilizing a three dimensional event display to confirm or reject vertex candidates. From quantitative values such as impact parameters, some candidates within a scan volume may be equally as likely as others to be the real interaction vertex. Viewing candidates in the 3D display can reveal useful information not otherwise obtained. This is discussed in section 4.2.2.

The primary goal of Fermilab experiment 872 was achieved by making the first direct observation of tau neutrinos in the interaction ν_τ + N -> τ + X. Furthermore, modern emulsion technology was successfully used and improved in the DONUT experiment

While emulsion detector technology has been significantly advanced, some problems do remain. Distortion problems are inextricably coupled to emulsion detectors. However, the impact of distortion can be minimized by requiring extremely controlled processing procedures and environment. Work is being done at Nagoya University to develop equipment and strategies to improve processing environments.[35] The inability in some cases to precisely predict vertex position will continue until automatic scanning rates, computer memory, and computer processing times are capable of handling the increased amount of data which would accompany larger scan volumes. Since scanning rates have increased by a factor of ~40 over the last 5 years and are expected to increase by another factor of ~25 in the next 5 years, the impact of this problem is being lessened as well[36].

Despite these difficulties nuclear emulsion has reemerged as an important sub-micron particle detector. The current importance of neutrino physics and the necessary ability to detect short lived particles make the technology developed in E872 very promising for future high energy physics experiments. Oscillation experiments such as OPERA[37] are presently using some of the same technology which was developed in E872. The use of emulsion analysis techniques presented in this theses will further enhance the usefulness of this old technology.

References

[1] W. Pauli, December 4, 1930 letter to colleagues, reprinted in *W. Pauli, collected scientific papers*, Editors R. Kronig and V. Weisskopf, Vol 2, p. 1313, Interscience, New York 1964
[2] F. Reines and C. Cowan, Phys. Rev. 92, 8301, 1953
[3] G. Danby , *et al*., Phys. Rev. Lett. 9, 36, 1962
[4] B. Pontecorvo, Soviet Physics JETP 37,1236,1960 [translated from 37, 1751 ,1959]; T. D. Lee, Rochester Conference 1960, p.567.
[5] M. Perl , *et al*., Phys. Rev. Lett 35, 1489, 1975
[6] Y. Fukuda, *et al*., Phys. Rev. Lett. 81, 1562, 1998
[7] SNO Collaboration Phys. Rev. Lett. 87, 071301, 2001
[8] ARGUS Collaborations Phys. Lett. B 202, 149, 1988
[9] LEP Collaboration Phys. Lett. B 202, 149, 1988
[10] C.C.Powell, P.H.Fowler, D.H.Perkins *The Study of Elementary Particles by the Photographic Method*, New York: Pergamon, 1959
[11] K. Niwa, *private communication* 1998
[12] W.M. Yao, , *et al*.,(Particle Data Group), J. Phys. G 33, 1, 2006
[13] R. Schwienhorst, Ph.D. Thesis, University of Minnesota 2000
[14] S.Aoki, *et al*., Nuclear Tracks 12, 249, 1986
[15] S.Aoki, *et al*., N Nuc. Instr. Meth. B51 466, 1990
[16] K. Hoshino, *private communication*, 1998
[17] K. Okada, *private communication*, 1998
[18] Walter H. Barkas, Nuclear Research Emulsions, Academic Press, 1963
[19] K. Kodama, *et al*., Nuc. Instr. Meth. A 516, 2004
[20] N. Saoulidous, Ph.D. Thesis, University of Athens, 2003
[21] V. Highland, Nuc. Instr. Meth. 129: 497, 1975
[22] B. Rossi, *High Energy Particles*, Prentice-Hall, 1952
[23] K. Kodama, *et al*., Nuc. Instr. Meth. A 493, 2002
[24] M. Nakamura, *private communication*, 1998
[25] M. Komatsu, *private communication* , 1998
[26] R. Brun, , *et al*., ROOT: An Object-Oriented Data Analysis Framework. URL root.cern.ch/
[27] B. Lundberg, K. Niwa, and V. Paolone, Ann. Rev. Nucl. Part. Sci. 53: 199, 2003
[28] K. Kodama, *et al*., Phys. Lett. B 504, 218, 2001
[29] E. Maher, Ph.D. Thesis, University of Minnesota, 2005
[30] R. Schwienhorst *et al*., Phys. Lett. B 513, 23, 2001

[31] J. Sielaff, Ph.D. Thesis, University of Minnesota, 2003
[32] G. Cowan, *Statistical Data Analysis*, Oxford University Press, 1998
[33] G. Ingleman, J. Rathsman, and A. Edin, LEPTO-The Lund Monte Carlo for deep inelastic lepton-nucleon scattering, Comp. Phys. Comm. 101, 108, 1997
[34] R. Brun, *et al*., GEANT Detector Description and Simmulation Tool, CERN Program Library,
W5013 1998
[35] T. Kotaka, *private communication*, 1998
[36] T. Nakano, *private communication*, 2006
[37] H. Pessard (OPERA), arXiv:hep-ex/0504033, 2005